

**SPATIAL EXTENT OF GEO-MECHANICAL PROPERTIES VIA
QUANTITATIVE SEISMIC INTERPRETATION**



By

Jawad Ahmed

M.Phil. Geophysics

2020-2023

Department of Earth Sciences

Quaid-i-Azam University Islamabad, Pakistan

CANDIDATE’S DECLARATION

I hereby declare that the M.Phil. Research work submitted bearing the title **“RESERVOIR CHARACTERIZATION OF KADANWARI AREA CENTRAL INDUS BASIN PAKISTAN USING WELL DATA AND SEISMIC DATA”** is a result of my research work. Jawad Ahmed M.Phil. Candidate

CERTIFICATE

This dissertation submitted by **JAWAD AHMED S/o NOOR Ilahi** is accepted in its present form by the Department of Earth Sciences, Quaid-i-Azam University Islamabad as satisfying the requirement for the award of M.Phil. Degree in Geophysics.

RECOMMENDED BY

Dr. Aamir Ali
(Supervisor)

Dr. Aamir Ali
(Chairman)

External Examiner

Department of Earth Sciences Quaid-i-Azam University

Islamabad

ACKNOWLEDGMENT

All appreciation be to **Allah Almighty**, the master of the universe, who gives unlimited blessing to His creation beneficent. He creates the universe in seven days and shares mysteries about the universe with us in Quran e Pak to explore the universe by the thirst for knowledge and wisdom.

I would like to pay my special gratitude to my thesis supervisor **Dr. Aamir Ali** of the earth science department who allowed me to do wonderful research on reservoir characterization of the Kadanwari area, Central Indus Basin Pakistan using well and Seismic data.

I wish to thank all facilities of earth science whose valuable knowledge was a milestone in the completion of the dissertation.

I am very grateful to Mr. Zahid Ullah Khan Senior Geophysicist at LMKR and Mr. Yawar Amin (senior Phd Student) for all appreciative to acknowledge my depth to all those experts who were involved in research work and put those ideas in a solid position. But most important acknowledge my beloved family, specially my parents for my encouragement, support and sacrifices throughout my study. Their too much appreciation, smooth motivation, and their love and trust made me strong enough to complete my goal. I also wish to tahnk the whole faculty of my department for providing me the academic base, which has enable me to take up this study I pay my thanks to clerical office who helped me a lot and all others who have contributed to the successful completion of this study

Jawad Ahmed

FEB 2023

DEDICATION

Every challenging work needs self-effort as well as guidance of elders especially those who are closed to our heart. I want to dedicate my humble efforts to my parents, teachers and siblings. I dedicated it to place where much of this wasw invented, elobrated and where a friendship developed that even the writing of a dissertation could not spoil.

ABSTRACT

A proper understanding of reservoir architecture is needed to extend solution about hydrocarbon exploration. In this study seismic interpretation, petro-physics and geo-mechanical analysis are used to characterize the Kadanwari area of central Indus basin, Pakistan. More specially the seismic based estimation of geo-mechanical properties are performed to examined their spatial variations. The 3D 12Km² block and one well Kadanwari-01 is used in this study.

Two horizons E-sand and B-sand are marked on seismic data with help of 1D forward modelling. Seismic interpretation give us the information about the presence of horst and graben structures favourable for hydrocarbon accumulation. The result of petro-physical analysis (hydrocarbon saturation 60-80% , effective porosity 9-10% and Vsh 33-35%) gives us the information about the potential zone which is gas in this area. Petro-physical's result shows that kadanwari well-01 is successful in producing economical quantity of hydrocarbon. This also demands to analyze geo-mechanical properties of study area in order to get optimum potential prospect zone for enhancing the production rate .

Geo-mechanical properties are estimated to construct rock mechanical model (RMM) by using wire-line data. The RMM incorporates GMP's including young's modulus, bulk modulus, shear's modulus, unconfined compressive strength, friction angle, overburden-stress, pore pressure, minimum and maximum stress. The spatial variations of GMP's are extracted at reservoir scale using seismic inversion integrated with multi attribute and neural networking algorithms (PNN).

The seismic interpretation gives us proper structural information. Our result of GPM's modelling matches the standard values obtained in laboratory which are required for production. There is also indication of favourable GPM's on spatial maps at reservoir scale which is indication of hydrocarbon accumulation. GPM's also helps us to minimize drilling risks and give us information about optimum prospect zone for drilling.

TABLE OF CONTENT

SR.NO.	PAGE NO.
1. INTRODUCTION	16
1.1 INTRODUCTION.....	16
1.2 PROJECT AREA	18
1.3 DATA UTILIZED.....	18
1.4 OBJECTIVE & AIMS OF REAEARCH.....	18
1.5 METHODOLOGY	19
2. PHYSICAL GEOLOGICAL AND TECTONIC FRAMEWORK.....	22
2.1 INTRODUCTION.....	22
2.2 TECTONIC SETTING AND STRUCTURE GEOLOGY OF INDUS BASIN	22
2.3 TECTONICS SETTING OF MIDDLE INDUS BASIN.....	23
2.3 STRATIGRAPHY OF MIDDLE INDUS BASIN.....	25
2.4 DEPOSITIONAL FACIES AND SEQUENCE STRATIGRAPHY OF THE STUDY AREA	26
2.4.1 CHILTAN FORMATION.....	28
2.4.2 SEMBER FORMATION	29
2.5 PETROLEUM SYSTEM OF CENTRAL INDUS BASIN.....	30
2.5.1 SOURCE ROCK	30
2.5.2 RESERVOIR ROCK.....	31

2.5.3	SEAL ROCK	32
3.	SEISMIC DATA INTERPRETATION.....	35
3.1	SEISMIC INTERPRETATION	35
3.2	BASE MAP:	35
3.2	METHODOLOGY:.....	36
3.4	SEISMIC HORIZONS TRACKING:	37
3.5	DEMARICATION OF E & B SAND AND FAULT MARKING:.....	37
3.6	CONSTRUCTION OF CONTOUR MAPS	39
3.6.1	TIME CONTOUR MAPS OF E-SAND AND B-SAND	39
4.	PETROPHYSICAL AND GEO-MECHANICAL PROPERTIES.....	44
4.1	INTRODUCTION.....	44
4.2	GEOPHYSICAL WELL LOGS TRACKS	44
4.2.1	LITHOLOGY LOGS:.....	45
4.2.1.1	CALIPER LOGS (CALI)	45
4.2.1.2	SHALE VOLUME (VSH).....	45
4.2.1.3	SPONTANEOUS LOG (SP).....	46
4.2.2	RESISTIVITY LOGS TRACK:.....	46
4.2.3	POROSITY LOGS TRACK:.....	47
4.2.3.1	SONIC LOG	47
4.2.3.2	DENSITY LOG (RHOB).....	48

4.2.3.3	NEUTRON LOG.....	48
4.2.4	AVERAGE POROSITY.....	49
4.2.5	EFFECTIVE POROSITY.....	49
4.2.6	RESISTIVITY WATER (RW).....	49
4.2.7	WATER SATURATION (SW):.....	49
4.2.8	RESULT OF PETROPHYSICAL ANALYSIS.	50
4.3	ESTIMATION OF GEO-MECHANICAL PROPERTIES.....	54
4.3.1	ROCK MECHANICAL MODEL (RMM).....	54
4.3.2	DETERMINATION OF LITHOLOGIES BY USING ROCK PHYSICS	55
4.3.3	VPVS RATIO VS. ACCOSTIC IMPEDENCE (AI).....	55
4.4.4	LAMBDA –RHO VS. VPVS RATIO.....	57
4.4.5	LAMBDA-RHO VS. MU-RHO.....	59
4.4	ESTIMATION OF ELASTIC PROPERTIES.....	60
4.4.1	YOUNG’S MODULUS	60
4.4.2	BULK’S MODULUS.....	61
4.4.3	SHEAR’S MODULUS.....	61
4.4.4	POISSON’S RATIO.....	62
4.4.5	UNCONFINED COMPRESSIVE STRENGTH (USC) AND FRICTION ANGLE (FANG).....	62
4.5	OVER BURDEN STRESS.....	64

4.6	PORE PRESSURE	65
4.7	MINIMUM HORIZONTAL STRESS	66
4.7.1	DETERMINATION OF MINIMUM HORIZONTAL STRESS.....	66
4.8	SIGNIFICANCE OF RMM.....	66
5.	SEISMIC BASED ESTIMATION OF GEO-MECHANICAL PROPERTIES	70
5.1	INTRODUCTION SEISMIC INVERSION:.....	70
5.2	MODEL BASED INVERSION:	70
5.2.1	METHODOLOGY:.....	71
5.2.3	EXTRACTION OF WAVELET:.....	72
5.2.4	INITIAL LOW FREQUENCY MODEL (LFM):	72
5.2.5	INVERSION ANALYSIS:.....	73
5.2.6	INTERPRETATION OF MBI RESULTS:.....	74
5.3	SPATIAL DISTRIBUTION OF GEOMECHANICAL PROPERTIES VIA SEISMIC INVERSION:.....	77
5.3.1	MULTI ATTRIBUTE AND PROBABILISTIC NEURAL NETWORKING:.....	78
5.3.2	SPATIAL DISTRIBUTION OF V_p/V_s RATIO:.....	78
5.3.3	SPATIAL DISTRIBUTION POISSON'S RATIO:	82
5.3.4	SPATIAL DISTRIBUTION LAMBDA -RHO:.....	86
5.3.5	SPATIAL DISTRIBUTION OF PORE PRESSURE:.....	90

5.3.6 SPATIAL DISTRIBUTION OF MINIMUM AND MAXIMUM STRESSES	95
6. DISCUSSIONS AND CONCLUSIONS	101
6.1 DISCUSSIONS:	101
6.2 CONCLUSIONS	102
7. REFERENCES	104

List of Figures

List of Figures.....	xi
Figure 2.1: Regional tectonic map and location of Kadanwari gas field, source; (Ahmad et al., 2011).	24
Figure 2.2: Generalized sequence stratigraphy of the middle indus basin, source: (Khalid et al., 2014)	28
Figure 3.1: Base map representing in-lines and cross-line of Kadanwari area including three wells(Kadanwari-01, Kadanwari-03, Kadanwari-06).	36
Figure 3.2: Interpreted the seismic section on Inline 2110.....	38
Figure 3.2: Map of E-sand showing time contours. Yellow, White & Red indicates shallow part while Blue and Green shows deeper part (C.I = 0.01sec).....	40
Figure 3.3: Map of B-sand showing time contours. Yellow, White & Red indicates shallow part while Blue and Green shows deeper part (C.I = 0.01sec).....	41
Figure 4.1: Petrophysical assessment Kadanwari-01 well at E-sand. Lithology is shown in track(1). Resistivity in Track (2). Porosity in track(3). track. Volume of shale, effective porosity and water saturation are shown in remaining tracks.....	51
Figure (4.2.1): Petrophysical assessment Kadanwari-01 well at B-sand. Lithology is shown in track(1). Resistivity in Track (2). Porosity in track(3). track. Volume of shale, effective porosity and water saturation are shown in remaining tracks.....	52
Figure 4.2: Petrophysical assessment Kadanwari-01 well at B-sand. Lithology is shown in track(1). Resistivity in Track (2). Porosity in track(3). track. Volume of shale, effective porosity and water saturation are shown in remaining tracks.....	53
Figure (4.3): Cross plot showing P-impedance and VpVs ratio for well Kadanwari -01. Depth interval for lower guru E & B sand is (3318-3338) & (3505-3797). The red eclipse show the gas sand zone.....	56
Figure (4.4): Cross plot showing VpVs ratio & P-impedance for well Kadanwari -01. Depth interval for lower guru E & B sand is (3318-3338) & (3505-3797). The red eclipse show the gas sand zone.....	57
Figure (4.5): Cross plot of lambda-rho and VpVs ratio for well Kadanwari -01. Depth interval for lower guru E & B sand is (3318-3338) & (3505-3797). The red eclipse show the gas prone sand	58
Figure (4.6): Cross plot of lambda-rho and VpVs ratio for well Kadanwari -01. Depth interval for lower guru E & B sand is (3318-3338) & (3505-3797). The red eclipse show the gas prone sand	59
Figure (4.7): Cross plot of lambda-rho and Mu-rho for well Kadanwari -01. Depth interval for lower guru E & B sand is (3318-3338) & (3505-3797). The red eclipse show the gas prone sand	60
Figure (4.8): RMM for lower guru E-sand. Track (1) represent static and dynamic modulus, Track (2) represent bulk's & shear's modulus. Track (3) represent poisson's ratio. Track (4) represent USC , Friction angle & Tensile strain.....	63

Figure (4.9): RMM for lower guru B-sand. Track (1) represent static and dynamic modulus, Track (2) represent bulk's & shear's modulus. Track (3) represent possion's ratio. Track (4) represent USC , Friction angle & Tensile strain.....	64
Figure (4.10):Track (1) blue color shows pore pressure, Green colour show minimum horizontal stress , Red color shows maximum horizontal stress and black color shows vertical stress for E-sand (3318-3338) & B-sand (3505 -3797).	67
Figure (4.11):Well-bore instability for E-sand (3318-3339) of lower guru.....	68
Figure (4.12):Well-bore instability for B-sand (3505-3797) of lower guru.	69
Figure (5.1): Acoustic impedance estimation workflow followed	71
for model based inversion (Sen., 2006)	71
Figure (5.2) : Extracted wavelet from seismic and well data. Blue dotted line shows average phase.	72
Figure (5.3): Initial low frequency impedance model for Lower guru E (3318-3338) & B sands (3505-3797).....	73
Figure (5.4): Inversion analysis for Kadanwari well-01	74
Figure(5.5): Inverted acoustic impedance section and black arrow shows low value of impedance.	75
Figure (5.6): Time slice of E-sand representing low impedance values.	76
Figure (5.7): Time slice of B-sand representing low impedance values.....	77
Figure (5.8): Results from PNN of predicted and real VpVs ratio with correlation of .988417.....	79
Figure (5.9): Spatial variation VpVs ratio for inline 2112 with black arrow represents the value of VpVs ratio of E (3318-3339) & B (3507 -3797) sand.	80
Figure (5.10): Time slice of E-sand and black eclipse represent potential prospect zone.81	
Figure (5.11): Time slice of B-sand and black eclipse represent potential prospect zone.82	
Figure (5.12): Results from PNN of predicted and actual possion's ratio with correlation of 0.983404.	83
Figure (5.13): Spatial variation of possion's ratio for inline 2112 with black arrow represents Low values of E (3318-3339) & B (3507 -3797) sand.....	84
Figure (5.14): Time slice of E-sand with low possion's ratio and black eclipse represent potential prospect zone.	85
Figure (5.15): Time slice of B-sand with low possion's ratio and black eclipse represent potential prospect zone.	86
Figure (5.16): Results from PNN of predicted and real LMR with correlation of .995102.	87
Figure (5.17): Spatial variation LMR for inline 2112 with black arrow represents the value of LMR values of E (3318-3339) & B (3507 -3797) sand.....	88
Figure (5.18): Time slice of E-sand with low LMR values and black eclipse represent potential prospect zone.	89
Figure (5.19): Time slice of B-sand with low LMR values and black eclipse represent potential prospect zone.	90
Figure (5.21): Results from PNN of predicted and actual PP with correlation of .984331.	91

Figure (5.22): Match between predicted and actual pressure. 92

Figure (5.23): Spatial variation of PP for inline 2112 with black arrow represents the high value of Pore pressure for E (3318-3339) & B (3507 -3797) sand..... 93

Figure (5.24): Time slice of E-sand with high pore pressure values and black eclipse represent potential prospect zone..... 94

Figure (5.25): Time slice of B-sand with high pore pressure values and black eclipse represent potential prospect zone..... 95

Figure (5.21) : correlation between predicted and actual pressure is.998649. 96

Figure (5.22): Match between predicted and actual pressure. 97

Figure (5.23): Spatial variation of **shmin** for inline 2112 with black arrow represents the high value for E (3318-3339) & B (3507 -3797) sand..... 98

Figure (5.29): Time slice of E-sand with high Shmin values and black eclipse represent potential prospect zone 99

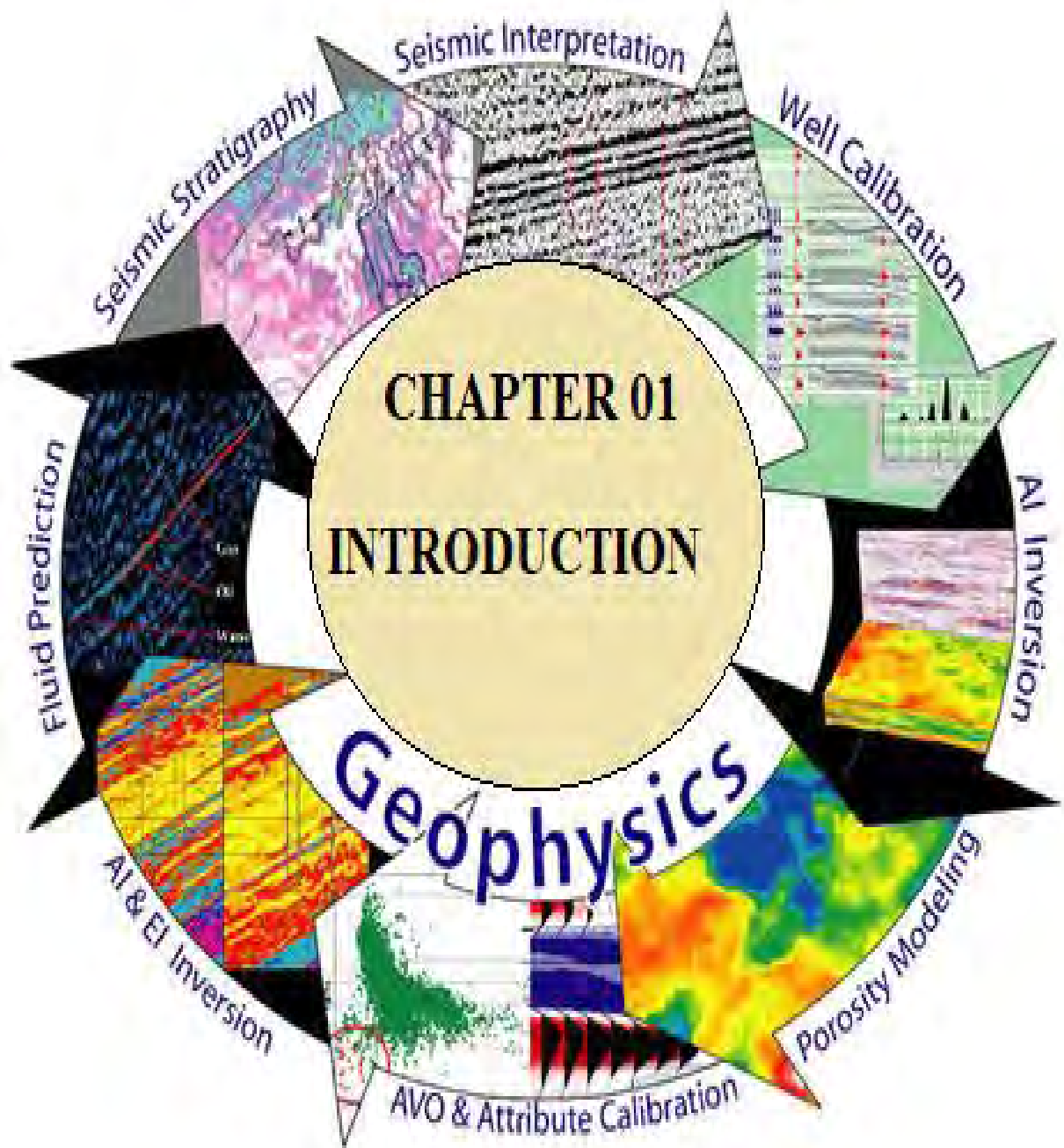
Figure (5.30): Time slice of B-sand with high Shmin values and black eclipse represent potential prospect zone 100

List of Tables

Table 4.1: Petrophysical Analysis of Kadanwari-01 well for E-sand & B-sand. 54

Table 6.1 :Rock physics and geo-mechanical values calculated for E & B sand. The standard values are also given 102

CHAPTER-01



CHAPTER 1

1. INTRODUCTION

1.1 INTRODUCTION

Hydrocarbons are a major resource to cope up with the significant needs of global economic structure as well as global energy structure. The global energy sector is currently working to transition from conventional to unconventional resources (such as tight oil and gas, coal bed gas, and shale oil and gas). Both resources are the main difference from each other (Jia et al. 2012). This research's primary significance is to increase reservoir characterization and the precision of rock mechanics and porosity prediction. (Zhen Liu, 2017).

For the prerequisite measure of field development, three-dimensional data is used to avoid financing lapses. The seismic reflection method is envisaged as a critical vicissitude in hydrocarbon investigation in both conventional reservoirs and unconventional reservoirs. In three dimension seismic data, we can prognosticate changes of pore pressure and fluid saturation in the reservoir environment (Yilmaz, 2001).

To this study, the given data comprises 3D seismic data and well log data. Many geophysical tools are used here for reservoir characterization, such as included seismic attributes, petrophysical investigation, and post-stack seismic inversion. All this work is done in integration with given 3D seismic and well data for estimation and future developments in the Kadanwari area. The seismic data interpretation and seismic attributes analysis is carried by using 3D seismic data to confirm the subsurface structure geology and reservoir extension, while petro-physics analysis and post-stack seismic inversion are carried through well log data for lithology confirmation and reservoir estimation. Seismic 3D data interpretation is a very fast process in fewer fracture strata but is very slow for more complex strata i.e. low impedance zone.

Petro-physical analysis of reservoir zone is one of the crucial parameters in borehole elucidation. The gross pay zone in volume of data is mostly calculated by the reservoir characterization in between reservoir zone which determined the significant volume of the productive zone for hydrocarbon accumulation. The petro-physical parameters tie with seismic data at the well data (Eshimokhai, 2012;

Schlumberger, 1989). Thus inside information of permeability and porosity incorporated physical fluid properties which are a good indicator of productive field (Benedicuts, 2007). More depth study of the whole reservoir is not possible, elucidation of good data can helpful for reduction of uncertainty chance.

Last two decades, seismic inversion is envisage as a significant tool in the oil exploration industry for the identification of hydrocarbon zones and reservoir characterization. Seismic data have more information about the subsurface interface and by applying seismic inversion to transforms these properties into layers properties. These properties can be directly correlated with well log data, in this way inversion help for improvements of characterization of the reservoir (Li and Zhao, 2014). Seismic Inversion applied on data to transfer seismic to blocky response corresponding acoustic impedance (AI). Acoustic impedance is a common method to interpret the geological boundaries layers, delineate reservoir properties, and detection of sweet spots (Barclay et al., 2008). Compare seismic inversion image with the traditional amplitude image, Geoscientists come to concede that seismic inversion image has more resolution than traditional one. This method leads to better estimation of reservoir characteristics such as Net pay, porosity, etc. (Pendrel, 2000). Different types of inversion algorithms can give a helpful bridge for reservoir development and management. It is also observed that Acoustic Impedance (AI) inversion analysis help to reveals the best approach in the identification of reservoir and its distribution.

The theoretical and applied science used to study mechanical behavior of geological material is call geo-mechanics that is used to minimize risk related to well in reservoir zone. the geo-mechanical properties significantly reduce the uncertainty related to well.(Archer & rasouli .,2012; Najibi et al.,2015).The GPM's analysis enhance the accuracy or reservoir parameter and well bore stability from micro to macro scale(Whaley.,2019;Eyinla & Oladunjoye.,2014).the well stability depends on stress components of well lithologies during drilling may cause great risk to rock stability(Qobi et al.,2012).for accuracy of our GPM's analysis we used empirical relation of well and seismic data. (Horsfal et al.,2014;Slota-Valim.,2013; Eyinla & Oladunjoye.,2014).

The GMP require to calculate reservoir elastic properties such as young's modulus, shear and bulk's modulus, pore pressure, minimum and maximum stress, unconfined compressive strain and friction angle. In this study we investigate the reason of successful production in kadanwari well 01 by using rock physics and geo-mechanical properties. Multi attributes and probabilistic neural networking (PNN) is used for seismic based estimation of geo-mechanical properties (Soubotcheva et al.,2001).

In this study we focused on following questions.

- How geo-mechanical properties are linked with well bore stability?
- How PNN can be effective to determine spatial distribution of GMP?
- How spatial distribution of GMP's gives information about optimum potential prospect zone?

1.2 PROJECT AREA

The study area is located in Sindh city of khairpur district, Pakistan. Its geographical coordinates are 27° 00' 00" to 27° 18' 00" latitude N and 69° 06' 00" to 69° 21' 00" longitude east as shown in figure (1.1). This area is located 75km SE of Sukkar, 285km away from Hyderabad, 70km far away from khairpur city, and 360kmNE of Karachi. Geologically this area is situated in the Middle Indus basin reservoir in the research work is lower Guro which is divided into seven units of different sand intervals (H, G, F, E, D,B, C)(Ahmad & Chaudhary, 2002) and bounded by Punjab in the northern side, Kirthar sub-basin in the southern side, Indian shield toward the east and by Kirthar fold belt (KFB) toward the western margin. Upper Guro formation is very effective for cap rock.

1.3 DATA UTILIZED

The three dimensional (3D) seismic cube ($12km^2$) of kadanwari area is utilized lies in middle Indus basin and three wells, kadanwari-01 , kadanwari-06 and kadanwari 03 are used in this research study. The seismic data consists of in-lines and cross-lines 141 and 155 respectively .3D seismic data is of high resolution and integrated with wire line data .Lower Goru sand are target in this area.

1.4 OBJECTIVE & AIMS OF REAEARCH

The leading objectives of this research are:

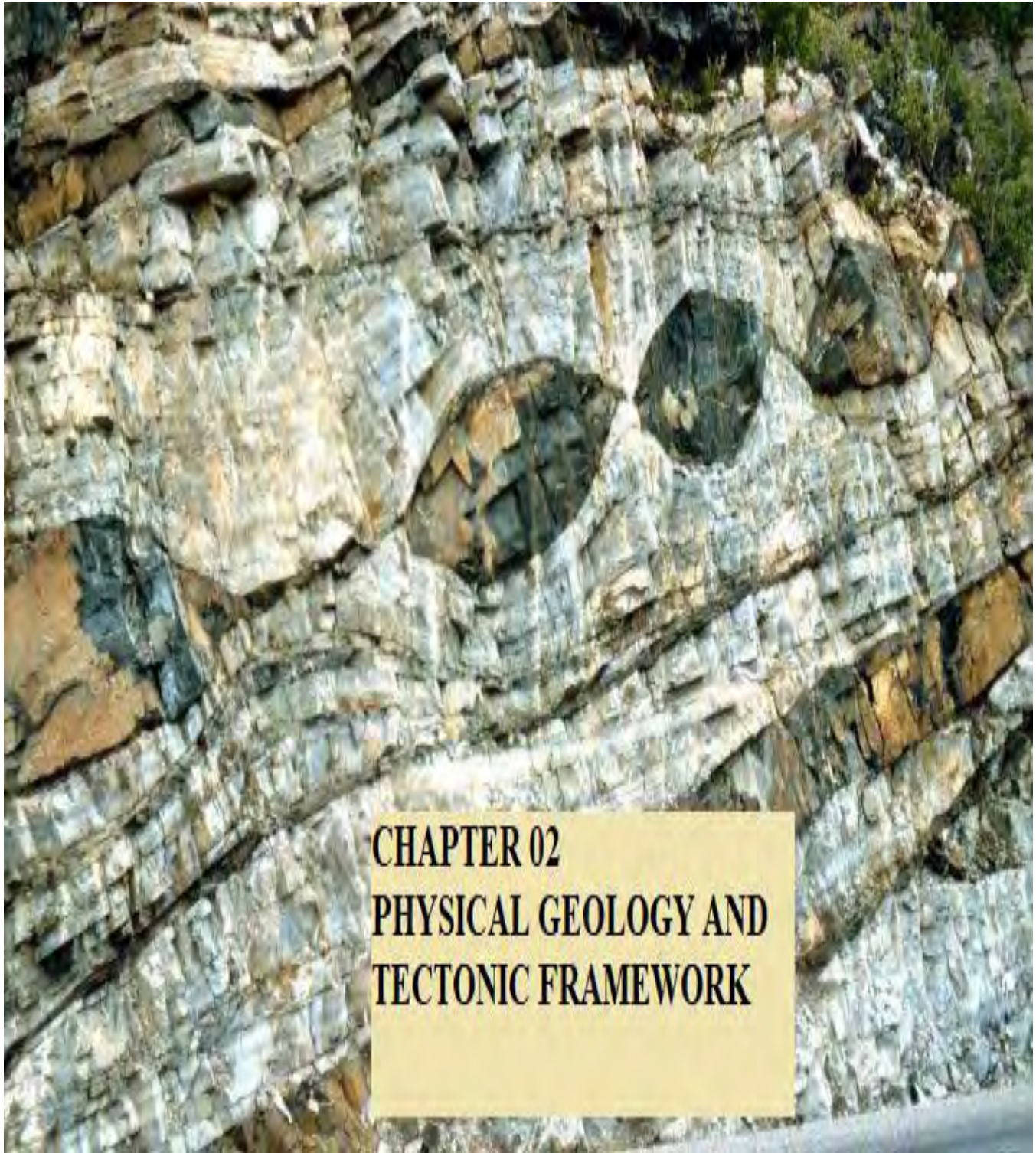
- To characterized reservoir rock in terms of structure elements.
- To perform petro-physical and geo-mechanical analysis on lower Goru sands.
- To examine the spatial behaviour of geo-mechanical properties the seismic based estimation of GMP is done by PNN and multi-attribute techniques.
- To identify the potential prospect zone in order to enhance production.

1.5 METHODOLOGY

An integrated approach is applied for reservoir characterization. The complete methodology is including petro-physical analysis, post-stack inversion. To achieve the main above mention objective following methodology is applied:

- The first step is seismic interpretation in which seismic base map is generated and two horizon (E-sand and B-sand) are picked on seismic section. Time contours are maps are generated to identify structure.
- Second step is to perform petro-physical analysis.
- Third step is to find geo-mechanical properties which are used to estimate rock mechanical model (RMM).
- Fourth step is spatial distribution of GMP which are estimated by using seismic inversion.

CHAPTER-02



CHAPTER 02
PHYSICAL GEOLOGY AND
TECTONIC FRAMEWORK

CHAPTER-02

2. PHYSICAL GEOLOGICAL AND TECTONIC FRAMEWORK

2.1 INTRODUCTION

Exploration of hydrocarbons is a difficult task in the subsurface without significant knowledge of the tectonic setting of the basin. Therefore an integrated approach has been adopted comprising of geological and geophysical knowledge to explore the sedimentary basin for petroleum prospective that consists of facies modeling, sedimentology, sequence stratigraphy, basin modeling, and petro-physics. This integrated knowledge develops a better understanding of the petroleum system of a basin. These are necessary elements for Hydrocarbon exploration (Nwaezeapu et. al., 2018).

The sequence stratigraphy is the most modern tool that is applied worldwide to explore stratigraphic traps in sedimentary basins to discover hydrocarbon reservoirs (Dutton & Barton, 2003). The tectonic setting and depositional history of the basin are studied through various techniques, i.e. paleogeography, paleoenvironment, and basin configuration. Due to a lack of knowledge about the sequence stratigraphic framework of the Lower Indus Basin various stratigraphic traps in the early Cretaceous Lower Goru Formation remain intact and could not be explored (Ahmad et al., 2004).

The study area that is the Kadanwari oil field is located in the Middle Indus Basin. Geographically it lies in the district Khairpur of Province Sindh. Geologically the Kadanwari Field is a sandwich between Kirthar fold belt and Chaman fault in the west, Indian shield with different Highs e.g. Jaisalmer High and Aravalli in the east, Indus trough and Indus offshore in the south, and Mari-kandkot high in the north (Nasir et al., 2011) as display in figure 2.1.

2.2 TECTONIC SETTING AND STRUCTURE GEOLOGY OF INDUS BASIN

Pakistan has a very distinctive geological environment because of its location at the intersection of two large domains. The Indo-Pak Continental Plate, which makes up the southern region, is part of the Gondwanan domain, whereas the Karakoram Block, which makes up the northern region, is part of the Tethyan domain and has complex assemblages and crustal structures.

Indus basin is a broad and important region for petroleum exploration. It is divided into three sub-basins (Kazmi and Jan, 1997) that are listed below.

- Upper Indus basin
- Lower Indus basin
- Middle Indus basin

2.3 TECTONICS SETTING OF MIDDLE INDUS BASIN

Sargodha High in the east and Sukkar Rift in the west geologically define the boundaries of the Middle Indus Basin. Suleiman Fold and thrust belt in the west, as well as Indian Shield rocks. During cretaceous times rifting of the Indian Plate towards the north in Thythes Ocean resulted in normal. The development of numerous horst and graben structures in this basin is due to rifting. Geological investigations of this area show various hotspots due to the rising of magma from the asthenosphere in Paleozoic also affected the stratigraphy of the area (Shah, 1997).

The following tectonic conditions make up the majority of the Central Indus Basin:

- Punjab platform.
- Sulaiman depression.
- Sulaiman fold belt.

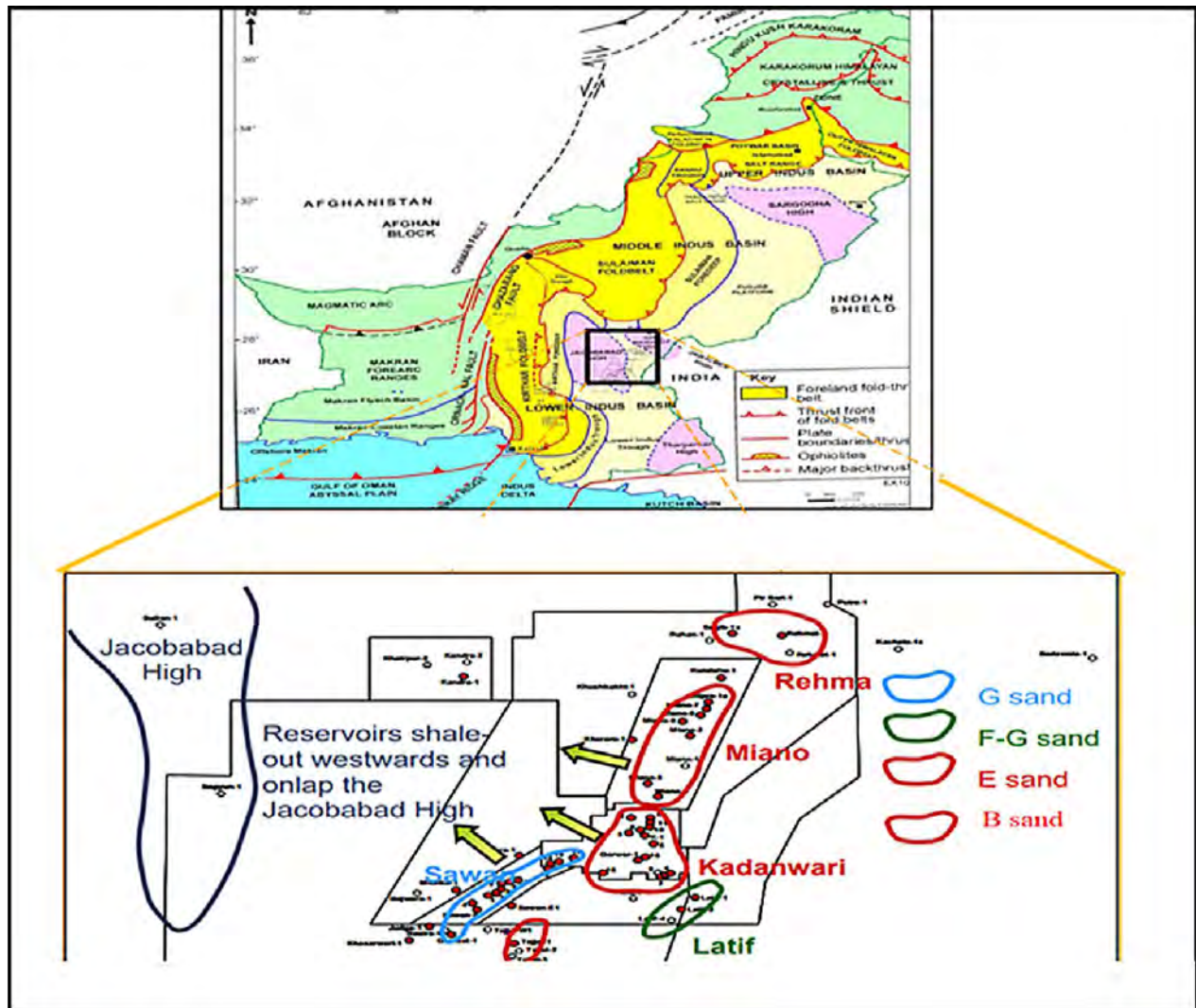


Figure 2.1: Regional tectonic map and location of Kadanwari gas field, source; (Ahmad et al., 2011).

The Kadanwari Gas Field lies in the north of Province Sindh which is about 350 km NE of Karachi (Fig. 2.1). Three major tectonic events configured the structural evolution of the Lower Indus Basin, i.e. Uplifting and erosion in late cretaceous, wrench faulting in late Paleocene, and uplifting of Jacobabad High in late tertiary to early quaternary (Abbasi et al., 2016).

The tectonic development of the Indian Plate is related to two main events, Rifting of Gondwanaland in the Mesozoic era and the Indian and Eurasian Plate collision in the Tertiary age. These two main events play a vital role in the development of Petroleum Play in this region.

The stratigraphic units in the middle Indus Basin exhibit depositional history of the Indus basin that goes back to Pre-Cambrian times. Throughout the basin evolution, depositional processes were affected

enormously by tectonic. The main source of sediments that controlled sedimentation were Indian Shield rocks (Shah, 1997).

2.3 STRATIGRAPHY OF MIDDLE INDUS BASIN

The tectonic history of the Middle Indus basin evolves over time in several periods. An significant tectonic event occurred when the Indian plate started to migrate and separate from Madagascar during the late Jurassic to early Cretaceous geological time. (Kazmi and Jan, 1997). According to Ahmed and Choudhary 2015, The source rock are organic-rich shales of Sembar Formation (lower creataceous). The sand of Lower Goru formation lie above Sembar shale. Due to rifting , a marine basin was formed in between both land Masses and large-scale sinistral movement happen along Transform Fault which was the Early Cretaceous period. In fact in this period record that this separation in the area by Normal Faults. The Boundary between the Cretaceous and Tertiary period is highlighted as an unconformity of the K-T boundary which is due to erosion. Influx of sediments during a tertiary time created a dome-shaped structure just above the unconformity between the early Paleocene Ranikot Formation and the late Paleocene Dunghan Limestone (Kadri, 1995). In Late Paleocene tear faults with larger throw and masking wrench faulting having NNW– SSE orientation cut through sembar. These wrench faults are a significant “flower”-type cross-section on seismic data. The third phase of the event is in the Late Tertiary to present Holocene result in uplifting of Jacobabad-Khairpur & Mari-Kanddhkot highs of NW-SE orientation and also responsible for structural and stratigraphic traps in the central Indus basin.

In Late Paleocene tear faults with larger throw and masking wrench faulting having NNW– SSE orientation cut through sembar formation in Kadanwari area. These wrench faults are significant “flower”-type cross-sections on seismic data and dominantly separated the structure into several compartments of faults.

The Jacobabad-Khairpur High's Late Tertiary to Maghalayan inversion, a tectonic event, had a significant impact on the Kadanwari region during the third phase. This event is s major reason behind the structural elevation of depositional strata of the distal part in Lower Goru than the proximal part & also enables stratigraphic and structural traps in highs. Late Cretaceous age strata are truncated Tertiary unconformity but NNE–SSW orientated faults are rarely founded above base Tertiary unconformity, and several hundred meters of strata are missing and estimated to erode (Ahmad et al., 2002).

These strike-slip faults are near to vertical trend and found even in chiltan formation. Due to complex pattern and trans-tensional regime display negative flower structure. The sinistral displacement of small-scale lateral movement is responsible for negative flower fault in the en-echelon pattern. Stemming from fact, overall this stresses counter the tectonic framework and structure configuration in the area in Late Tertiary. In collectively sands of the Lower Goru were deposited in an environment of shoreline to estuarine submitted to both long tidal influence and shore currents. These two processes influenced the sand supply and class of sands. Lower Goru formation has a package of sand shale layers. These sands are major reservoirs having different reservoir characterization even within few kilometers (Ahmad et al., 2011).

2.4 DEPOSITIONAL FACIES AND SEQUENCE STRATIGRAPHY OF THE STUDY AREA

The pictorial summary of sequence stratigraphy of study area is given in figure 2.2, which formations of various lithology and ages with their associated Groups.

Different reservoir sands of the Lower Goru formation have been formed by only a few depositional facies. The Lower Goru sequence in general consists of ten depositional facies types. Out of these ten facies, three facies are found reservoir facies in the Kadanwari area as (1) Upper shoreface tidal channel, upper shoreface barrier bar medium to courser size grains of sands, upper shoreface rips current or ebb delta sands, (2) distributary channel courser grain size sands, mouth bar sands, and (3) transgressive tidal channel having medium-courser grain size sands (Ahmad et al., 2004). E-sand is prograding shore-face deltaic front which were deposited due to distributary channels and mouth bar (Heikal et al., 2011).

Sediments were deposited in E-1 chamositic shale blanket, Gritty Transgressive, E-2 and, E-4 courser grain size shore-face sand, E-3 Transgressive Hot hereolithics, E-5 cleaning upward shore-face sands with fine grains, E-6 lower shoreface shale with thin sands/offshore, and E-5 and E-4 are more productive (Ahmad et al., 2002).

Stratigraphic of study area comprises of pro-gradational wedge shore-face sand body and turbidities lobes overlying on thick basinal sembar shale of pelagic /bathyal referred to the deltaic marine environment. The lower Goru sand comprised deltaic marine sand-shale, sand deposit on stand plain, and basin ward barrier bar shore-face to distal offshore setting on the ramp. In the present era Eastward tilt near to structural highs in the study area provide stratigraphic traps.

In early cretaceous time, sembar formation deltaic silliciclastics and lower Guro formation were on the top of the carbonates of chiltan limestone. Carbonates after chiltan limestone were terminated in late Jurassic time unconformity. As a result, again rifting between the Indian plate and the African plate is linked with tectonic changes and environmental changes.

In late Jurassic time, Kimmeridgian/Oxfordian unconformity and Titho-Nian stage condensed section were established due to the absence of sediments supply. This sembar formation has removed the structural complexity of the area and shows flatten on the seismic section. Thus erosion of the topset toward the east shows Initial part of the wedge was uplift and on the front of the wedge was prograding and down stepping to the west. Sandy parolics of sembar sequence 1 and Lower Goru formation “A” lowstand system tracts were intercalation with Sembar sequence 2 of the shaly slope. As Relative Sea level rise and sediments supply to become equilibrium, prograding in sembar formation of sequence 2 and Lower Goru “A” sequence lowstand wedge get to a maximum limit. Sediments supply remain enough to attain aggregational parasequence set of sandy parolics which were transgressed onto A” sequence. Relative Sea level rise during some part of early Cretaceous and retrogradation of low sediments flux in late Cretaceous time in the basinal margin (Ahmad et al., 2004).

Cretaceous part is present throughout Pakistan, this part was highly tectonically unstable in most the parts. The early Cretaceous Guro formation belongs to Mona jhal Group which were subdivided into four major formations as mention below in ascending order:

- Sember formation
- Goru formation
- Parh limestone
- Mughal kot formation

The Main formations of the area are Lower Goru containing sands, chiltan formation, and Sember formation that is used for Hydrocarbon evaluation. Lower Goru formed during the Cretaceous period and chiltan from Jurassic period, chiltan formation is older than Goru formation (Ibrahim shah, 2009).

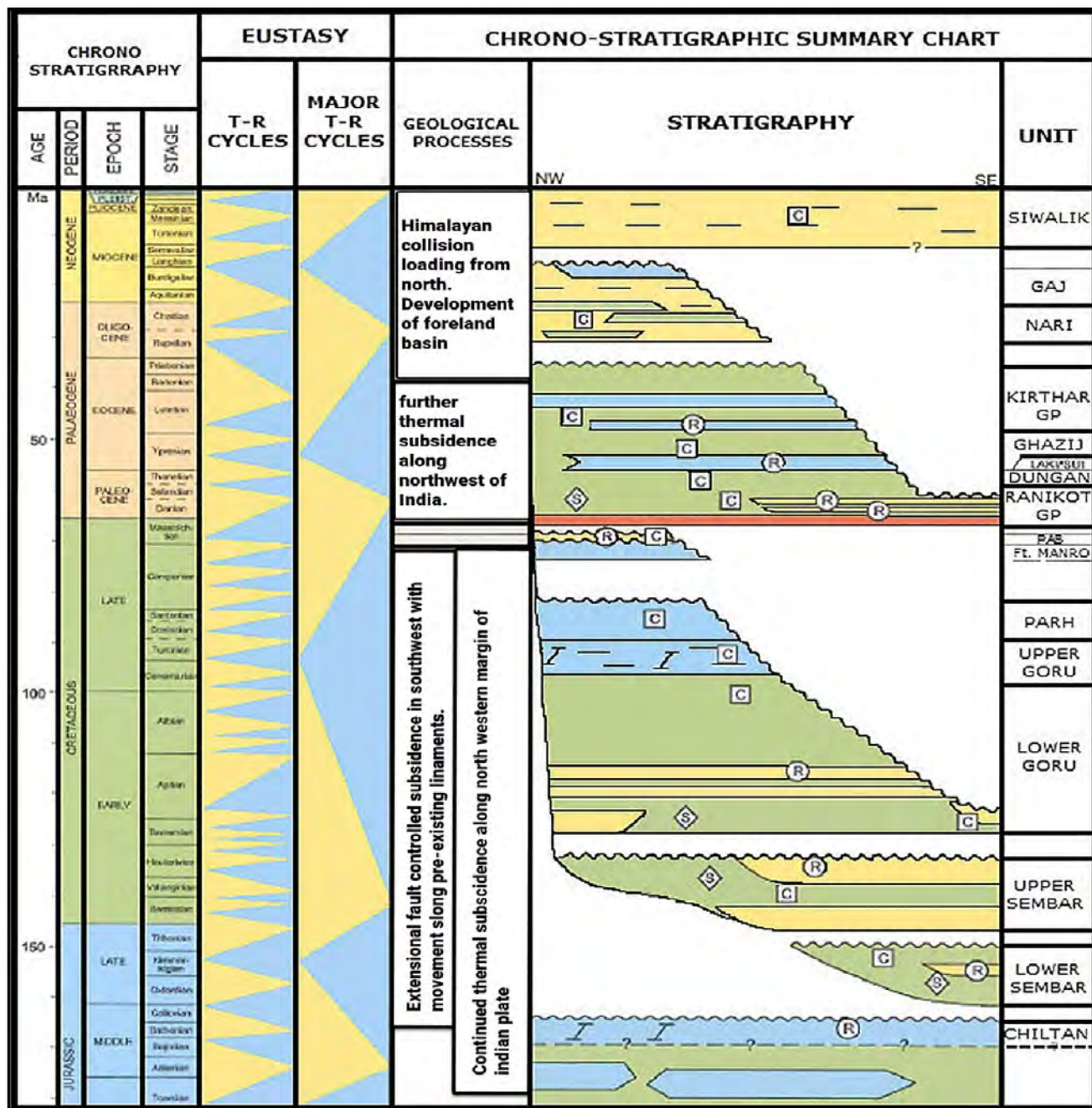


Figure 2.2: Generalized sequence stratigraphy of the middle Indus basin, source: (Khalid et al., 2014)

2.4.1 CHILTAN FORMATION

Rocks of the Jurassic age are present in the middle Indus basin in form of Shirinab, Mazar Dirk, and Chiltan formations. Chiltan formation has middle to late Jurassic age. The lower contact of Chiltan

formation with Shirinab formation is confirmable. It is affected by both Indian-Africa plates rifting, and eustatic sea-level rise in the middle Jurassic age. As a result, the depositional environment of chiltan formation is shallow marine. The lithology has consisted of massive dark Limestone, oolitic, shaly, and reefoid. The color of limestone varies with yellowish-brown, whitish-grey, and off-white. Chiltan formation in some area acts as a reservoir, shale above act as a cape rock and source at deep is much mature (Asim et al., 2014).

2.4.2 SEMBER FORMATION

Sember formation name was given by Williams after Sember passes through Murree hills to included belemnite beds and belemnite shale. These belemnite beds are also included in the Pab limestone and Goru formation. Age of Sember formation is early cretaceous with a deep marine environment. The lower contact of Sember formation is confirmable with the chiltan formation of the Jurassic age. It has silty black shale interbedded siltstone and rusty nodular weathered argillaceous limestone layers and greenish to weathered color Glauconite. Locally shale subordinated with sandstone with phosphatic nodules (Diagenetic facies of shale and limestone, sandstone) and pyritic are present in some basal areas. The thickness is varied, in some sections it may to 133m, and in some areas 262m in Mughal kot. The thickness of formation may decrease to some meters and then absent (Williams, 1959). Its lower contact with Jurassic age has disconfirmable contact with early cretaceous age as Mazar Dirk formations, while the upper contact of Sember formation is generally confirmable with the Goru Formation (Ibrahim shah, 2009).

2.4.3 GORU FORMATION

Goru Formation has been subdivided into two parts upper Goru and Lower Goru, and formation is broadly scattered in Sulaiman and Kirthar range. Both parts have Early Cretaceous age consists of interbeds of shale, limestone, and siltstone. The limestone of Goru formation is very fine in grain size and with fine bedded. Limestone has domination in both parts of Goru formation. Limestone is white, off-white, and light brown, and very soft to moderately hard. In the Lower Goru formation, shale is interbedded in a sandstone bed. The depositional environment of Goru formation is shallow marine, and deltaic deposits are found. Locally thickness is 536m but reduces to 60m in Quetta, and in subsurface average over 100m. The upper contact of the Goru group is confirmable with Parh

formation and the Lower contact of Goru Group is confirmable with Sember formation. The productive reservoir of Lower Goru formation is highly heterogeneous Sands (G, F, E, D, C, B, A) interbedded with shales. Two sands (G-sand and E-sand) are sources in the Lower Goru formation. E-sand act as conventional reservoir and rest of sands classified as the non-conventional reservoir. Sands (G, F, E, D, C, B) is present in Kadanwari-01 well and Kadanwari-03 well, E-sand is producing in most of the wells reservoir depth at 3318 m but F& D sand are in some wells and G-sand are got by hydro fracturing process.

2.5 PETROLEUM SYSTEM OF CENTRAL INDUS BASIN

The Potential of reservoir rock is found out by the combined studies and comprehensive knowledge of source rock, migration, reservoir rock, and source rock. According to extensive literature knowledge studies area comprises cap-rock (shale of Goru formation), reservoir rock (lower Goru formation), source rock (sembar formation), and traps (Kadari.,1995).

The oldest strata of sembar formation of the cretaceous period are organic-rich shale in the Kadanwari area(Kadari.,1995). The main source of Lower Goru sand is the Indian shield to SE. So depositional trend is presumed to NS, that's why more wells are distributed in NS of Kadanwari area. E-sand is productive in reservoir till 3340m depth.

2.5.1 SOURCE ROCK

In the early cretaceous period, the Indian plate had to move toward the north with the influx of detrital sediments comes with the Indian shield. Middle Indus basin has extensional regime during lower to mid cretaceous age as linked with seawater circulation at NW margin of the Indian plate and middle to the upper period of the cretaceous time associated with clastic deposits. Sembar formation was deposit during marine environment average thickness of 0 to 260 meters. By critically analyze by geochemistry study shale of sembar formation is a more beneficial potential source rock for oil and gas production of cretaceous throughout Indus foreland. Sembar contains mainly shales having a small amount of intercalation with sandstone and siltstone. The quality of source rock is thermal maturity, total organic-rich, and gas-prone kerogen. The early cretaceous period was favorable for organic life because of sea-level rise, basin preserves organic material, and time with effective temperature turn organic material into hydrocarbon. Furthermore, a geochemical study shows large-scale hydrocarbons produce from lower cretaceous shale of sembar formation. In addition, Sembar formation contains an average TOC

content of 1.4%, Type III Kerogen, and vitrinite reflectance values ranging from 0.6% to 1.6%, depending on the stage of thermal development. These show that Indus Basin on the western side has more thermally maturity than the eastern side of the Indus basin due to deep buried. The thermal maturity of Sembar Shale is greater in the westward and less in the eastward(Wandrey et al., 2004).

2.5.2 RESERVOIR ROCK

Between the Jacobabad-Khairpur high and the Mari-Kandhkot high, the Central Indus Basin is a potential hydrocarbon zone. Several gas fields have been discovered in the Central Indus basin, Kadanwari gas field was by Eni Pakistan is producing field. Reservoir sands were charged by organic-rich Sembar shale and shale with lower Goru formation.

Thermal activity for hydrocarbon generation was started in Paleocene - Oligocene period. The hydrocarbons generation phase was associated with late cretaceous to early Tertiary and the most significant part of HC formed in Eocene. The most potential reservoir in the study area is the cretaceous sandstones, Paleocene Ranikot formation sandstones, and late Eocene Sui limestone. However, liquid HC generation of late Cretaceous may be trapped in a westward dipping detached stratigraphic wedge (Ahmad et al., 2004).

The migration was started and entraps during Eocene –Miocene, and structural traps developed in the upper Cretaceous-Tertiary. Furthermore, cretaceous sandstone having Goru sands and Peb sandstone. In the central Indus basin package of sands of the lower Guro formation act as a reservoir. Gas reserve in Kadanwari field is more than others field of the area may be due to up-dip hydrocarbons migration as this area lie on Jacobabad-Khairpur high (Jadoon et al., 2019). The depositional environment of the reservoir is a delta and shallow marine sandstone. The principal reservoir sandstone has porosity values of 30 percent and permeability vary up to 1 to > 2000mK (Wandrey et al., 2004).

Lower Goru formation containing a full package of six sands packages which are E, B, C, F, G and D sand. B-G and E-sand is a presumed reservoir rock. The most producing reservoir sand of area are D-sand, E-sand, F-sand, and G-sand. The gas production begun from E and D sands. In this study work E and B sand are major producing sands in kadanwari-01 well.

2.5.3 SEAL ROCK

The shale in the lower Indus basin behaves as a cap rock, inter-bedded with reservoir sands in lower Goru and overlying on that (Kadri.,1995).The faults provide as a pathway for the migration of hydrocarbons from Sembar shales of the Sembar formation into the Lower Goru reservoir, and they also serve as an impermeable seal for traps (Jadoon et al., 2019).

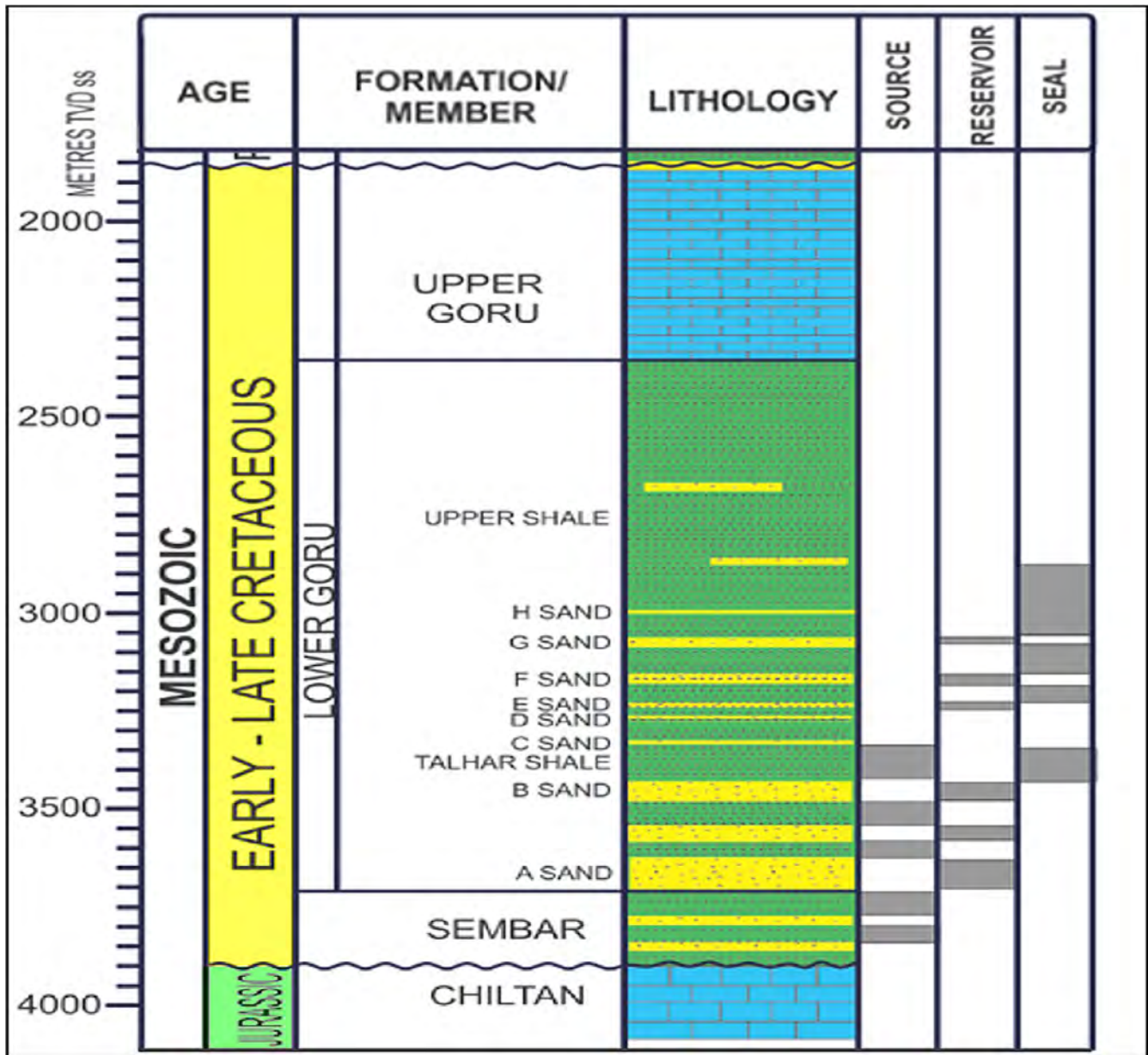
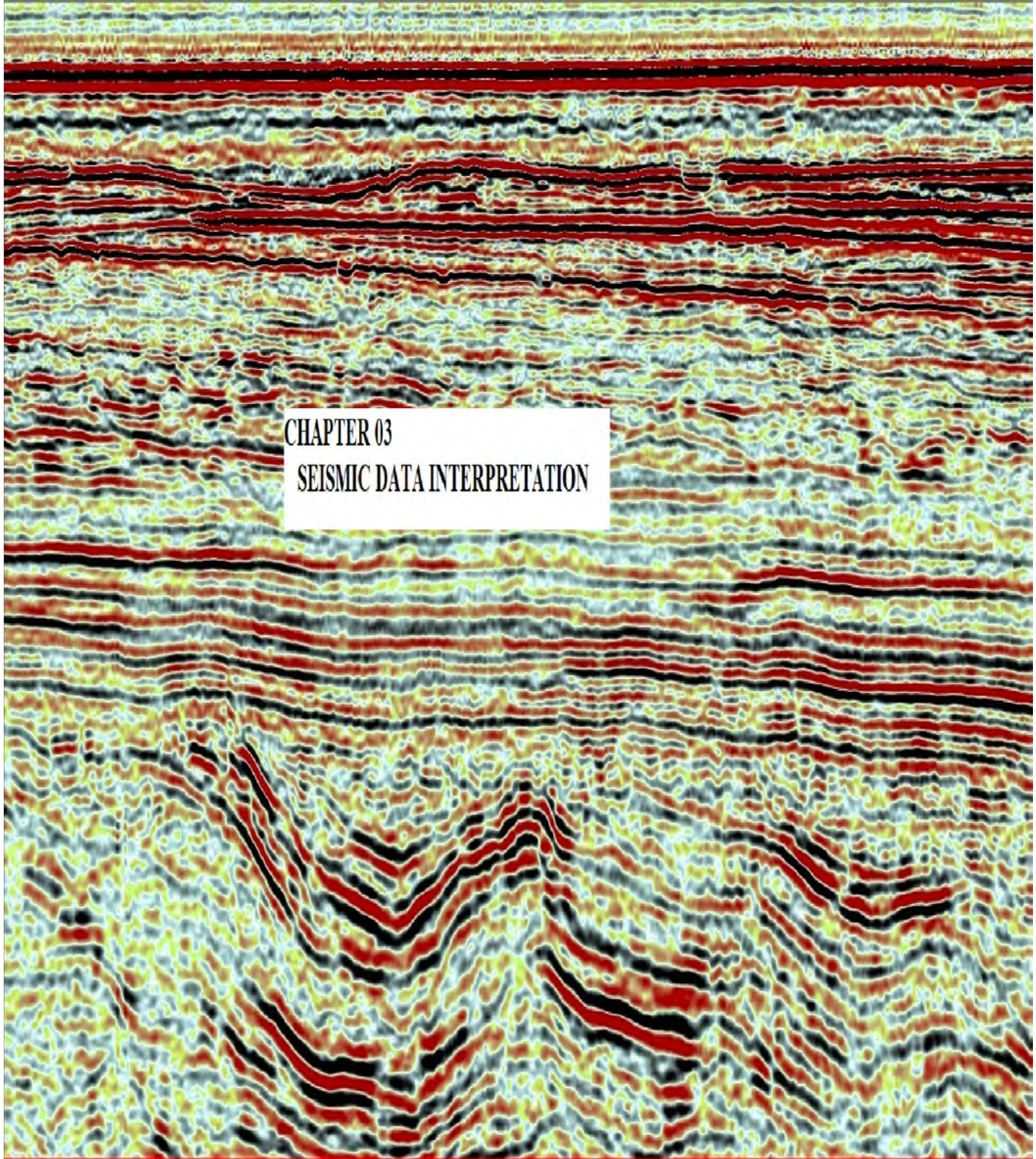


Figure 2.3: Stratigraphy of MIB (Kadanwari wells)[2000-4000meters](Courtesy; Preimer oil Pakistan).

CHAPTER-03



CHAPTER 03
SEISMIC DATA INTERPRETATION

Chapter-03

3. SEISMIC DATA INTERPRETATION

3.1 SEISMIC INTERPRETATION

Three dimensional (3D) seismic interpretation act as a key role seismic exploration regarding subsurface features. In seismic horizons are picked and then transferred to other lines for investigation over whole (3D) cube (Bacon et al.,2007).3D seismic is very commanding tool in seismic delineation of hydrocarbon(Tonnies.,2005;Aurnhammer.,2006).To start Seismic data interpretation, we must have some sort of data; in-line and cross-line (Seismic section), shot points (Base map), Wells, Velocity data (from VSP and check shop), formation tops of the wells for identification of Horizons and Logs data (Saroor, 2010). The seismic interpretation was accomplished by doing different procedures and steps. The main steps are as follow to interpret seismic data are;

1. Cubic Base map of Kadanwari area
2. Generate synthetic seismogram
3. Faults prediction
4. Horizons tracking
5. Fault polygon generation on E-sand and B-sand
6. Time, depth contour map generation

3.2 BASE MAP:

A map that can be used by geoscientists to represent all kinds of data for interpretation. The Base map is prepared with the help of the Geographic Reference System (GRS) latitude & longitude of the given data are loaded into the software .Baser Map gives detail information about inline and cross-line. The preparation of base map is carried out by importing SEG-Y and navigation files of seismic line in Kingdom suite .The well data is in Las format. The well (Kadanwari-01) is loaded and show the location and orientation of the wells on the base map The Figure (3.1) shows base map of Kadanwari area. All three wells and in-lines and cross-lines are posted on map.

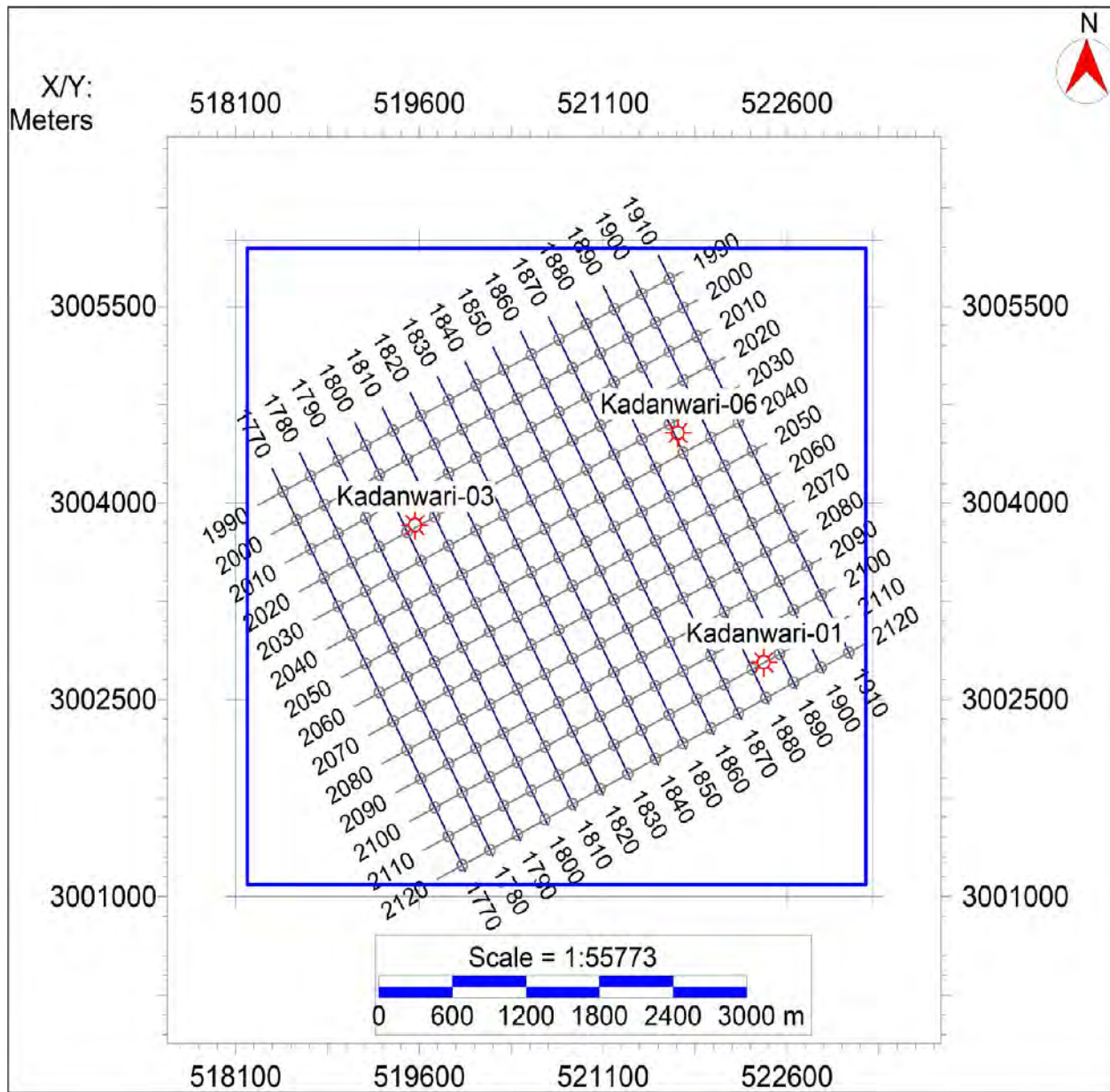


Figure 3.1: Base map representing in-lines and cross-line of Kadanwari area including three wells(Kadanwari-01,Kadanwari-03, Kadanwari-06).

3.2 METHODOLOGY:

The seismic interpretation procedure started with synthetic seismogram in which we tie seismic data with synthetic seismogram and correlated with well tops(Bacon et al.,20017) .The velocity is generated from sonic , density is obtained from density log and there product results in acoustic impedance. The impedance is convolved with extracted wavelet to get synthetic trace. The trace is match with original

trace. Seismic events are tied with tops with the help of synthetic seismogram. Best seismic to well tie depend on quality of well data, seismic data, wavelet and processing quality (Lines & Alam, 2013).

Two horizons are picked on 3D seismic cube (E-sand and B-sand) at each 5 line interval. Two faults are marked on seismic section and then fault polygons are marked. The grids are generated after fault and horizon picking. The last step is generation of time and depth contours \maps. The gridding and contouring are last steps used to examine lateral variation of structure are present in area.

3.4 SEISMIC HORIZONS TRACKING:

Horizons picking is a major task in seismic data interpretation. The formation tops help to mark horizons on the seismic section. After synthetic seismogram is a tie with seismic section, two seismic horizons have been picked on inline 2110 using well tops of Kadanwari-01. The name of marked horizons is E-sand and B-sand of Lower Goru. Some in-lines are interpreted by using Kingdom software as shown in figure 3.1. Based on available data of Kadanwari, total 27 inlines are interpreted for structure marking at the interval of 5. To understand the structure of the Kadanwari area on well K-01 on Inline 2110 is displayed in figure 3.1. It is observed that horizons are dipping toward the west side and on shallow depth toward the east side. Some faults are observed on all inline sections e.g. F1 and F2, which are the major faults.

3.5 DEMARCATION OF E & B SAND AND FAULT MARKING:

Faults prediction and marking on seismic section is possible with enough literature knowledge about the geology of study area and faults correlation. Fault correlation defines dip direction, an extension of fault on different formations, and heave and throw of faults. The structure of the study area is associated with a wrench or Negative flower structure. As faults in the Kadanwari area are strike-slip faults in NW-SE orientation and linear vertically extent to lower Cretaceous and Jurassic Chiltan formation. Interpretation of structure on seismic section suggests the significant movement of faults along with Cretaceous age and Tertiary age result in left-lateral strike-slip faults. Some faults are observed on all sections e.g. F1 and F2, which are the major faults that are extended to late Cretaceous & Chiltan formation. Some fault splays of this master fault terminate against major faults but splay faults are not accessed in my seismic cube. And fault splays are observed only till lower Goru formation and majorly pass through the reservoir.

Fault polygons show the sub-surface discontinuities by displacing the contours. By inspecting the available seismic data, it is crucial to identify the faults and determine their lateral extent in order to construct fault polygons. Fault polygons are constructed by interpretation of faults and the faults are correlated with each other. It represents faults trend on inline and cross line sections. The polygons can be constructed in two ways: Manual and auto-generated. Manual fault polygon is generated by adding nodes and the digitization of faults on the map. It shows lateral Extension of fault trend by manually joining similar faults on the map. Auto-Generate fault polygons are generated by the software. Figures 3.2 and 3.3 show the polygons of the E-sand and B-sand of the lower Goru. At B-SAND and E-SAND levels, two faults polygons are generated.

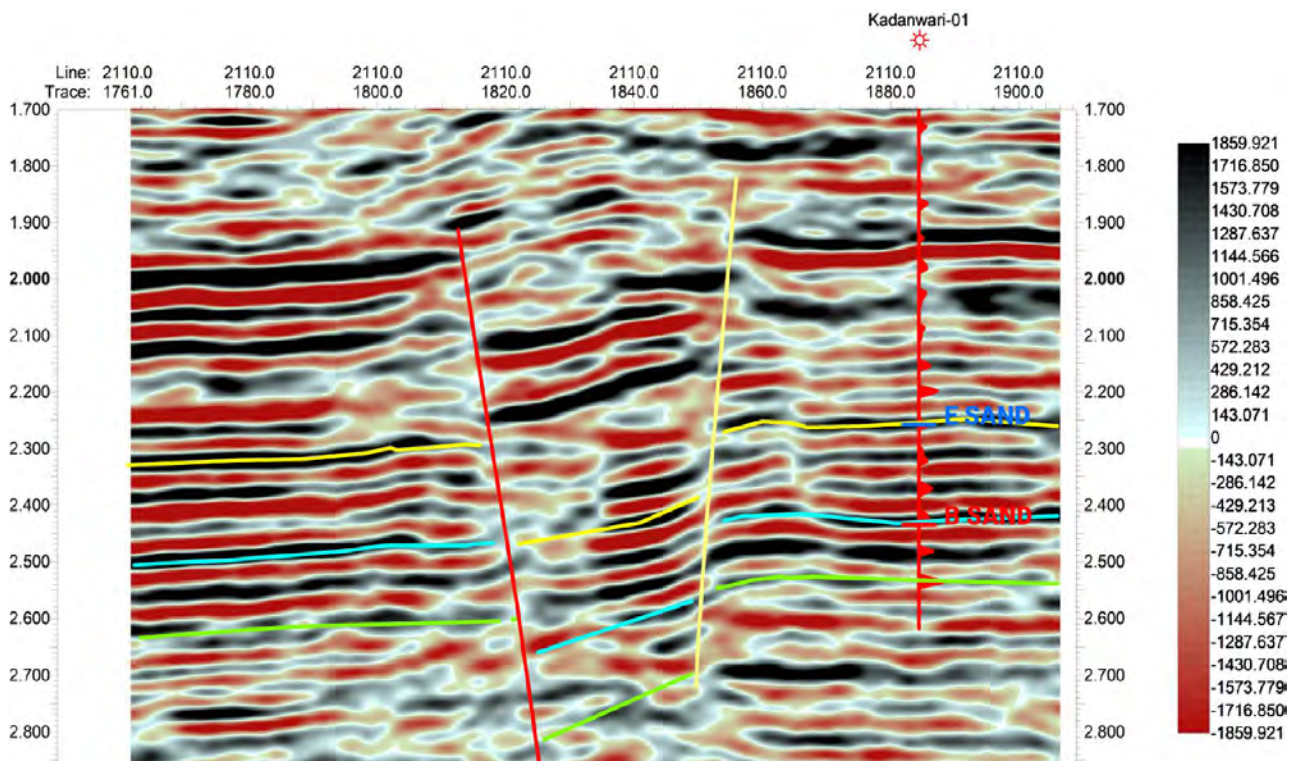


Figure 3.2: Interpreted the seismic section on Inline 2110

3.6 CONSTRUCTION OF CONTOUR MAPS

Contour maps generation is the final step of seismic data interpretation. First, generate a grid on horizons by using a contour tool for contour maps construction. The last step in interpretation is creating time and depth contours maps of the subsurface from the arrival time of the seismic wave. Contour maps show the real picture of earth 3D to the 2D earth surface. These contour maps show the dip of faults, folding, and the difference in the terrain by contour lines. For depth contour map construction, time-depth relation help to convert time section to depth section by using mathematical tool $S = V * T/2$. To convert the time to depth section we need a 1D velocity function.

3.6.1 TIME CONTOUR MAPS OF E-SAND AND B-SAND

Time contours maps are generated after picking horizons and faults. Faults polygons are formed to separate contours along fault. The time contour map of E-sand & B-sand ranges from (2.231- 2.470 & 2.395 – 2.667)sec. Units of time contour are second or sec. On the time contour map, it is shown that the fault trap bound the structure, and hydrocarbons are accumulated.. The Contour interval is 0.04s. The time contours maps of E-sand & B-sand are displayed in Figure (3.2 & 3.3). The color bar depicts the area's elevation. Red to green colors indicates the shallowest area, and blue colors indicate the deepest part. The depth contours are not generated because velocity cube data at different common depth points are not available.

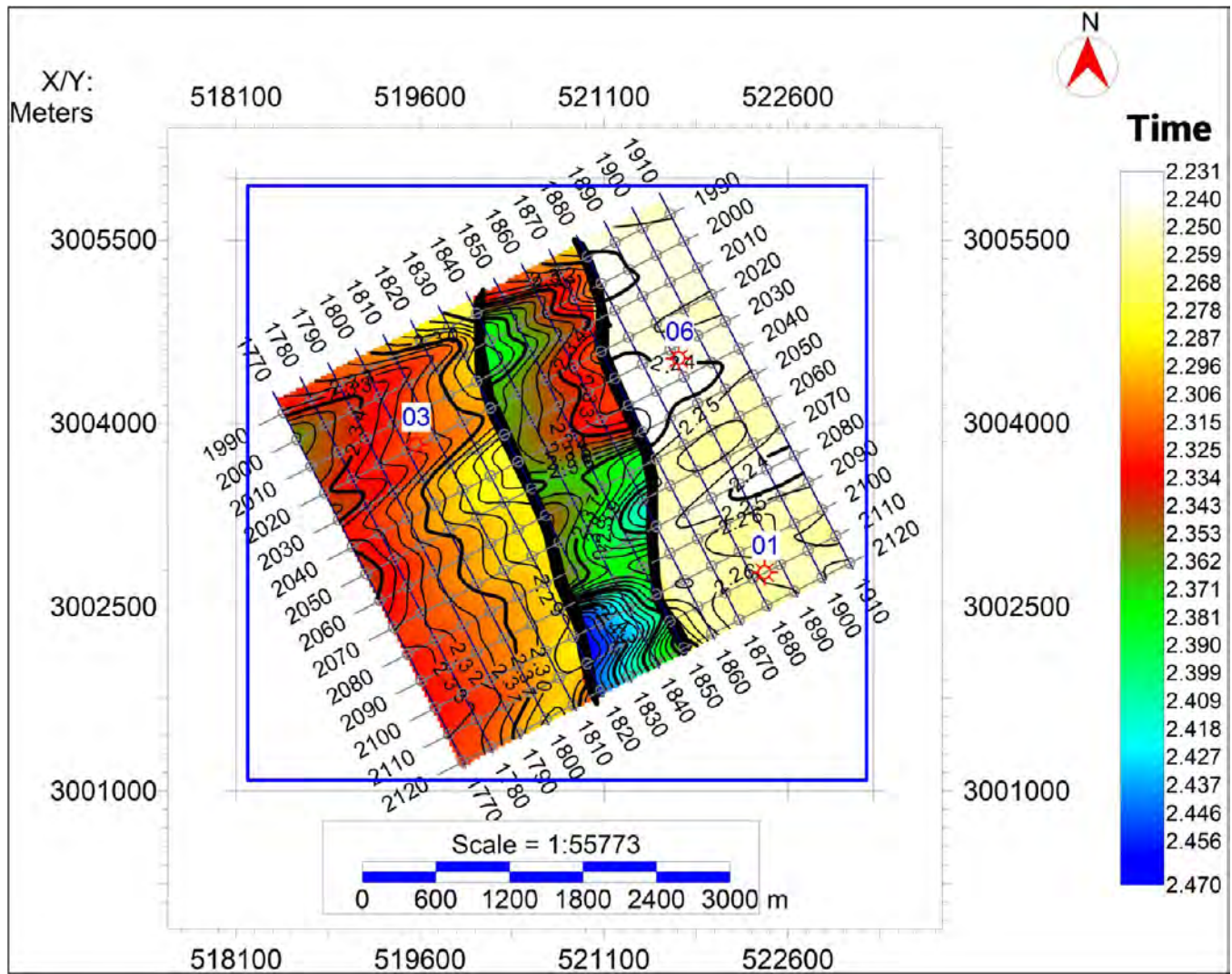


Figure 3.2: Map of E-sand showing time contours. Yellow, White & Red indicates shallow part while Blue and Green shows deeper part (C.I = 0.01sec)

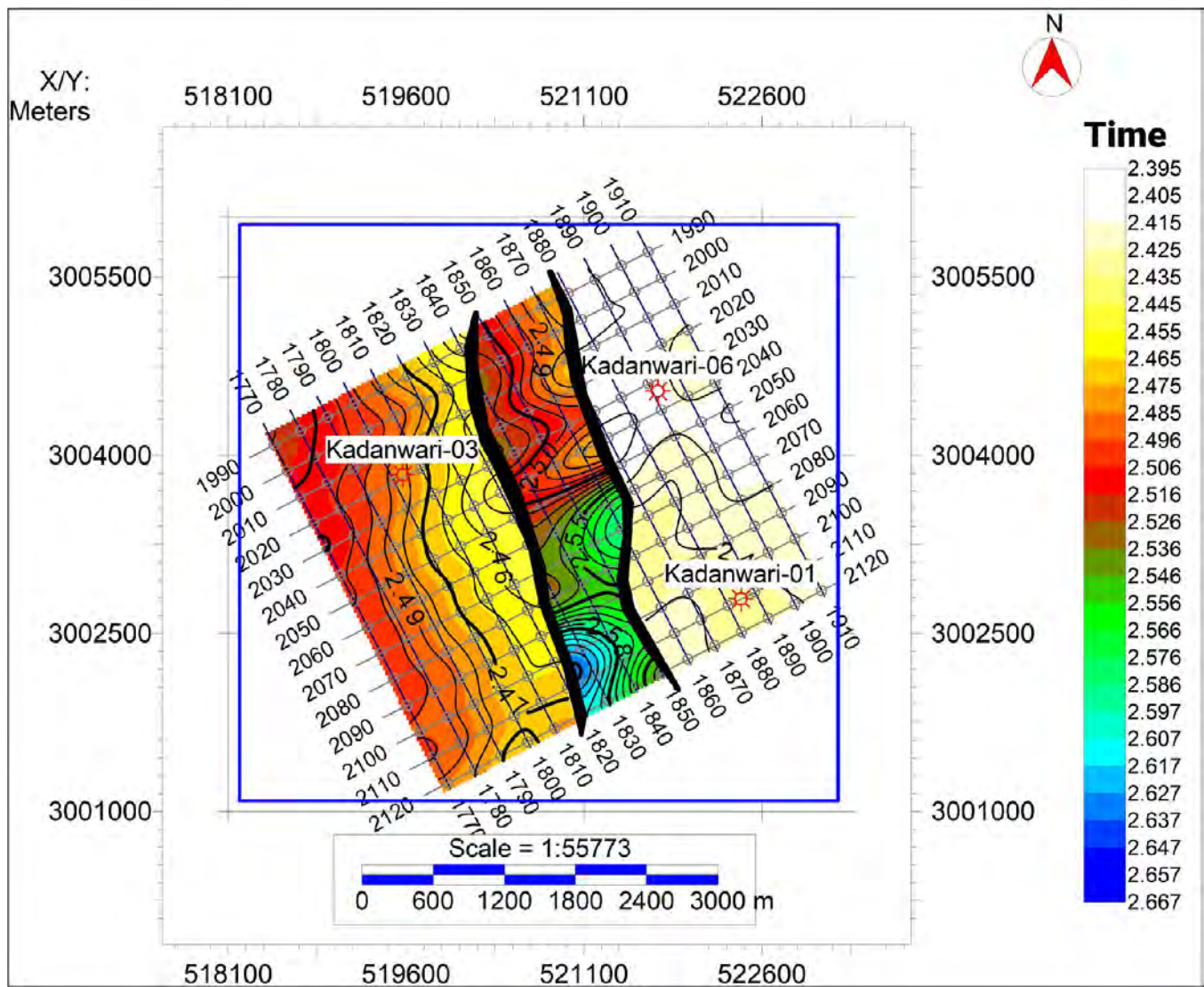
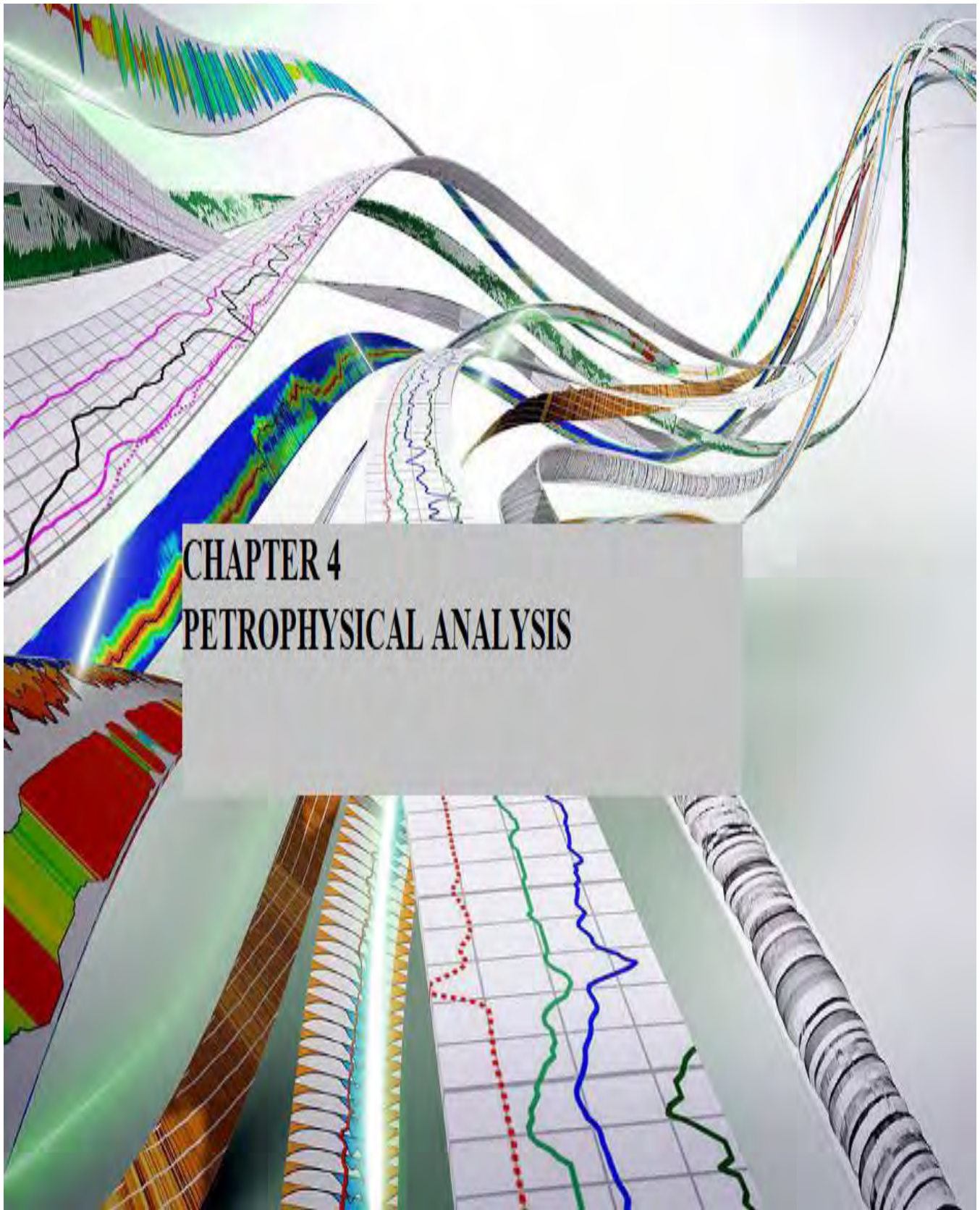


Figure 3.3: Map of B-sand showing time contours. Yellow, White & Red indicates shallow part while Blue and Green shows deeper part (C.I = 0.01sec)

CHAPTER-04



CHAPTER 4
PETROPHYSICAL ANALYSIS

4. PETROPHYSICAL AND GEO-MECHANICAL PROPERTIES

4.1 INTRODUCTION

Petro-physical analysis gives a deep insight of fluid and its identification and quantification in reservoir (Ali et al., 2014). The physical; property of rock and fluid is done by petro-physical analysis (Asquith et al., 2002). Petro-physical analysis study of physical and chemical properties change relation with fluid interaction in rocks. Petro-physics need core data, production data and well logs data to determine porosity, volume of shale, water saturation. This analysis help for the prediction of the productive zone in the area (Ali et al., 2015). when we integrate petro-physical results with rock physics we identify the potential prospect and non-prospect zone which help geoscientist. (Daniel., 2003).

GMP's measured both dynamically and statically. In static measurement the core specimen is required and exposed to increment stress until fracturing occur in order to find GMP's in laboratory. The dynamic geo-mechanical properties are computed by using p-wave velocities from well log and seismic (Al-Shayea, (2004); Hongzhi; (2005); Chan et al., 2006).

Sine 1950 scientist used sonic and density logs to calculate dynamic mechanical properties for reservoir study which include young's modulus, bulk modulus, shear's modulus, unconfined compressive strength, friction angle, overburden stress, pore pressure, minimum and maximum stress. These values are convert to static value to estimate reservoir mechanical properties (Najibi et al., 2015; Archer & Rasouli., 2012).

All above mentioned geo-mechanical properties are calculated to estimate RMM. Firstly we perform Petro-physics then RMM is estimated to understand rock strength, failure and deformation.

4.2 GEOPHYSICAL WELL LOGS TRACKS

Well Log curves used for the identification of a potential zone can be classified into three tracks: Lithology track, resistivity track, and porosity track.

4.2.1 LITHOLOGY LOGS:

Three logs include in track 1 (Lithology track).

- Caliper log (CALI)
- Gamma-ray log (GR)
- Spontaneous log(SP)

4.2.1.1 CALIPER LOGS (CALI)

Caliper logs are commonly used to determine the diameter, size, and shape of the borehole with depth. Caliper log is an important indicator of breakouts and cavity washouts. We use this log to check QC for other logs. If caliper logs have not been properly run then resistivity and porosity log do not give correct results. Caliper log gives a greater response for shale and lesser for sandstone.

4.2.1.2 SHALE VOLUME (VSH)

Natural radioactivity of formation is determined by using gamma-ray logs. Gamma-ray logs usually measure high-energy radioactive radiation from the formation. It is powerful tools to identify lithologies. Gamma ray values for sand stone and carbonates rocks are very low and high for shale because of organic content(Asquith and Gibson.,2004).Formation having a radioactive substance that releases gamma-ray in form of electromagnetic energy. When emitted gamma-ray strikes with the electron of formation, energy is transferred. This emitted gamma-ray detect on the detector of gamma-ray. Gamma-ray logs especially use for the differentiation of sandstone and shale. All emission of radioactivity in the subsurface is due to potassium, uranium, and thorium elements (Archie, G.E., 1942).

Lithology identification is an important tool for reservoir characterization. The major application of gamma-ray logs is the determination of reservoir thickness, lithology identifications, the correlation between different wells, and the prediction of the volume of shale The range of gamma-ray API values is 0 to 150. Sandstone is defined as having gamma-ray levels below 75 API, and shale is defined as having gamma-ray values between 75 and 150 API. This is because sandstone has fewer radioactive elements than shale, that's why it is an important tool for reservoir identification. Vsh is determine by formula (Asquith and Gibson.,2004) given below.

$$V_{sh} = \frac{GR_{Log} - GR_{min}}{GR_{max} - GR_{min}}, \quad (4.1)$$

where GR_{Log} show gamma-ray log values, GR_{min} means the minimum value of GR log and GR_{max} means the maximum value of GR log.

4.2.1.3 SPONTANEOUS LOG (SP)

Spontaneous potential (SP) is used to differentiate potential between surface rock and borehole. SP log term as self-potential log and natural potential difference. Along with the determination of reservoir thickness, depositional environment, and water resistivity in the formation, SP log also uses for the identification of permeability. Shale baseline deflect on reservoir interval with depth. This deflection changes with depth. SP curve deflection will not occur in the reversed permeable zone. This is a piece of important information for the identification of the thickness of the reservoir. SP negative abnormal deflection will occur on the permeable zone and help to find permeability of the reservoir. SP log is used to differentiate the salinity of mud filtrate and formation water in sandstone and shale. SP deflection will be negative when the salinity of formation water is higher than mud filtrate and vice versa.

4.2.2 RESISTIVITY LOGS TRACK:

The typical application of the resistivity log is the resistivity of hydrocarbon saturation determination in the reservoir and permeability of rocks. Several logs tools are used to determine the resistivity of water in rock pores. These resistivity logs are classified into two divisions (based on conditions) such as induction logs and electrical resistivity logs. Induction logs are further divided into lateral logs. These induction logs are

- Lateral Log Deep (LLD),
- Lateral Log Shallow (LLS)
- Micro spherically Focused Log (MSLF)

Lateral log Deep (LLD) has deep penetration in the un invaded zone and LLD is used for the investigation of saline water. Lateral log Shallow has less penetration than LLD and usually use for mud cake medium resistivity. Micro-spherically focused log is used to measure resistivity in the undistributed zone and flushed zone. Which can be used to measure the Residual Hydrocarbon Saturation (RHS) close to the borehole. MSFL is a good indicator of the relative movement of hydrocarbons. In the water-bearing zone mud filtrate fully flushed the invaded zone. The ratio method is used for the calculation of resistivity of formation water (R_w).

$$\frac{R_w}{R_t} = \frac{R_{mf}}{R_x}, \quad (4.2)$$

Where R_w is formation water resistivity, R_{mf} denotes the mud filtrate resistivity, R_x denotes the invaded zone resistivity, R_t is true resistivity.

4.2.3 POROSITY LOGS TRACK:

Porosity logs are used to calculate the volume of space available in rocks. Porosity determination is a key parameter for reservoir characterization. Porosity describes space available for hydrocarbons or water accumulation. The porosity of formation is determined by using density logs such as sonic, density and Neutron log.

A combination of logs is used to measure the porosity of the reservoir. These logs depend on lithology, fluid types in pores, drilling environment, and pore's geometry in addition to porosity.

4.2.3.1 SONIC LOG

The sonic log is helped in the calculation of the transient time of high frequency of impulse with Formation depth. The sonic log (DT) is also term as acoustic log or porosity log. The instruments used for the sonic log are the transmitter which is the source for acoustic signal and the receiver which are helpful in measurements of acoustic pulse arrival time at the receiver. The acoustic impulse travels both in attenuation and dispersion of signal through rocks. The time needed for P-wave to arrive at a certain distance across 1 ft of formation depth is called interval transient time. The reciprocal of transient time is called the acoustic velocity of the wave.

Applications of the sonic log:

- ✓ Depth conversion (T-D chart formation)
- ✓ Lithology indicator
- ✓ Porosity calculation

The transient time of sound waves depends upon the geometrical shape of pores cementation of rock, and matrix. The Wyllie time average formulation is mostly used for measurements of porosity from the sonic log.

$$\phi_{sl} = \frac{\Delta t_{sl} - \Delta t_{ma}}{\Delta t_f - \Delta t_{ma}}, \quad (4.3)$$

where

ϕ_{sl} is the porosity calculation from the sonic log

Δt_{sl} Formation's interval transit time measured by the sonic log

Δt_{ma} Rock's matrix interval transit time examine in the laboratory

Δt_f Interval transit time saturating fluid in pores of rocks are examined in the laboratory Sandstone has high velocity (low acoustic transient time) than shale with the same porosity values. Application of sonic log is increase with the combination of other logs;

- The porosity of formation determination by using acoustic transient Time
- Mechanical properties of the formation such as the size of grains with Density log.
- Synthetic seismograms generation by using sonic log with Density log.
- Lithology indicator with Neutron log and Density log.

The hydrocarbons present in reservoir rocks of formation are found by sonic log porosity and need some more correction. These corrections result in Gas prons sonic porosity values are 0.7φsl and in oil are 0.9φsl.

4.2.3.2 DENSITY LOG (RHOB)

The density log is useful for the prediction of bulk density. It may be computed by multiplying the fluid density by its relative volume and matrix density by its relative volume.(Tittman and Wahal, 1965).

The radioactive source in the density tool emits gamma-ray radiation in the formation. These rays travel through the formations and lose energy and scattered more. The detector fixed in density tool is used to count the rate of gamma rays emits. The gamma-ray count rate is related to bulk density.

$$\phi D = \frac{\rho_{ma} - \rho_b}{\rho_{ma} - \rho_f} - Vsh \frac{\rho_{ma} - \rho_b}{\rho_{ma} - \rho_f}, \quad (4.4)$$

where ρ_{ma} rock matrix density, ρ_b is bulk density, ρ_f is density of the fluid in rocks, and Vsh is the volume of shale.

4.2.3.3 NEUTRON LOG

Neutron logs (NPHI) are available for measurements of the hydrogen content in the formation rocks. Hydrogen content mainly constitutes in water and hydrocarbon and water present in the pores of rock is a good indication for porosity. Neutron logs are used for the direct calculation of porosity. Typically application of neutron log is porosity measurements, lithology indicator and give a response on gas effects. In the clean shale-free formation, only oil and water-filled in the formation can measure by using Neutron logs. When there is more gas in the pores of rocks than liquid fill, the density of the neutron log will be decreased due to the less hydrogen content in the gas. As in shale,

hydrogen is present OH series and clay contains water in the matrix of shale. This is the main limitation in the neutron log due to gas effects.

4.2.4 AVERAGE POROSITY

As the name mention, the mean porosity produced by summing several logs and dividing it by the total number of logs used to calculate porosity is known as average porosity. The method is given below which is useful for estimation of the Average porosity of the zone of interest

$$\phi_{avg} = \frac{\phi_n + \phi_d + \phi_s}{3}, \quad (4.5)$$

Where ϕ_{avg} is average porosity, ϕ_d is density porosity, ϕ_s is sonic porosity.

4.2.5 EFFECTIVE POROSITY

Effective porosity is considered as the porosity of formation rocks which is useful for the contribution of liquid flow through rocks pores. It is ratio between the volume of interconnected void space of porous rocks and the bulk volume of rock without shale impacts in that rocks. The effective porosity values decrease to zero, where shale is highly concentrated in the zone. Effective porosity is a supreme tool for the estimation of hydrocarbon saturation and water saturation. The effective porosity is envisaged for the determination of suitable reservoir rocks (Asquith & Gibson, 2004).

4.2.6 RESISTIVITY WATER (RW)

The Formation water resistivity (Rw) is mandatory for the assessment of water saturation (Sw). Rw is directly dependent on the temperature of formation and salinity. Different techniques i.e SP method ,resistivity cross plot method ,picket plot and apparent Rw method are used for calculating Formation's resistivity.

4.2.7 WATER SATURATION (SW):

Water saturation (Sw) is an important tool in estimating hydrocarbon reservoirs and analyzing Oil initial in place (OIIP) and Gas initial in place (GIIP) for the oil and gas industry. The late cretaceous Lower Goru reservoir contains variable amount of clay mineral.

Water saturation is defined as percentage of water in pore volume of rock also known as formation water. Two model to calculate saturation of water are given below.

- Archie's model
- Indonesian model

Here the mathematical model of (Archie's formula was used to calculate S_w . Archie formula is used for clean and shale-free sand reservoirs. While Indonesian formula is used for both reservoirs of clean and shaly sand.

Archie's model works on the base of resistive material in the formation is saltwater. In petrophysical interpretation, Archie's formula for determination of water saturation (S_w) is given below.

$$S_w = \sqrt[n]{\frac{F \times R_w}{R_t}}, \quad (4.6)$$

$$F = \frac{a}{\phi^m},$$

Where F is Formation factor. Where S_w represent Water saturation, R_w Formation water resistivity, ϕ is effective porosity, R_t is formation true resistivity, a is Tortuosity factor, m is the Cementation factor having value 2, and n is the Saturation exponent. In this study we calculate water saturation by Indonesian model.

Hydrocarbon Saturation is the derived from water saturation formula. In petrophysical interpretation, the hydrocarbon saturation is calculated by subtraction of S_w from 100.

$$S_{hc} = (100 - S_w)\%$$

4.2.8 RESULT OF PETROPHYSICAL ANALYSIS.

Petro-physical analysis of both E-sand and B-sand shows that value of GR log is low which is indication of sand. There is also a significant separation between LLD and LLS so their is resistivity contrast. Their are crossover between Neutron and Density logs which are indication of hydrocarbon. The porosity is good up to 11% which is good for clastic rocks. Effective porosity is a significant indicator for reservoir assessment. The high values of effective porosity are the function of a good reservoir. Hydrocarbon zone is easy to identify with the incorporation of maximum resistivity log and porosity log values, permeability high, and low water saturation values (40% for E-sand & 25% for B-sand), and less Vsh (33% for E-sand , 35% for B-sand). The saturation of water is low in E-sand and B-sand which is clear identification of hydrocarbon accumulation in economical quantity. . The collapse of borehole reflection in caliper log curves is shown as irregular effects an indicator of washout which increases wellbore diameter. Due to this irregular effect, the values of other logs are also affected. Effective porosity is a significant indicator for reservoir assessment. The

petro-physical analysis of lower goru E-sand (3318-3339) and B-sand (3505-3797) are shown in figure (4.1) and (4.2). Table (4.1) shows the estimated values of reservoir parameters for the E-sand & B-sand.

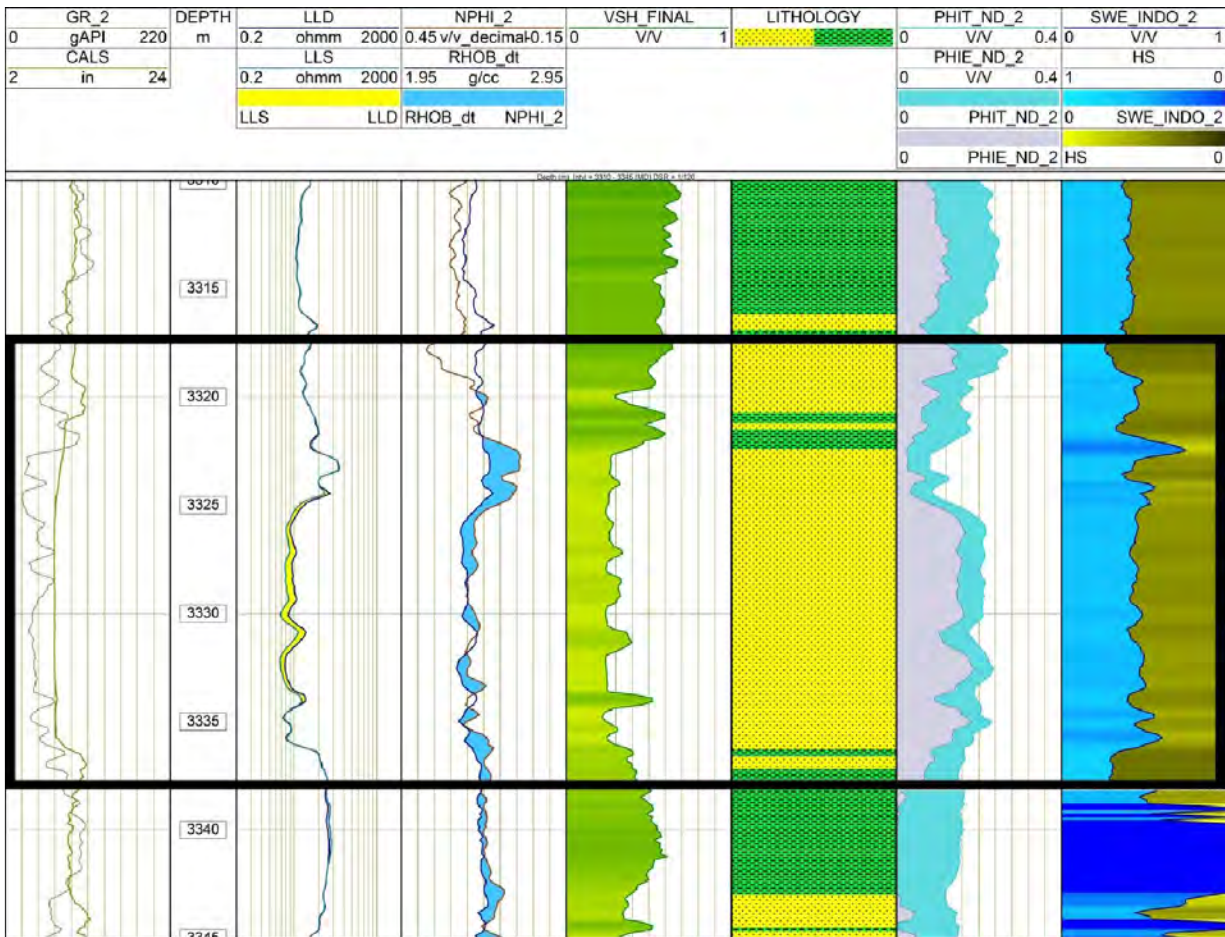


Figure 4.1: Petrophysical assessment Kadanwari-01 well at E-sand. Lithology is shown in track(1). Resistivity in Track (2). Porosity in track(3). track. Volume of shale, effective porosity and water saturation are shown in remaining tracks

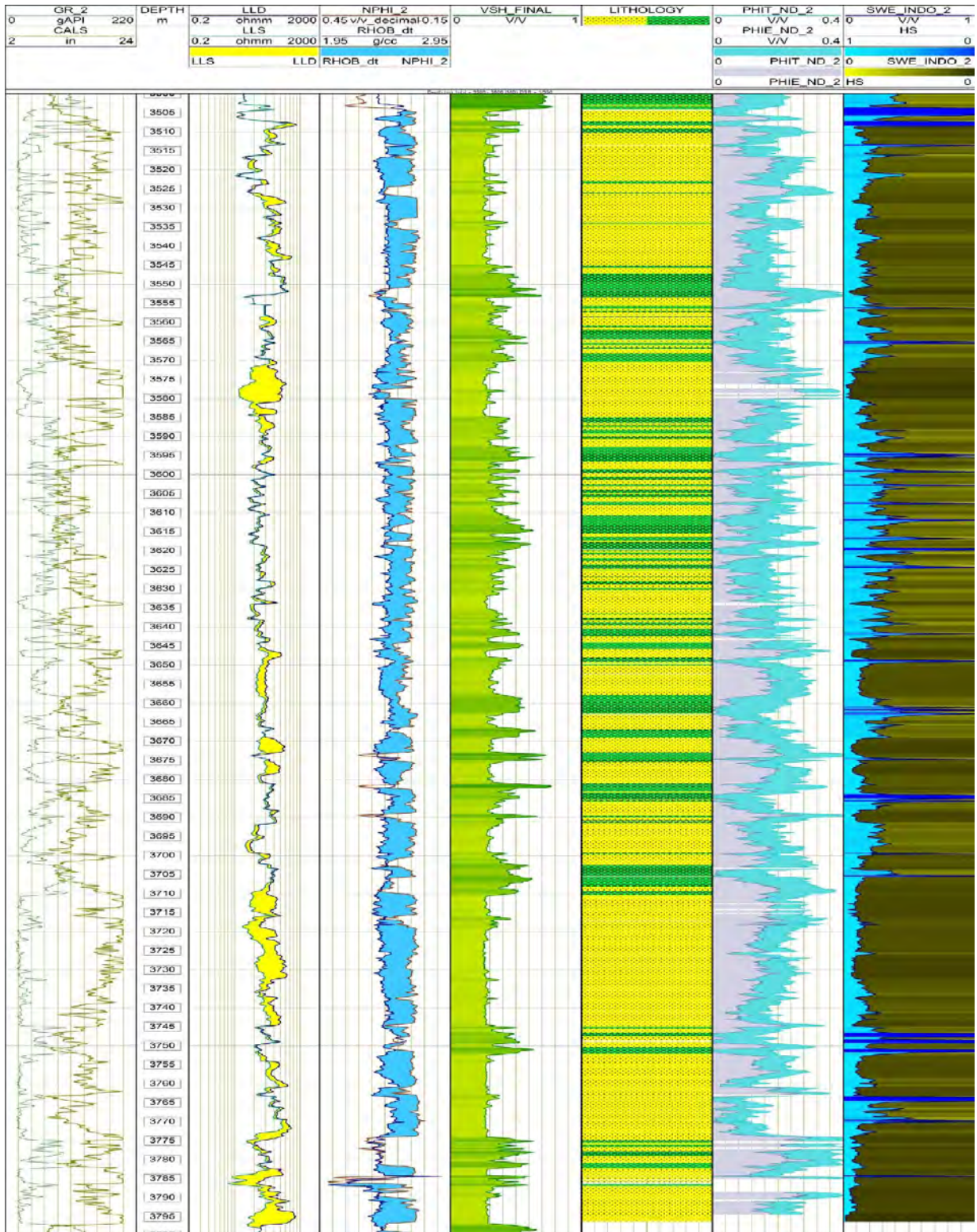


Figure (4.2.1): Petrophysical assessment Kadanwari-01 well at B-sand. Lithology is shown in track(1). Resistivity in Track (2). Porosity in track(3). track. Volume of shale, effective porosity and water saturation are shown in remaining tracks

GR_2	DEPTH	LLD	NPHI_2	VSH_FINAL	LITHOLOGY	PHIT_ND_2	SWE_INDO_2
0	gAPI 220	0.2 ohmm 2000	0.45 v/v_decimal 0.15	0	V/V	1	
6	CAL_1	LLS	RHOB_dt				
	in 12	0.2 ohmm 2000	1.95 g/cc 2.95				
		LLS	LLD RHOB_dt NPHI_2				
						PHIT_ND_2	SWE_INDO_2
						0 V/V 0.4	0 V/V 1
						PHIE_ND_2	HS
						0 V/V 0.4	1
						PHIT_ND_2	SWE_INDO_2
						0	0
						PHIE_ND_2	HS
						0	0

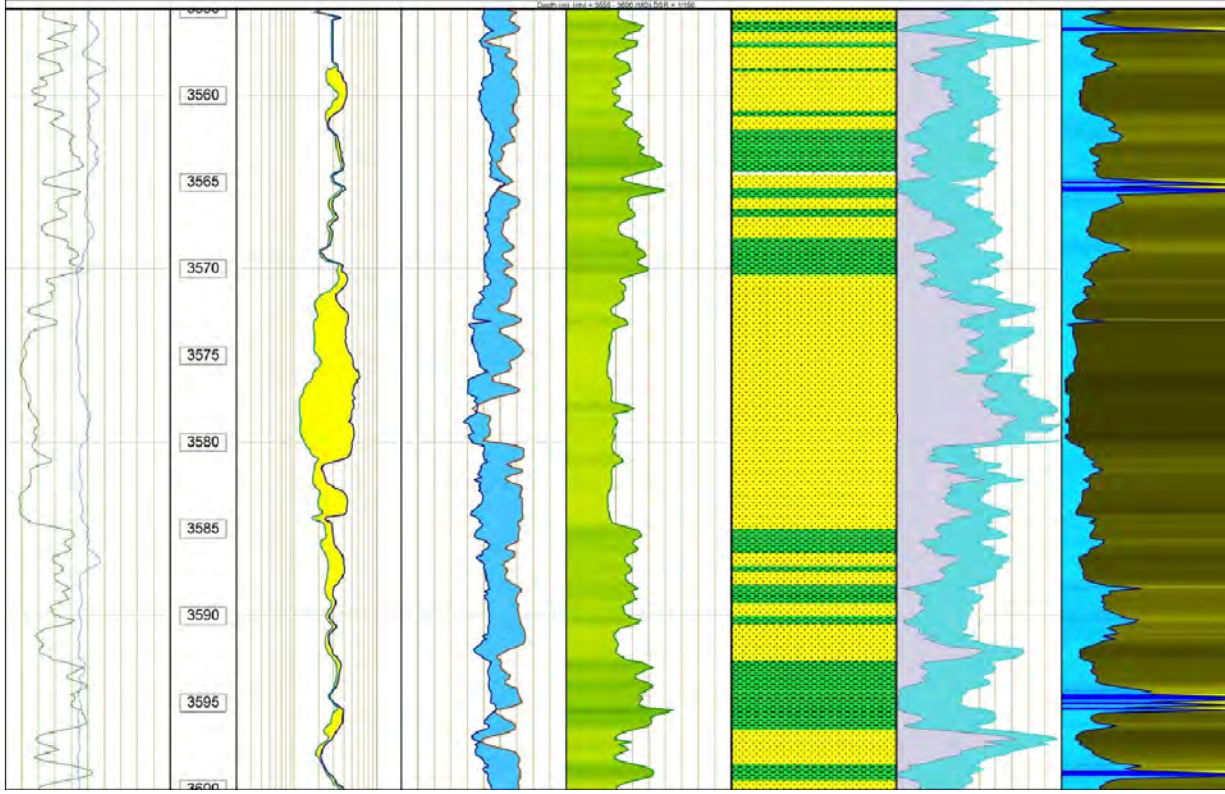


Figure 4.2: Petrophysical assessment Kadanwari-01 well at B-sand. Lithology is shown in track(1). Resistivity in Track (2).Porosity in track(3). track.Volume of shale,effective porosity and water saturation are shown in remaining tracks

Table 4.1: Petrophysical Analysis of Kadanwari-01 well for E-sand & B-sand.

Prospective Zones	Borehole name	Depth meter	Thickness meter	Vsh (%)	PHIE (%)	Sw avg (%)	HCS (%)
PZ-01	Kadanwari-01	3318-3338	20	31-33	9	0.40	60
PZ-02	Kadanwari-01	3505-3797	240	34-38	8	0.25	75

4.3 ESTIMATION OF GEO-MECHANICAL PROPERTIES

Geo-mechanical properties play a important role in minimizing drilling risk and maximizing the well productivity. It is helpful in failure analysis according to hooks law stress is directly proportion to strain .There are three types of deformation depending on force applied and describe by elastic moduli. The moduli are bulk ,shear and young’s moduli. Young’s moduli measure the ability of material to undergo elastic deformation while bulk and shear modulus define strength of material(Archer et al 2012; Eyinla and Oladunjoye.,2014).

The transverse strain to corresponding axial strain ratio on a material stretched along one axis is known as the Poisson's ratio. Poisson's ratio is a crucial mechanical characteristic that can be utilised to predict the geo-mechanical behaviour during well drilling (fjar et al., 2008).the pressure of fluid in pore space define as pore pressure (Zoback., 2007).The one principle stress which is use to gauge fraction propagation and geometry as well as barrier and safe mud zone which is helpful in well stability.

4.3.1 ROCK MECHANICAL MODEL (RMM)

The RMM or MEM is a detailed assessment of the rock strength and elastic characteristics, the status of in situ-stresses, and pore pressure of the reservoir and overburden formations. The key stages that must be followed in order to develop an RMM are listed below.

- Rock physics analysis help us to discriminate different formations like sandstone containing water , shaley sandstone and also give information about hydrocarbon prone sands.
- Estimate rock properties including elastic properties such as Young’s modulus (EM), strength properties mainly the uniaxial compressive strength (UCS), and tensile strength.

- Use the density log and pore pressure from existing techniques, such as sonic or resistivity logs based on the Eaton equation, to estimate the vertical stress.
- From the poro-elastic equation, maximum and minimum horizontal stresses can be determined.

The first step in to determine lithology by rock physics analysis. Cross-plotting of rock properties for fluid and lithology is carried out in kadanwari area using well 01.

4.3.2 DETERMINATION OF LITHOLOGIES BY USING ROCK PHYSICS

Rock physics is important tools which give us link between geophysical and geological parameters which is helpful in reservoir characterization.(Golyan,2012).To perform exploration effectively the characterization of reservoir in term of lithology and pore fluids is important. Sometimes we used unconventional tools in reservoir characterization (Satinder.,1998).The cross plot is used in this particular study.

Cross plots help to identify and detect anomaly and visual representation of more than two variables helpful in detecting anomalies visually to delineate lithology and other fluids present information (Omudu et al 2007). Cross plot analysis is used to discriminate and determine rock properties. Following cross plots are given below.

- V_p/V_s ratio vs. acoustic impedance (AI)
- $\lambda - \rho$ vs. V_p/V_s ratio
- $\lambda - \rho$ vs. $\mu - \rho$

4.3.3 VPVS RATIO VS. ACCOSTIC IMPEDENCE (AI)

This cross plot divides reservoir into different zones. The value of V_p/V_s ratio for gas sand ranges from 1.62 to 1.8 and for brine sand its values are greater than 1.8 and value of P-impedance should be low in presence of hydrocarbon.(Das and Chaterjee,2018).By using these values we can separate shale zone ,brine zone and hydrocarbon zones. In Figure (4.3) & (4.4) the low value of P-impedance and V_p/V_s ratio are shown which satisfy our result and there is clear indication of gas sand.

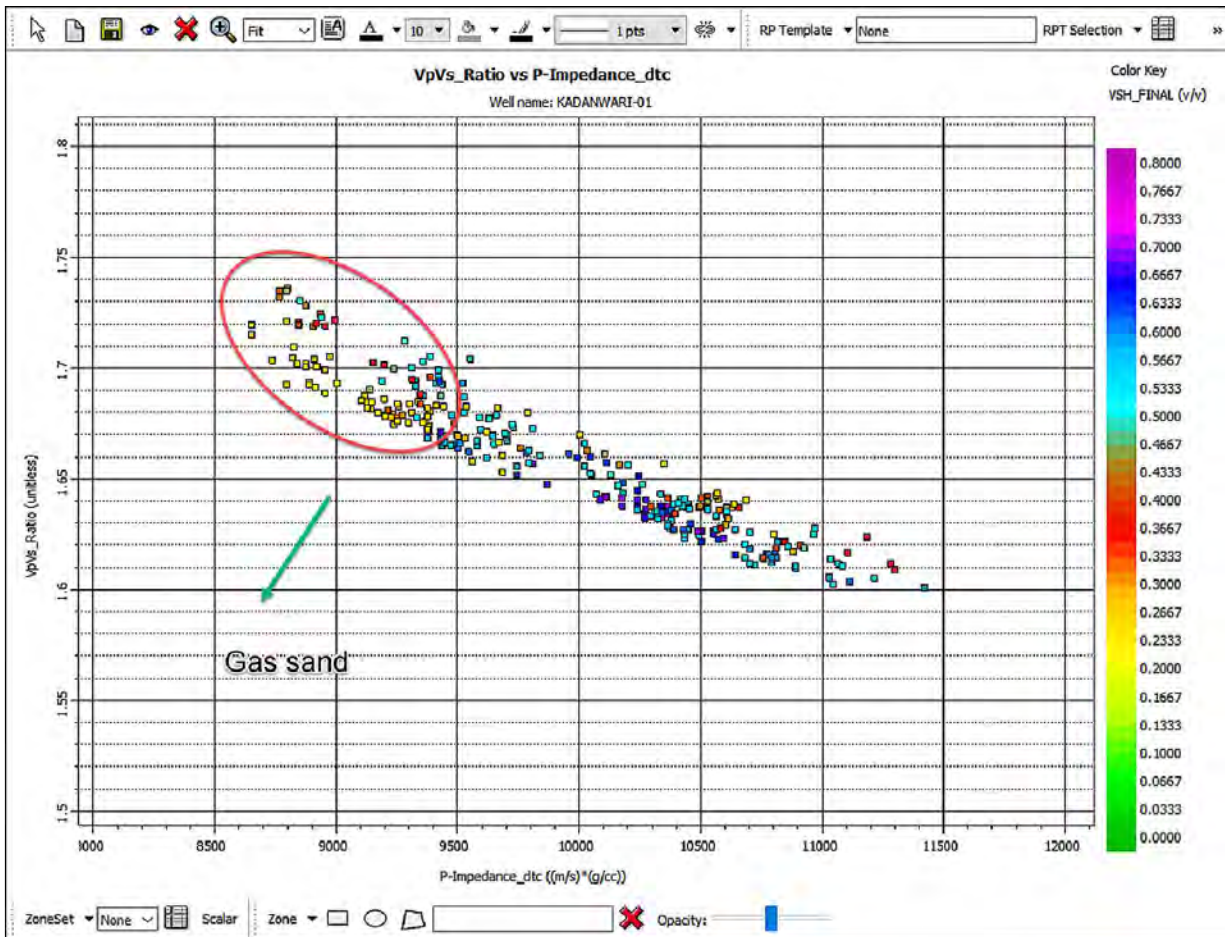


Figure (4.3): Cross plot showing P-impedance and VpVs ratio for well Kadanwari -01. Depth interval for lower guru E & B sand is (3318-3338) & (3505-3797). The red eclipse show the gas sand zone.

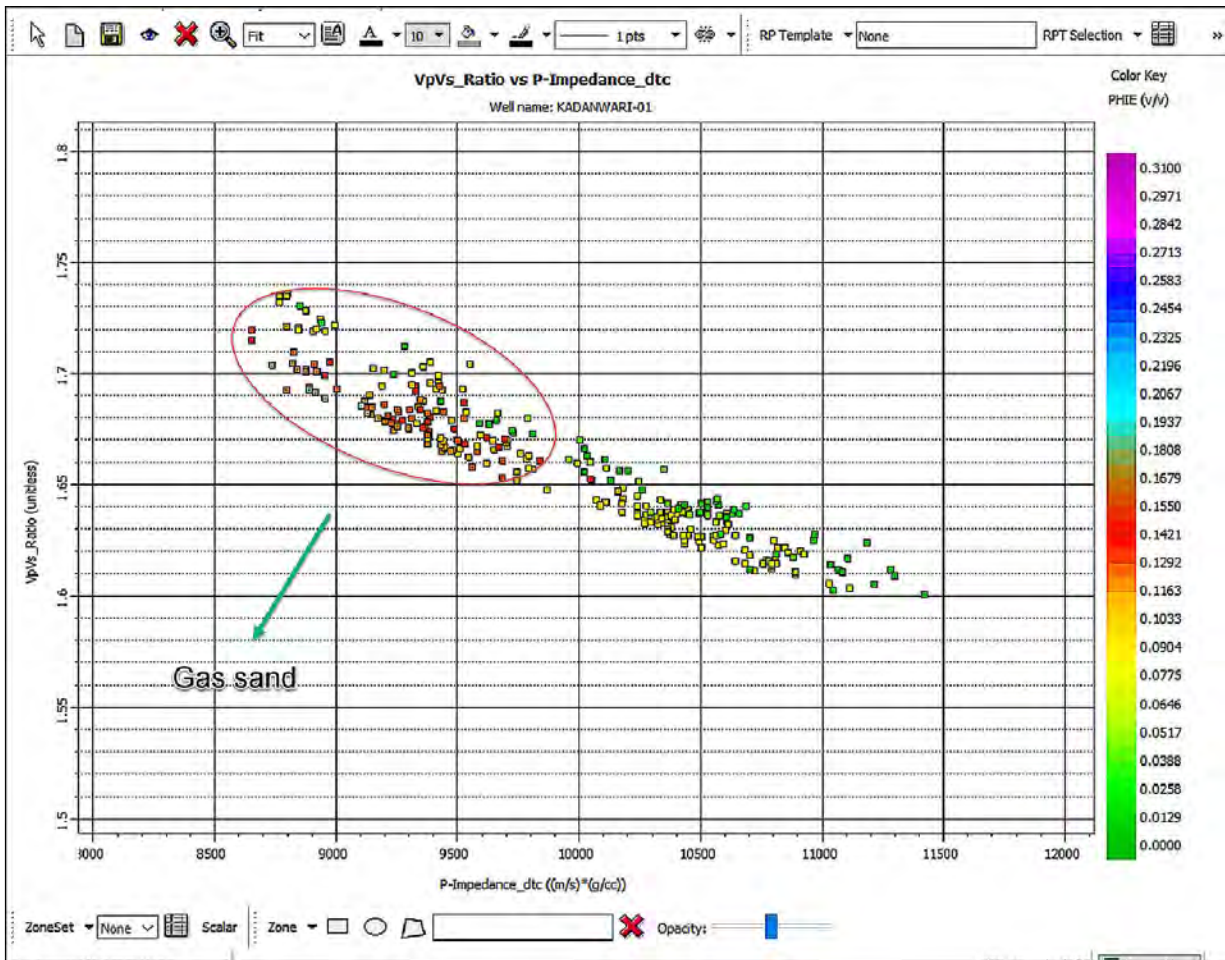


Figure (4.4): Cross plot showing VpVs ratio & P-impedance for well Kadanwari -01. Depth interval for lower guru E & B sand is (3318-3338) & (3505-3797). The red eclipse show the gas sand zone.

4.4.4 LAMBDA –RHO VS. VPVS RATIO

The term lambda is incompressibility and rho is density. The product of lambda and rho is very good in determining lithology. Thus all values of this cross plot are aligned against lambda -rho. The values of lambda -rho for gas sand are approximately closer to 20 GPa & the value of Vp/Vs ratio for gas sand ranges from 1.62 to 1.8. But when we encounter compacted sand their values show relative closer trend. The low lambda-rho and Vp/Vs ratio values for kadanwari's sand are in below figure (4.5 & 4.6).

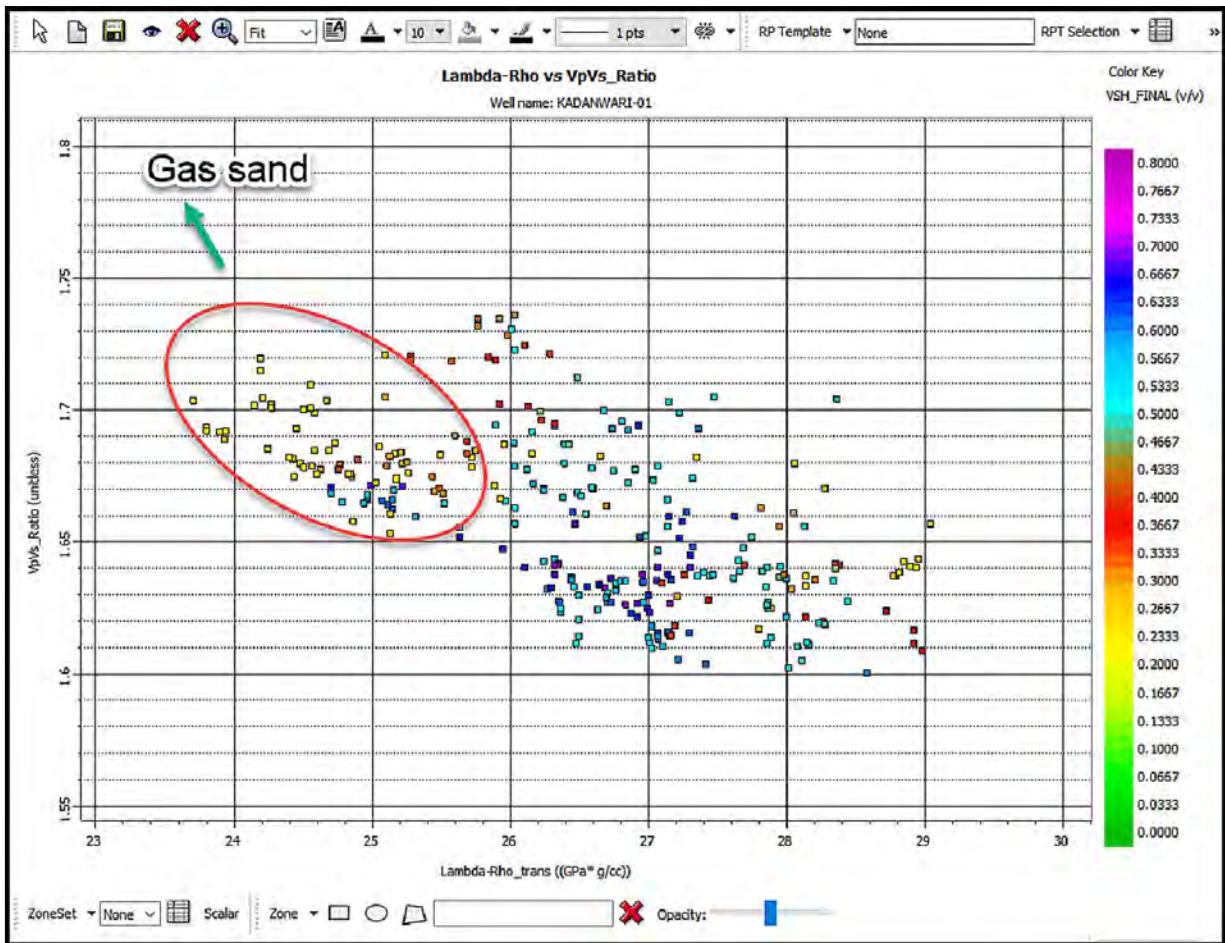


Figure (4.5): Cross plot of lambda-rho and VpVs ratio for well Kadanwari -01. Depth interval for lower guru E & B sand is (3318-3338) & (3505-3797). The red eclipse show the gas prone sand .

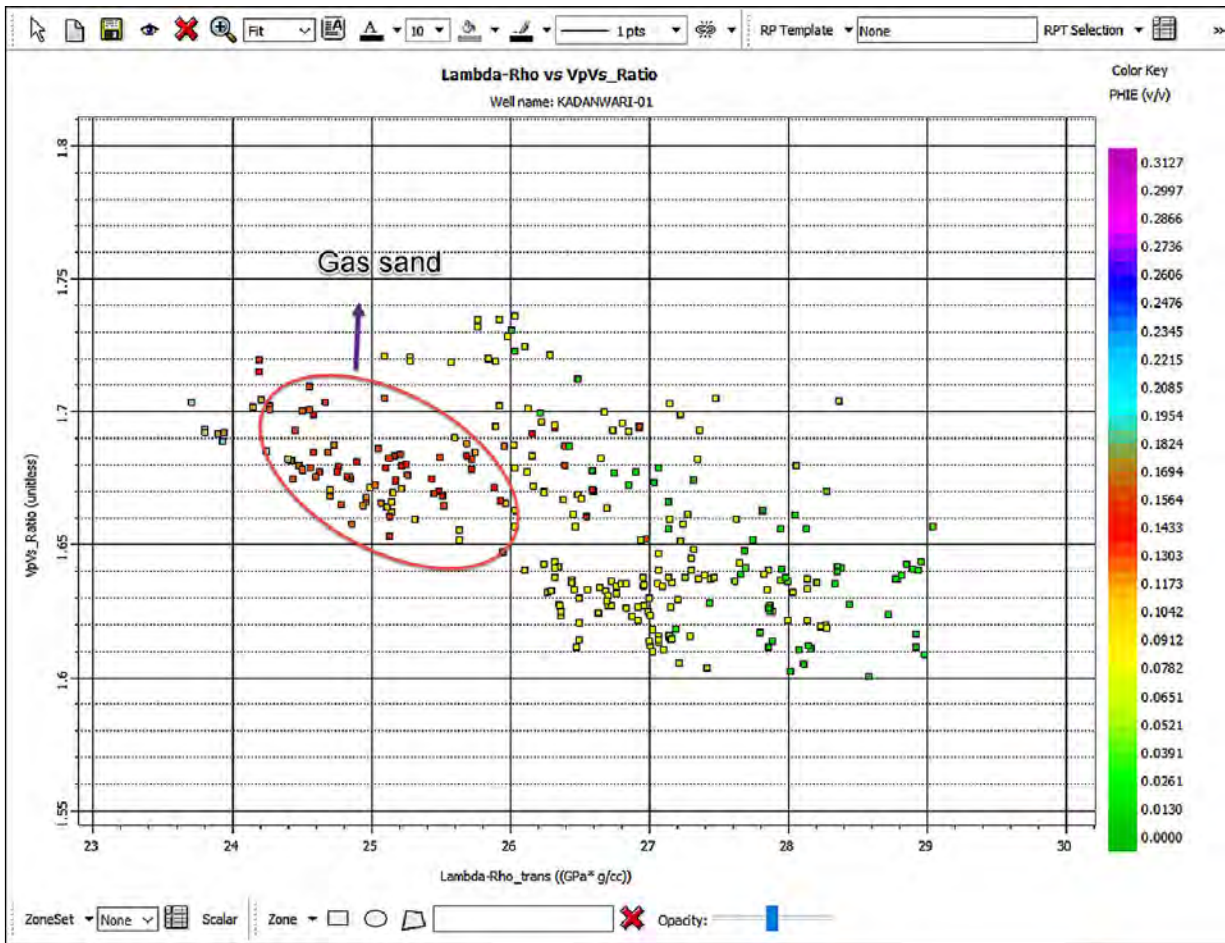


Figure (4.6;):Cross plot of lambda-rho and VpVs ratio for well Kadanwari -01.Depth interval for lower guru E & B sand is (3318-3338) & (3505-3797).The red eclipse show the gas prone sand .

4.4.5 LAMBDA-RHO VS. MU-RHO

The tem lambda is incompressibility and Mu- rho is rigidity. .the value of lambda –rho for gas sand are less than 20 GPa and value of Mu- rho should be greater than 15 GPa approximately (Das and Chaterjee ,2018).When we encounter compacted sand with low porosities the lambda rho values show some relative change behavior (Das and Chaterjee ,2018). Cross plot of LMR also separate Gas and water zone of lower guru sands. The below figure (4.7) show the low value of LMR which is satisfying our zone of interest.

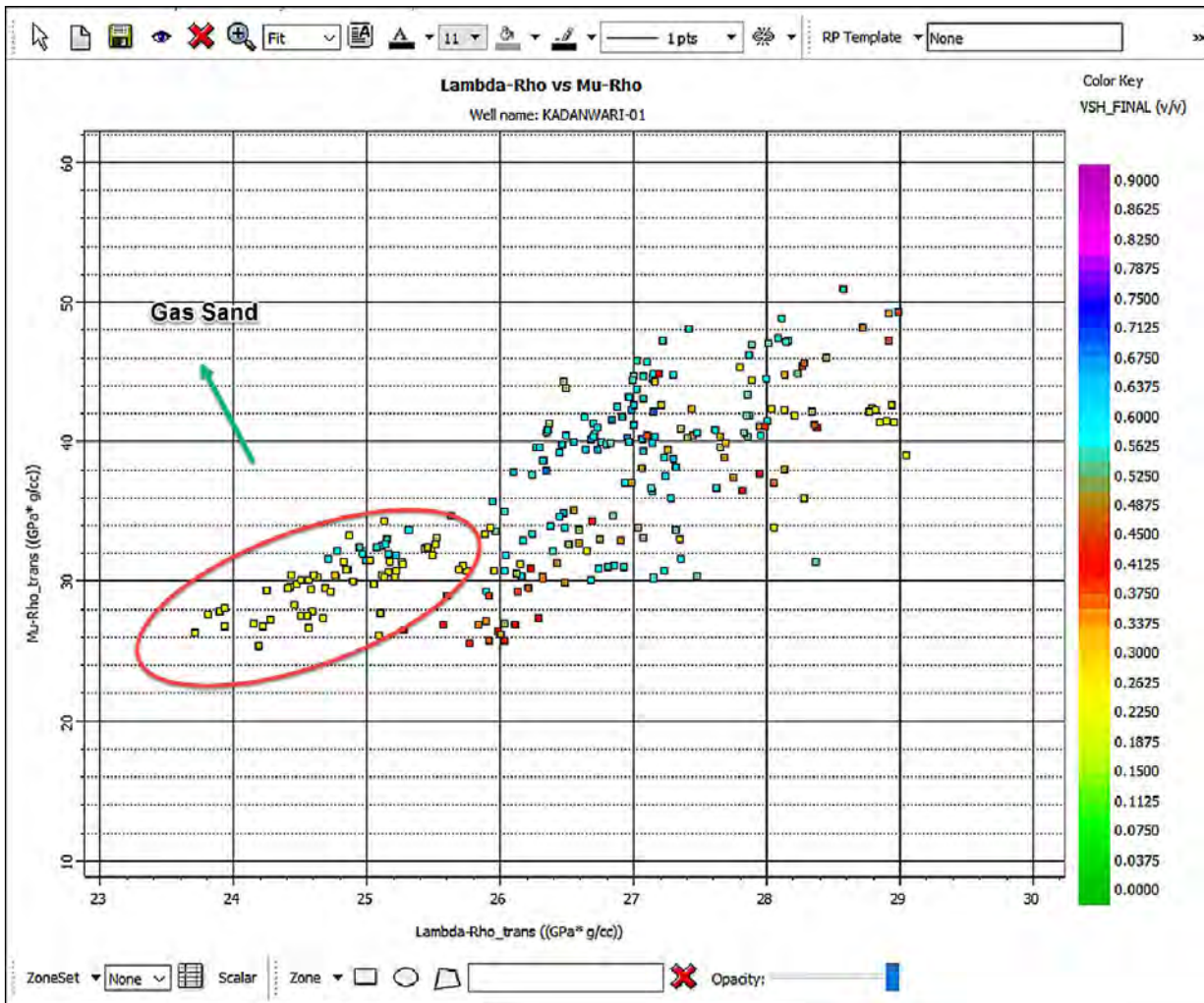


Figure (4.7):Cross plot of lambda-rho and Mu-rho for well Kadanwari -01.Depth interval for lower guru E & B sand is (3318-3338) & (3505-3797).The red eclipse show the gas prone sand .

After completion of first step we move on to second step of RMM. In this step we calculate elastic properties.

4.4 ESTIMATION OF ELASTIC PROPERTIES.

The Young’s modulus (E_{dyn}) and Poisson’s ratio (ν) are two dynamic elastic properties, are computed in relation with the rock density, ρ , and compression P-wave velocity and shear wave S-wave velocity .The elastic properties are calculated are given below

4.4.1 YOUNG’S MODULUS

In the context of linear-elastic deformation, Young's modulus is a fundamental parameter for defining the relationship between stress and strain in a material. The acoustic velocity data can be

utilized to derive Young's modulus from theoretical formulae. However, static Young's modulus is required for geo-mechanical analysis. Therefore, it must be transformed to static modulus if only dynamic modulus is provided. The young modulus is ratio of longitudinal stress to longitudinal strain uniaxial stress state. The relation used to calculate young's modulus given by (Archer & Rasouli.,2012;Eyinla &oladunjoye,2014;jamshidian et al .,2017) show in below equation.

$$E_{dyn} = \frac{\rho * Vs^2 (3Vp^2 - 4Vs^2)}{(Vp^2 - Vs^2)}, \quad (4.7)$$

where Vs is s-wave velocity , Vp is P-wave velocity and ρ is density and E_{dyn} is dynamic modulus.

The value of young modulus should be 27.66 with standard deviaton of 9.98 for gas sand. Figure (4.8) & (4.9) show the values of young's modulus for lower guru E-sand (3318-3338) & B-sand (3505 -3797) which are 32 GPa & 36GPa.

4.4.2 BULK'S MODULUS

The property of material to resist of isotropic squeezing is known as bulk modulus. If material with initial pressure P1 and volume V1 is subjected to isotropic pressure ,then resultant pressue is changes to P2 and volume changes to V2 which is smaller than V1,this volumetric decrease is known as bulk modulus(Archer & Rasouli,2012)It is given by following equation.

$$K_{sta} = \frac{E_{sta}}{3 * (1 - V_{sta})}, \quad (4.8)$$

where K_{sta} is Buk's modulus, E_{sta} is young staic modulus and V_{sta} is static passion ratio.The value of bulk modulus ranges from 8.75 GPa with standard deviation of 3.98 for Gas sands (Abbas et al.,2018). Figure (4.8) & (4.9) show the values of bulk's modulus for lower guru E-sand (3318-3338) & B-sand (3505 -3797) which are 5.34GPa & 6.906GPa.

4.4.3 SHEAR'S MODULUS

Resisting to shearing is known as shear's modulus. it is also calculated by sonic and density logs (Eyinla &oladunjoye,2014;Mavko et al.,,2009).The value of shear modulus should be up to 5.60with standard deviation of 2.60 (Abbas et al.,2018).The equation used to calculate shear modulus is given below

$$G_{sta} = \frac{E_{sta}}{3 * (1 - V_{sta})}, \quad (4.9)$$

where is G_{sta} shear's modulus. Figure (4.8) & (4.9) show the values of shear's modulus for lower guru E-sand (3318-3338) & B-sand (3505 -3797) which are 5.12GPa & 7.00GPa.

4.4.4 POISSON'S RATIO

Possion's ratio is defined as longitudinal contraction causes laterl elongation when stress is uniaxial (Fjar et al.,2008). By quantifying the lateral and axial deformations of the uniaxial compression test in the rock sample, one can calculate the static poisson's ratio. The lithology, confining stress, pore pressure, and porosity of a rock all affect its static Poisson's ratio.

$$V_{sta} = \frac{V_p^2 - 2V_s^2}{V_p^2 - V_s^2}, \quad (4.10)$$

where V_{sta} is static passion ratio

The value of poisson ratio V_{sta} is highly effected in presence of fluid.the value of poisson ratio should be low in rock containing hydrocarbon and approximately equal to 0.23 with standard deviation of 0.3(Abbas et al.,2018). . Figure (4.8) & (4.9) show the values of poisson's ratio for lower guru E-sand (3318-3338) & B-sand (3505 -3797) which are 0.22 & 0.19.

4.4.5 UNCONFINED COMPRESSIVE STRENGTH (USC) AND FRICTION ANGLE (FANG)

Unconfined compressive strength of formation is directly proportional to density because increase in density result in decrease in porosity. USC is related to mineralogy and porosity. The tensile strength of rock is 1/10 of USC (Xu et al.,2016).The value of USC for gas sand should be 66.38GPa with the standard deviation of 17 (Abbas et al.,2018)The formula for USC is (Bradford(1998).

$$USC = 2.28 + 4.1089E_{sta}, \quad (4.11)$$

where E_{sta} is static young's modulus.

Friction angle (FANG) is calculated by plumbs relation (1994).Which relates porosity and clay volume.

$$FANG = 26.5 - 37.4(1 - PHI - V_{clay}) + (1 - PHI - V_{clay})^2, \quad (4.12)$$

where PHI is porosity, V_{clay} is volume of clay .The value of FANG should be 42.35° with standard deviations of 4.96°.The Figure (4.8 &4.9) show values of friction angle(33° & 40°) ,USC (52GPa &70GPa) and tensile strength of E & B sands are given below.

DEPTH m	YSM_HAN		BSM_han		PR		TSTR_MPa	
	0	GPa 60	0	GPa 12	0	0.5	0	MPa 200
	YDM_HAN		SSM_han				UCS_YME_MPa	
	0	GPa 60	0	GPa 12			0	200
							FANG_FROMGR	
							0	deg 60

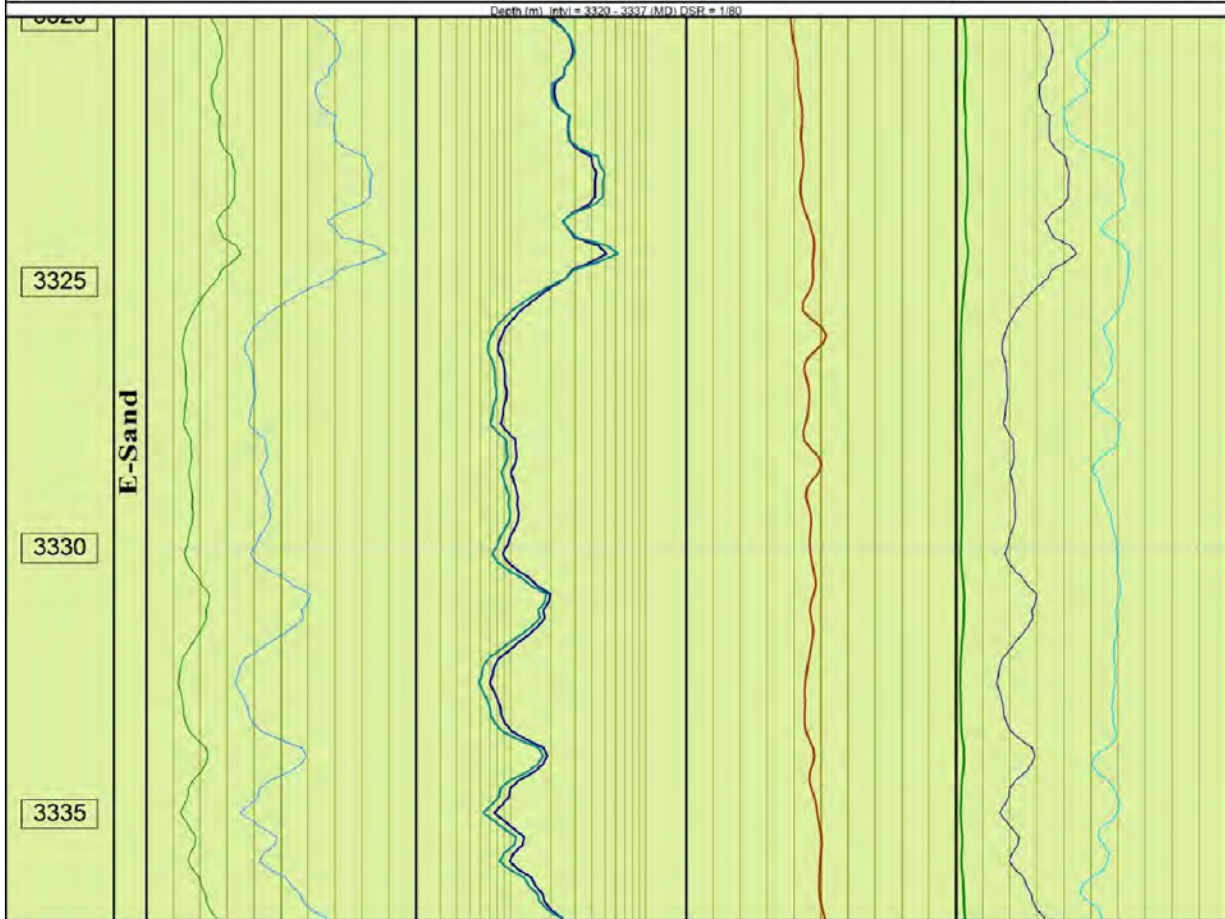


Figure (4.8): RMM for lower guru E-sand. Track (1) represent static and dynamic modulus, Track (2) represent bulk's & shear's modulus. Track (3) represent Poisson's ratio. Track (4) represent UCS, Friction angle & Tensile strain.

DEPTH	YSM_HAN		BSM_han		PR	TSTR_MPa	
m	0	60	0	12	0	0.5	200
	YDM_HAN		SSM_han			UCS_YME_MPa	
	0	60	0	12		0	200
						FANG_FROMGR	
						0	60

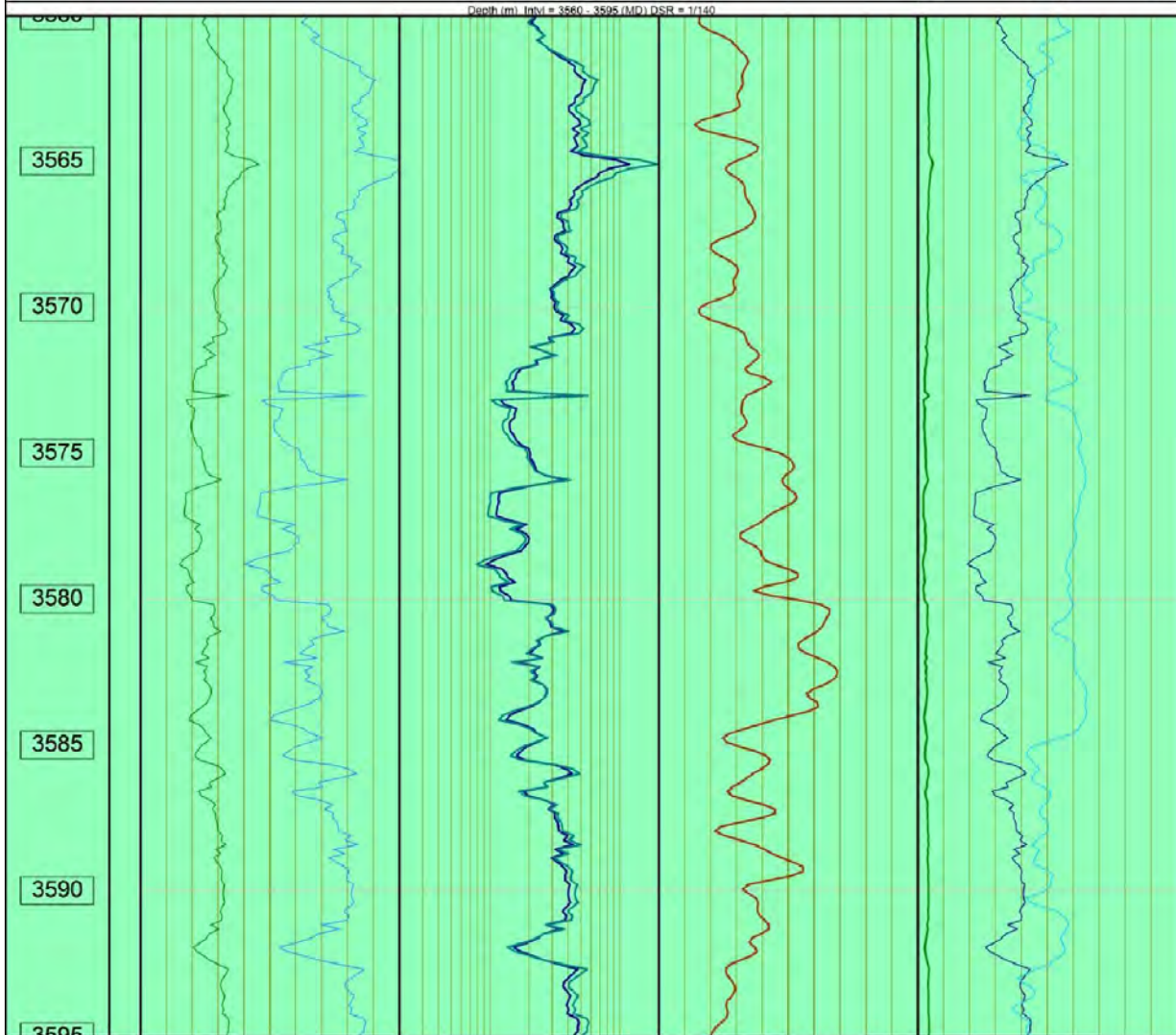


Figure (4.9): RMM for lower guru B-sand. Track (1) represent static and dynamic modulus, Track (2) represent bulk's & shear's modulus. Track (3) represent Poisson's ratio. Track (4) represent UCS, Friction angle & Tensile strain.

4.5 OVER BURDEN STRESS

The integration of rock density to the depth of interest results in the overburden stress (Sig V). The interval where density log is not available then available density log is extrapolated to estimate density of interval having no density log. Due to the accumulation of sediments, overburden pressure

directly increases with depth. At shallow depths, density log is typically not recorded. To determine rock density at the shallow depth, numerous empirical methods have been devised and put to use. The integration of rock densities can be used to predict the vertical stress if density varies with depth. In well-cemented and compacted formations, the vertical stress varies linearly with depth. The overburden stress is also calculated by given equation

$$\rho = 0.31V_p^{0.25}, \quad (4.13)$$

The overburden gradient is 1 psi/ft, and the average sediment density is between 1.8 and 2.2 g/cm³. (Fjar et al., 2008).

4.6 PORE PRESSURE

Pore pressure is pressure exerted by fluid on pore spaces of rock matrix. One of the essential aspects in geo-mechanical analysis and petroleum production is are pressure. It significantly affects the wellbore stability analysis and the deformation around the wellbore (Detournay & Cheng, 1988). Consequently, the pressure caused by the formation fluid can be used to define pore pressure.

Inaccurate pore pressure predictions can result in serious drilling accidents like kick and blowout as well as a considerable NPT during the drilling process. Pore pressure is hydrostatic at relatively modest depths (less than 2000 m), which means a continuous, interconnected column of pore fluid extends from the surface to that depth.

Indicating that the deeper formations are hydraulically isolated from the shallower ones, overpressure begins at depths of more than 2000 meters, and pore pressure rises quickly with depth. By 3800 m, the pore pressure reaches a level that is relatively near to the overburden stress, a situation known as hard overpressure. In the group of people who anticipate pore pressure, the effective stress is typically characterized as being obtained by subtracting the overburden stress from the pore pressure. The amount of effective stress decreases as overpressure increases. The following formula is used to determine pore pressure.

$$PP = \delta_v - \frac{\delta_e}{\alpha}, \quad (4.14)$$

where PP stands for pore pressure. δ_v donate the vertical stress, δ_e is effective stress and α is Biot's constant.

Pore pressure estimation coupled with stress used to characterize reservoir mechanically. Prediction of pore pressure help us to drill well safely and help us to identify the mud weight. While at basin

level it will help us to determine rock maturing , regional faulting behavior, fluid migration at large scale. In hydrocarbon zone pore pressure should be high (Huffman.,2002).The value of pore pressure for E-sand (3318-3338) & B-sand (3505 -3797) is shown in Figure (4.10) which are 34MPa & 37MPa.

4.7 MINIMUM HORIZONTAL STRESS

The one of principle stress used to identify the fracture geometry and propagation, safe mud window and barrier zone for maximizing reservoir production and well bore instability is known as minimum horizontal stress.(Bell,1997;Bell and Babocock.,1986;Maleiki et al.,2014;Warpinski and Teufel.,1999).

To determine S_{hmin} two methods are used, one is direct and second in indirect method.In direct method stress are measured directly by Leak off test ,extended leak of test, micro and mini fracture measurement and step rate test (Nolte.,1988;Carengie et al.,2002);Zoback.,2010;Fang and Khasksar 2011).

For in direct method we used different model such as Andrson model, Newberry Model and Poro elastic model (Fan et al.,2014; Pallikathekathill & Mawuli,2011; ,Zhang,wang, & Meng 2011).The direct method is so expensive so we use indirect method. In indirect method we must have lot of data.

4.7.1 DETERMINATION OF MINIMUM HORIZONTAL STRESS

It is calculated by poro-elastic model (Abdideh & Fathabadi.,2013).

$$S_{hmin} = \frac{v}{1-v} \delta_v + \frac{1-2v}{1-v} \alpha P_p + \frac{E_s}{1-v^2} \varepsilon_x + \frac{E_s v}{1-v^2} \varepsilon_y, \quad (4.15)$$

where S_{hmin} is minimum stress, v is passion ratio,Vertical stress is denoted by δ_v , α denotes Biot's constant, pore pressure is given P_p and $\varepsilon_x \varepsilon_y$ are strain components. The value of S_{hmin} for E-sand (3318-3338) & B-sand (3505 -3797) is shown in Figure (4.10) which are 47MPa & 50MPa.

4.8 SIGNIFICANCE OF RMM

RMM in concurrence with information like diagenetic evolution takes place in rocks, depositional history, structural geology , petrophysical analysis is very useful in following manner. Bore-hole analysis is very useful for well bore instability, breakout analysis and determination of safe window (Ashannezhad., 2016;tingay et al.,2008) which are shown in figure (4.11 & 4.12).RMM study is used to design well completion. It also help us to understand rock mechanical properties and subsurface

heterogeneities.(Dusterhoft et al.,2017). RMM is helpful in identifying sweet spots and facilitate hydraulic fracking (Jacobi et al.,2018).

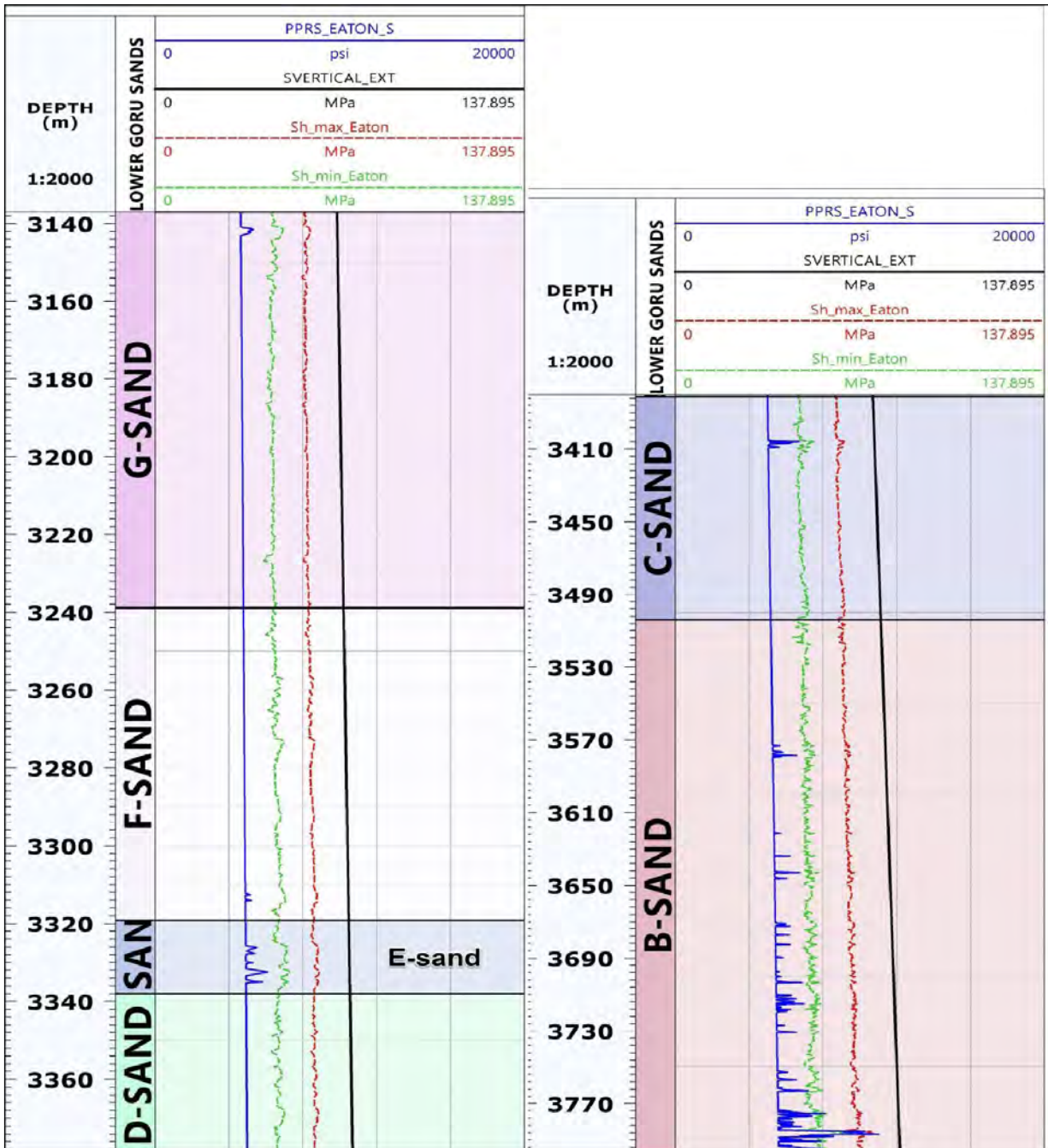


Figure (4.10):Track (1) blue color shows pore pressure, Green colour show minimum horizontal stress , Red color shows maximum horizontal stress and black color shows vertical stress for E-sand (3318-3338) & B-sand (3505 -3797).

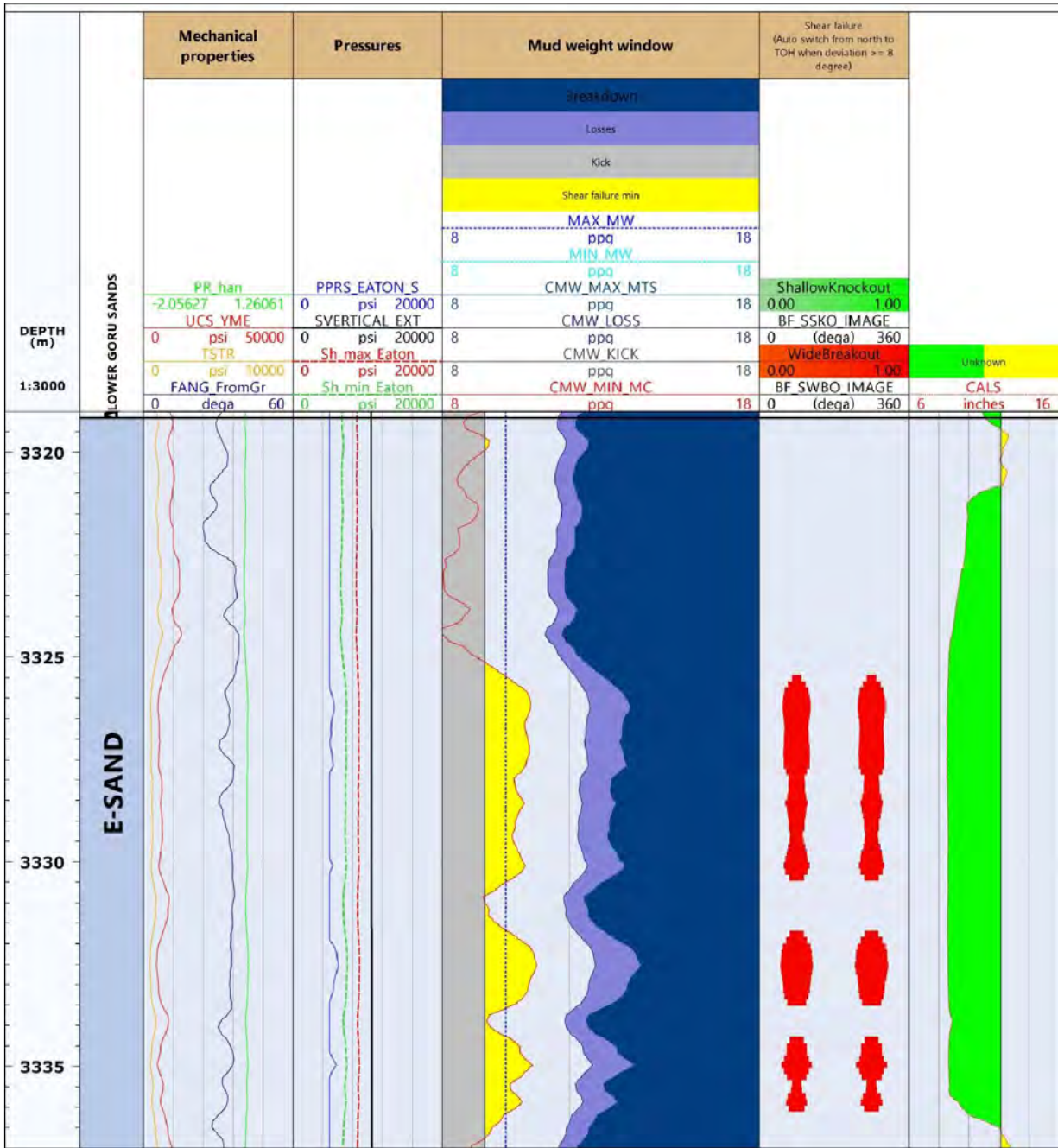


Figure (4.11): Well-bore instability for E-sand (3318-3339) of lower goru.

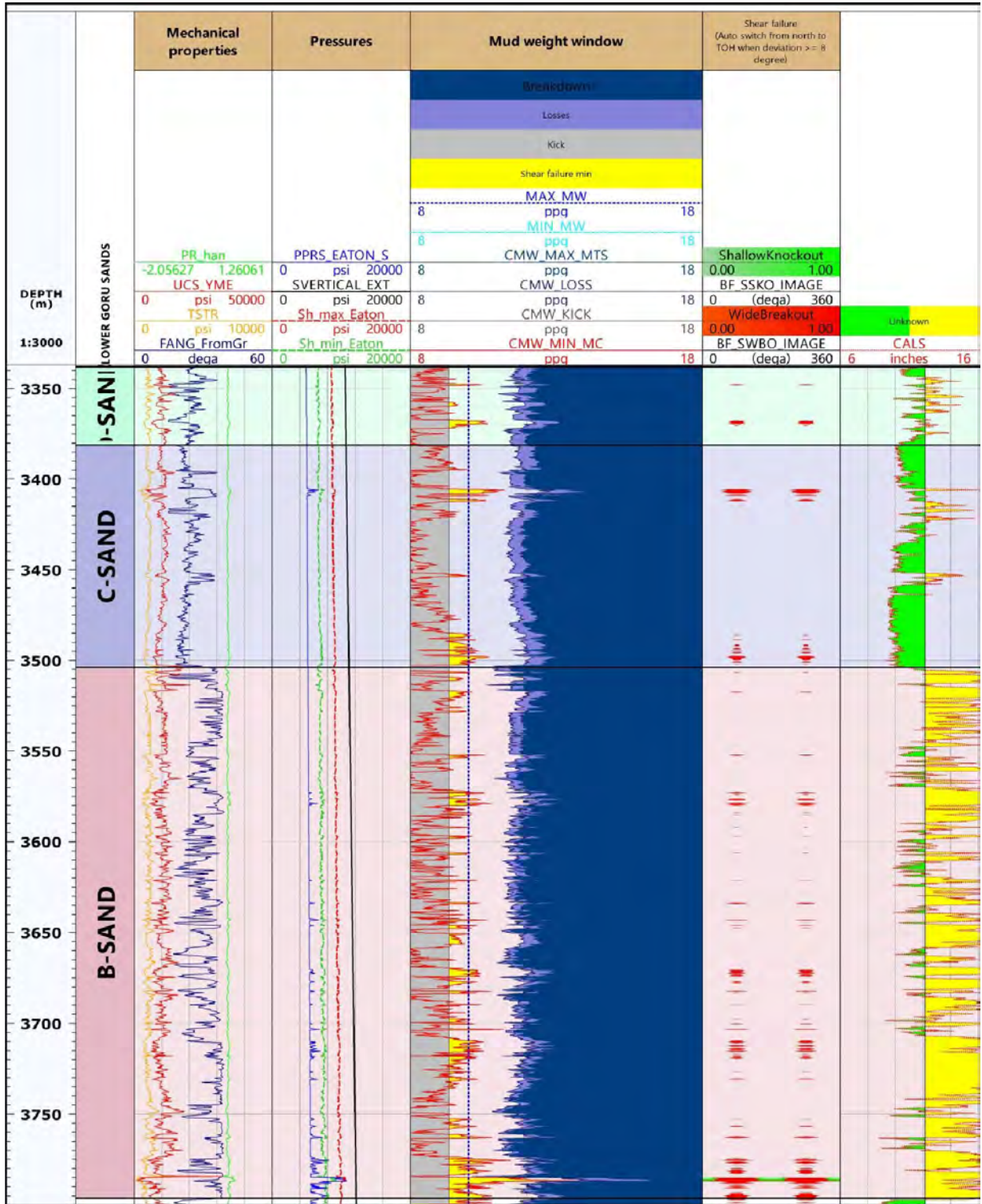


Figure (4.12): Well-bore instability for B-sand (3505-3797) of lower goru.

CHAPTER 5

5. SEISMIC BASED ESTIMATION OF GEO-MECHANICAL PROPERTIES

5.1 INTRODUCTION SEISMIC INVERSION:

Seismic inversion is basically defined as the transformation of seismic impedance to seismic amplitude. It makes hydrocarbon zones easier to interpret, map, and quantify (Ali et al.,2018).The seismic inversion is performed by de-convolution in which seismic trace is transformed to earth reflectivity series. To model subsurface geological structure seismic inversion is used where reflection data is used as input and controlling parameters are obtained from well logs(Sukmono.,2002).

The very optimum technique used for reservoir characterization is seismic inversion because in this technique the seismic data (interface property) is inverted to acoustic impedance (layer property). The correlation is made between layer property and petrophysical properties (porosity, Sw etc) the result obtained is further extended to seismic scale (Barclay et al.,2008).

The goal of seismic inversion is to evaluate reservoir properties this technique is helpful in characterization of reservoir and monitoring the changes occurring in rock due to production and substitution of fluids (Gavotti et al.,2014).

In present study firstly we perform model base inversion and in second part we predict geo-mechanical properties like elastic properties, poisson ratio, vpvs ratio, pore pressure, minimum and maximum stresses by using multi attributes and neural networking techniques.

5.2 MODEL BASED INVERSION:

The recursive inversion problems are avoided in MBI by changing the model iteratively to obtain best fit between observed and calculated data. We have stacked data to perform this inversion (Russell,B et al., 1991). MBI is based on convolution model. This equation is solved for reflectivity series if we consider noise as un corrected with seismic signal.

Seismic trace = source wavelet *Reflectivity + Noise

This equation is band limited and non-linear (Swisi et al., 2009) and solved iteratively. To control small amount of error hard constrained are applied. The soft constrained (vario-grams) are applied to

incorporate initial guess models but generally hard constrained are preferred (Gavotti.,2014).the schematic diagram of MBI is given below

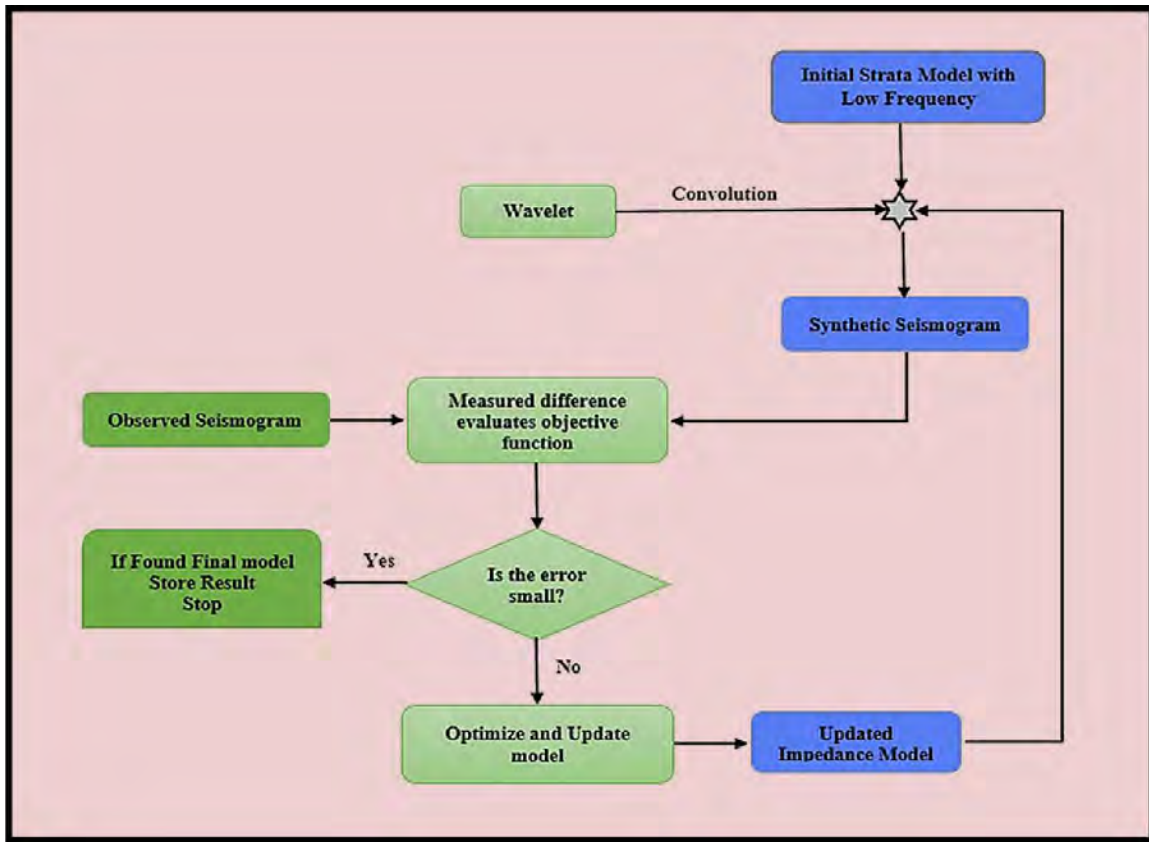


Figure (5.1): Acoustic impedance estimation workflow followed for model based inversion (Sen., 2006)

5.2.1 METHODOLOGY:

The methodology for MBI is given below:

- Acoustic impedance is calculated by sonic and density log of kadanwari well-01.
- Two horizons are picked to provide structural information.
- For initial impedance horizons are interpolated along well location.
- To constrain initial impedance by selecting block size.
- Statistical wavelet is extracted from seismic section.
- Synthetic trace is obtained by convolving earth reflectivity with extracted wavelet.

- Synthetic seismic trace is obtain by convolve earth reflective series with extracted wavelet which is different from observe trace.
- By using statistical technique we minimize misfit between observed and synthetic trace.

5.2.3 EXTRACTION OF WAVELET:

Source wavelet is extracted by conversion of reflectivity to acoustic impedance (AI). Source wavelet has a valuable role in seismic inversion. This wavelet is extracted from the time window of 2200-3000 ms having a wavelength of 100ms.

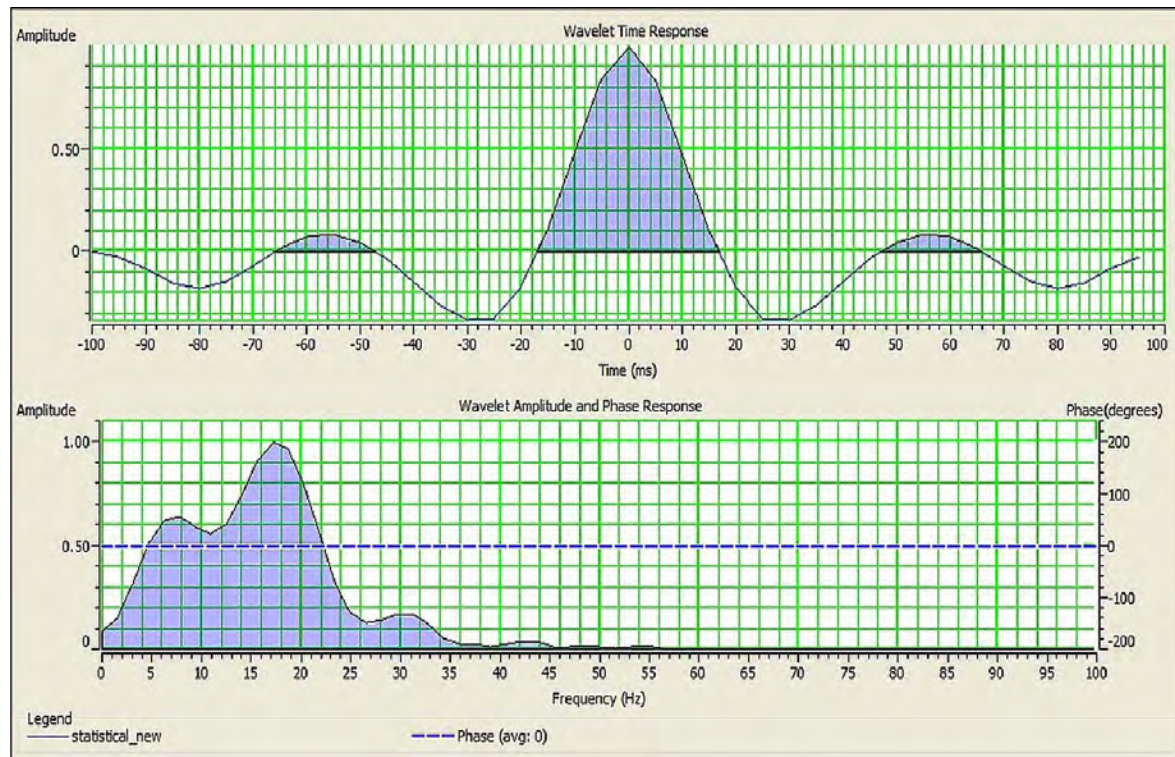


Figure (5.2) : Extracted wavelet from seismic and well data. Blue dotted line shows average phase.

This wavelet is used for 1-D forward model. The seismic in vicinity of well is used to improve control over wavelet.

5.2.4 INITIAL LOW FREQUENCY MODEL (LFM):

Generally acoustic impedance is divided into two types relative acoustic impedance and absolute. We used absolute impedance because it incorporates low frequency component (0-15Hz) in its algorithms that are used to invert seismic amplitude data. Absolute impedance is quantitative and qualitative(Cooke and Cant.,2010).Low frequency are neglected during acquisition and processing

steps but it is important role in inversion analysis and have certain impacts on inversion results. So in MBI low frequency are added to overcome ambiguity (Cooke and Schinder,1983).Initial low frequency model is shown in figure (5.3).

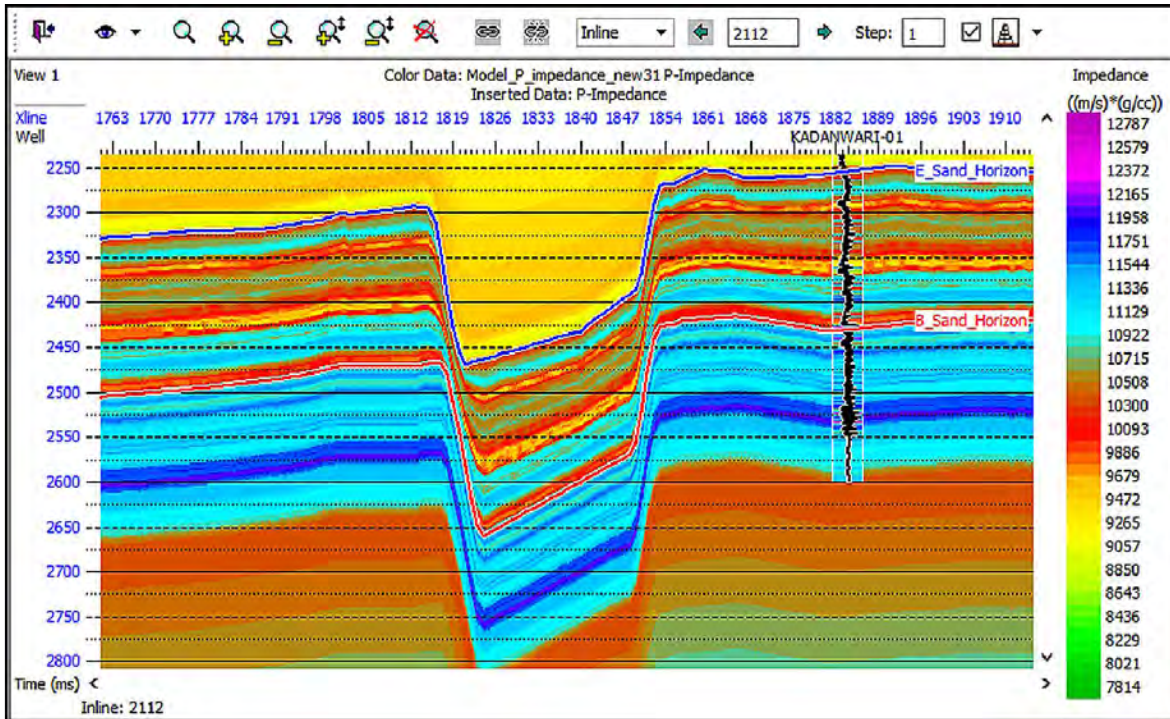


Figure (5.3): Initial low frequency impedance model for Lower guru E (3318-3338) & B sands (3505-3797).

5.2.5 INVERSION ANALYSIS:

The inversion analysis for Kadanwari well-01 and 3D seismic cube are in given figure. The coefficient of correlation is approximately (0.98) and the synthetic and observed traces are in shown in figure by red and black color. The estimated root mean square error between observed and modeled trace is 0.145. Root square error between impedance log and inverted trace is approximately 522.6 (m/s)*(g/cc).

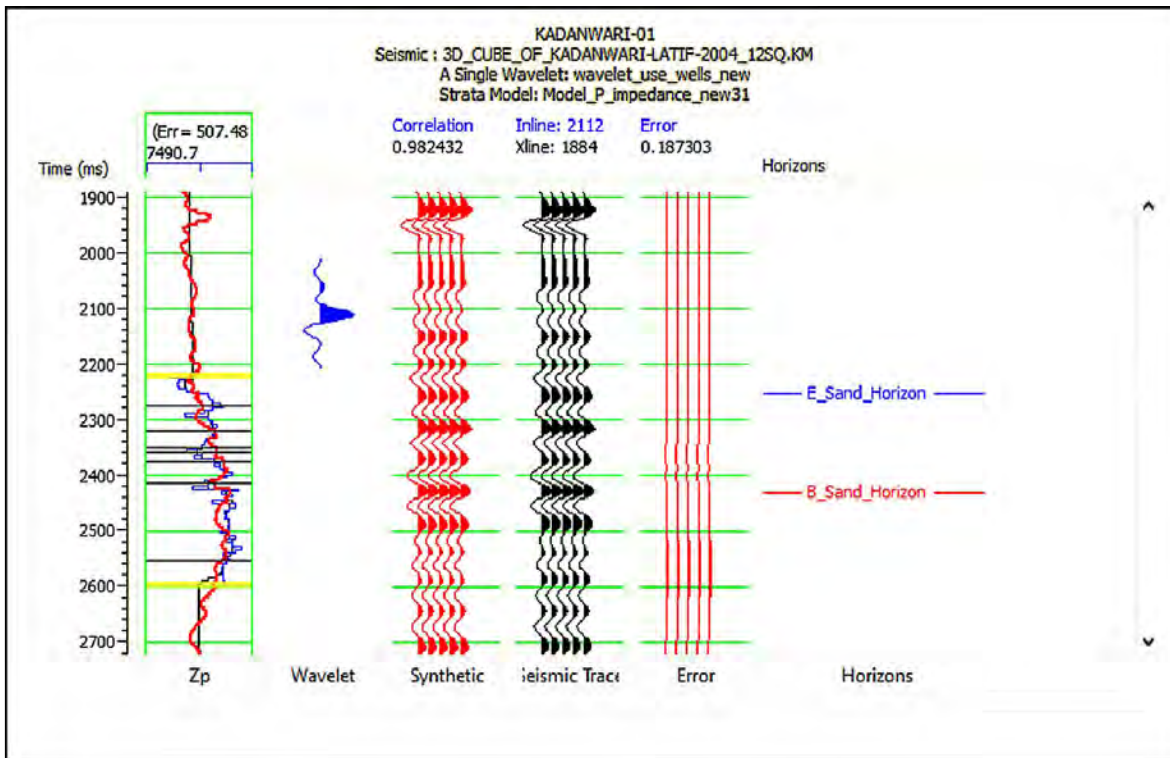
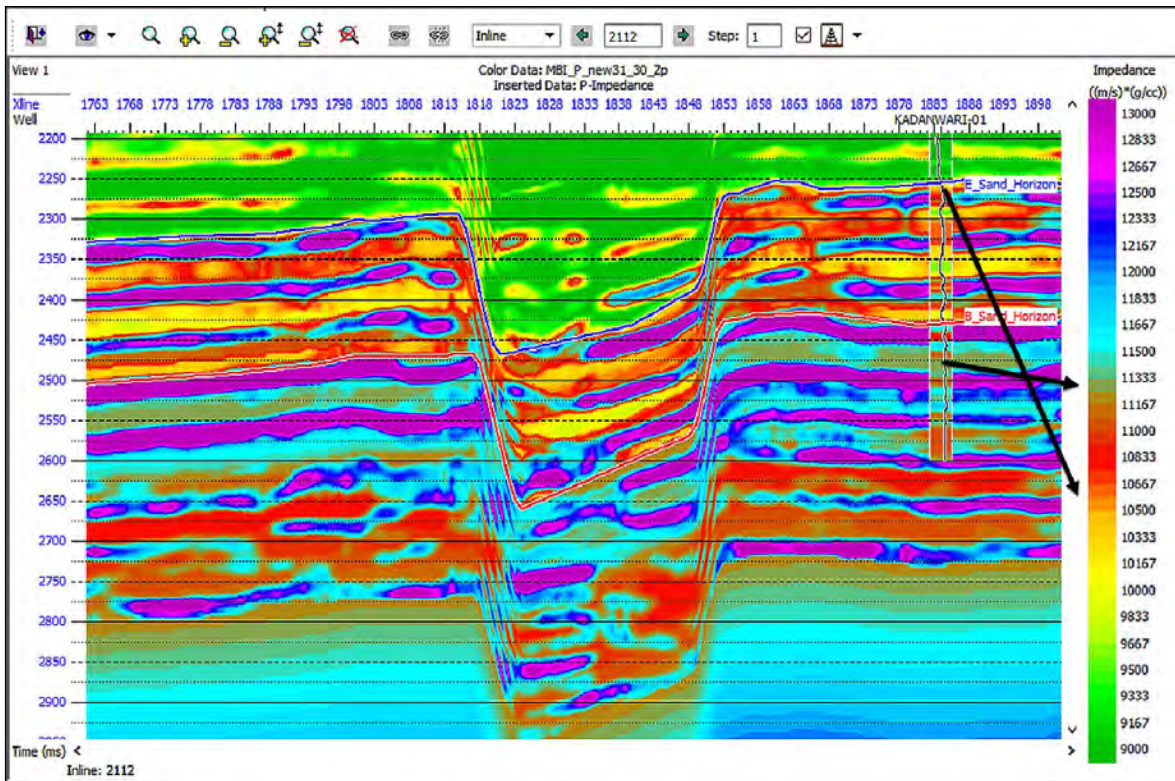


Figure (5.4): Inversion analysis for Kadanwari well-01

5.2.6 INTERPRETATION OF MBI RESULTS:

The model is interpreted by using color bar showing impedance. the inversion is applied on selected time window of (2200-3000 ms) where horizons of our interest lie. the inversion result are based on acoustic impedance modeling low acoustic impedance is associated with presence of hydrocarbon. in the study are we have low acoustic impedance which shows the presence of hydrocarbon. while higher values shows the presence of shale(gavouti.,2014).So E-sand (3318-3339) is main producing in kadanwari well-01 while B-sand (3505-3797) is minor producing zone. Inverted acoustic session is shown in figure (5.5) .Slices of E & B sand are also generated show in figure (5.6) & (5.7).



Figure(5.5): Inverted acoustic impedance section and black arrow shows low value of impedance.

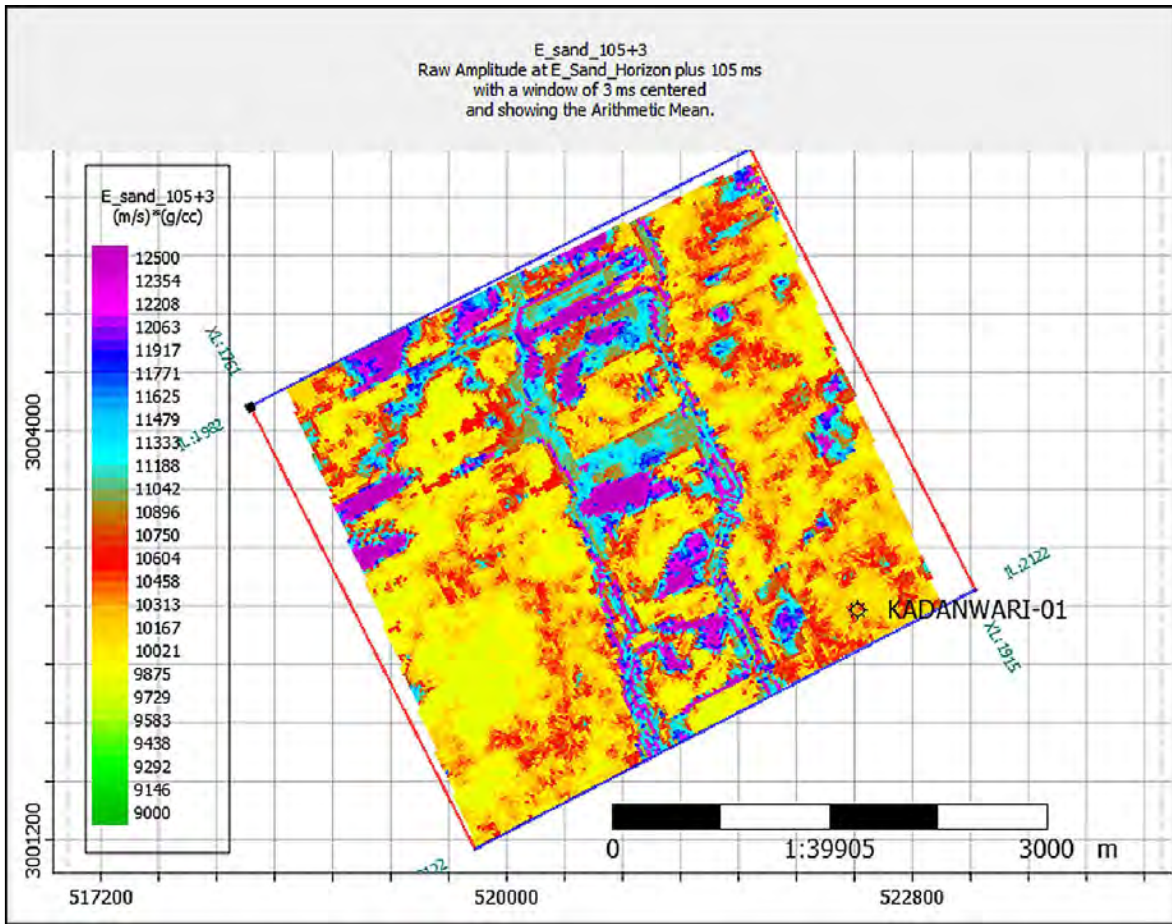


Figure (5.6): Time slice of E-sand representing low impedance values.

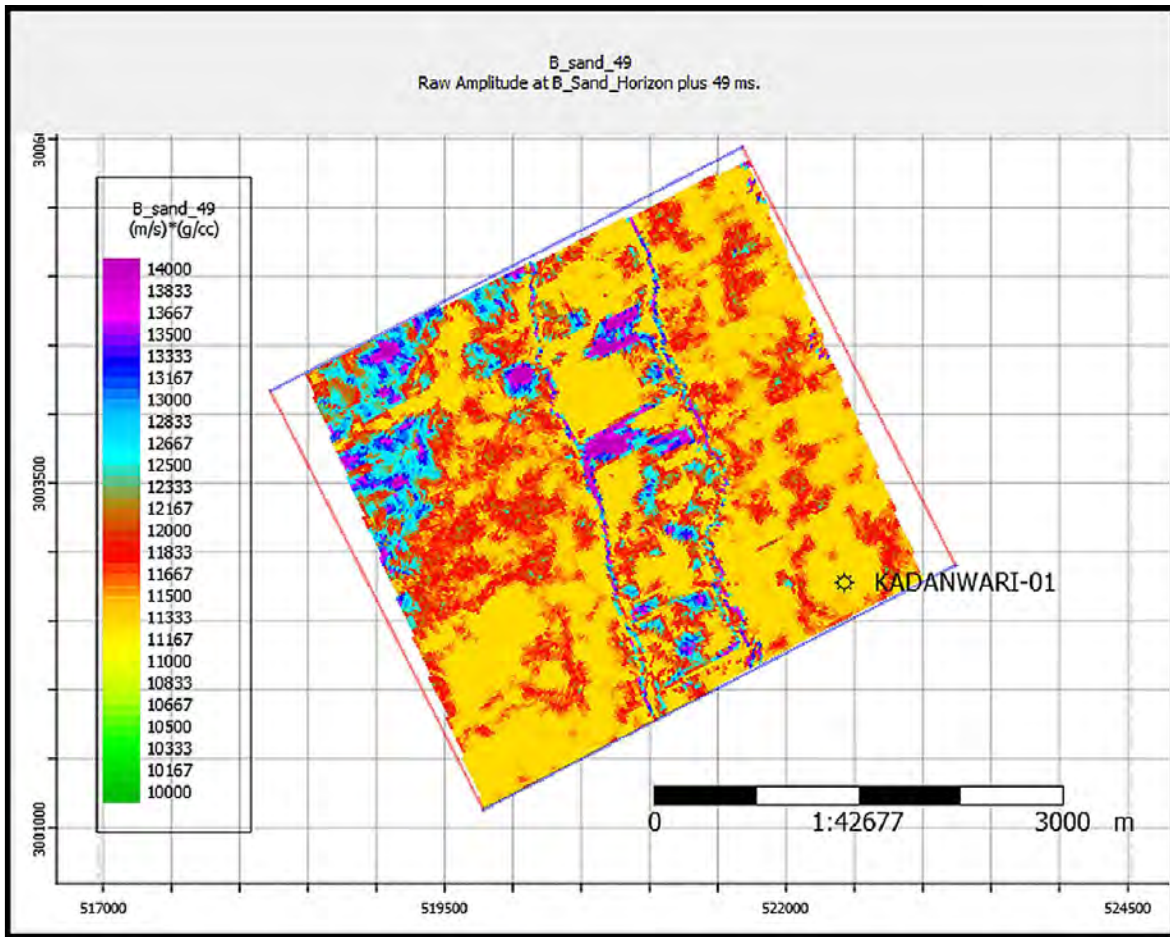


Figure (5.7): Time slice of B-sand representing low impedance values.

5.3 SPATIAL DISTRIBUTION OF GEOMECHANICAL PROPERTIES VIA SEISMIC INVERSION:

The purpose of seismic inversion is to build correlation between petro-physical and reservoir properties. In this thesis geo-mechanical properties are estimated using well logs and their spatial distribution is observed in order to avoid ambiguity in kadanwari -01 .by using neural networking and multi attribute analysis ,lambda-rho, mu-rho, young's modulus, passion ration, vpvs ratio, pore pressure ,minimum and maximum stress are inverted to find the reason either well is success or fail. Here as we know the kadanwari field is gas field so we find the reason of successful exploration. The techniques which are used to estimate spatial distribution are given below.

5.3.1 MULTI ATTRIBUTE AND PROBABILISTIC NEURAL NETWORKING:

The PNN and multi attribute analysis is helpful in seismic base estimation of geo-mechanical properties. The emerge module in HRS-9.2 software is used for this purpose in this module well data is merged with seismic data .well properties are calculated internally as well as can be used externally also (Soubotcheva,et al.,2001).

The step for PNN and multi attribute for study area is given below:

- The seismic data is examined at well location to determine sets of attributes.
- The relationship is derived from neural networking and multi attributes depending on demand.
- These relations are applied on 3D seismic cube to create volume of desired geo-mechanical properties.
- PNN is non linear , parallel processed techniques which mimics human brain roughly. This network is trained to make algorithms working .These networks are known as artificial neural networking.

The PNN and neural networking is intelligent technique and used as powerful tool to make more accurate reliable geo –mechanical properties. By using neural networking and multi attribute analysis the spatial distribution of lambda-rho, mu-rho, young's modulus, passion ration, vpv ratio, pore pressure, minimum and maximum stress are discussed below.

5.3.2 SPATIAL DISTRIBUTION OF VpVs RATIO:

In this chapter we estimate there spatial distribution by using seismic inversion and interpret their result to facilitate our research. According to Das and chaterjee (2018) the range of VpVs ration is 1.62 to 1.8 (Abbas et al 2018) for hydrocarbon zone. We use this value for lab reference because these values are of same lithology of different area. Model-based results for predicted inverted VpVs ratio are in good relationship with the actual VpVs ratio curve trend. Moreover, the relationship between predicted VpVs and observed VpVs ratio is cross-plotted as displayed in Figure (5.8). The spatial distribution of VpVs ratio is shown in Figure (5.9).Time slice of E-sand & B-sand are shown in figure (5.10 &5.11) depict that kadanwari-well-01 are drilled at good range of VpVs values which required for hydrocarbon occurrence. These values are relatively high because we use Vs which is generated by Han(1986) empirical equation. Black eclipse represent the potential prospect zone which have low values of VpVs and is is good position for drilling well to increase our production rate. The values of VpVs for E sand is 1.66 and for B-sand is 1.63.

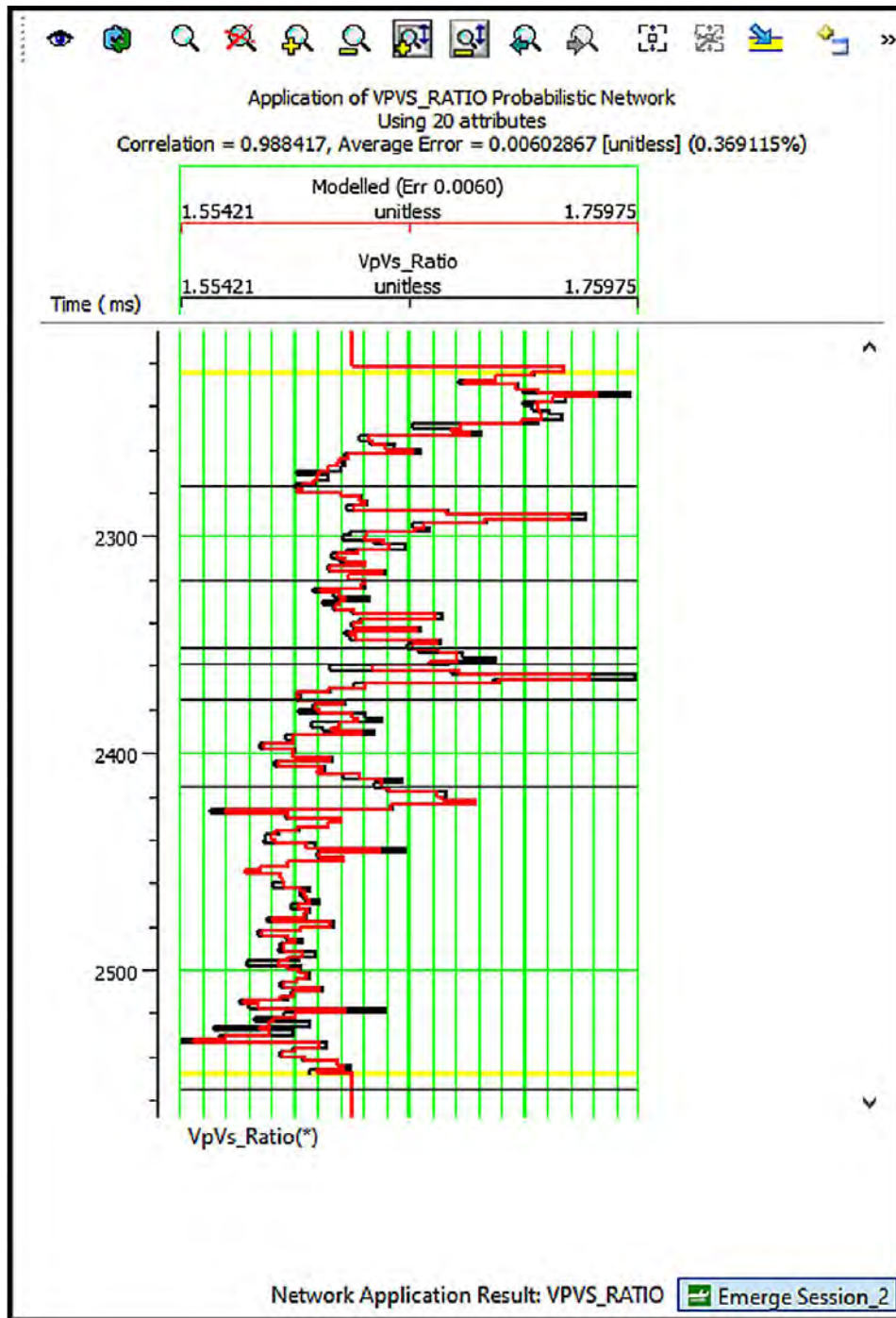


Figure (5.8): Results from PNN of predicted and real VpVs ratio with correlation of .988417.

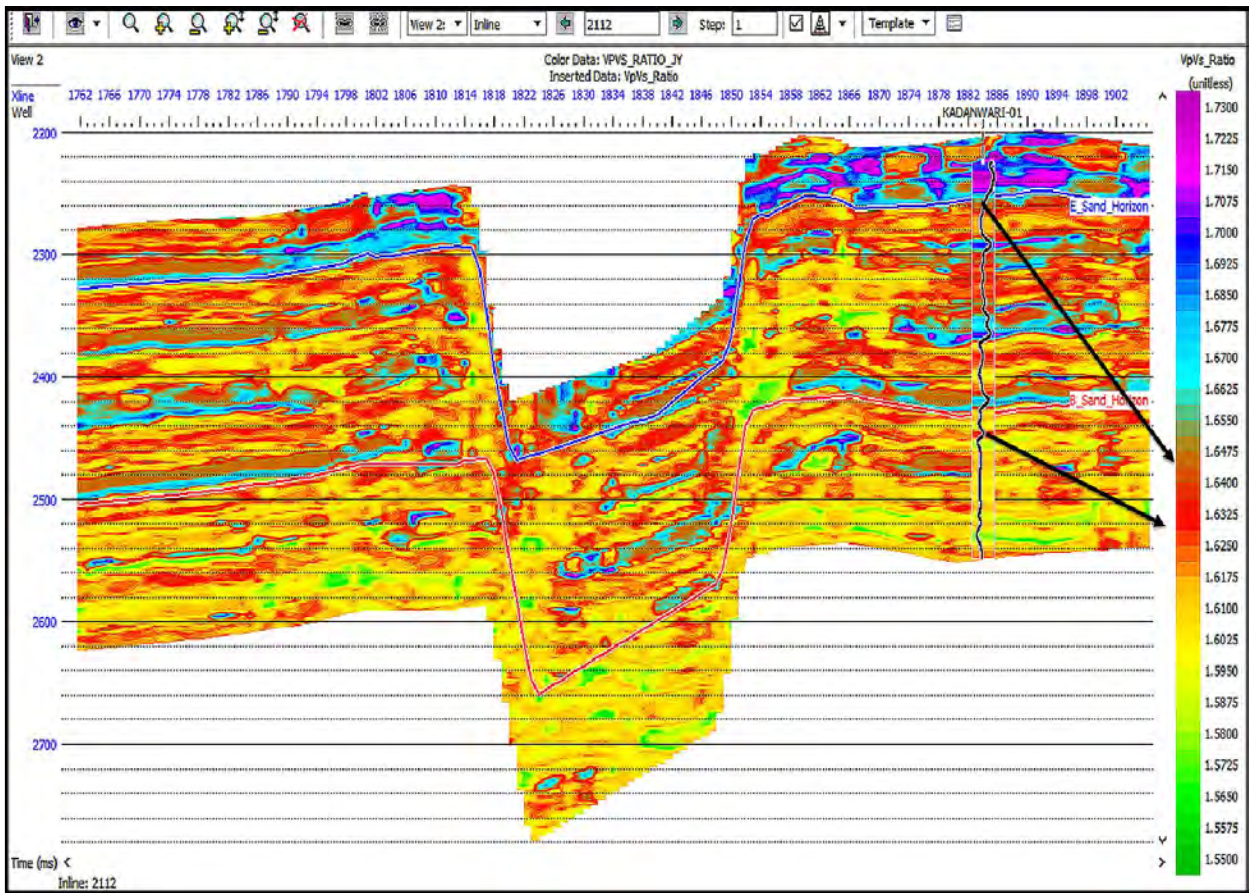


Figure (5.9): Spatial variation VpVs ratio for inline 2112 with black arrow represents the value of VpVs ratio of E (3318-3339) & B (3507 -3797) sand.

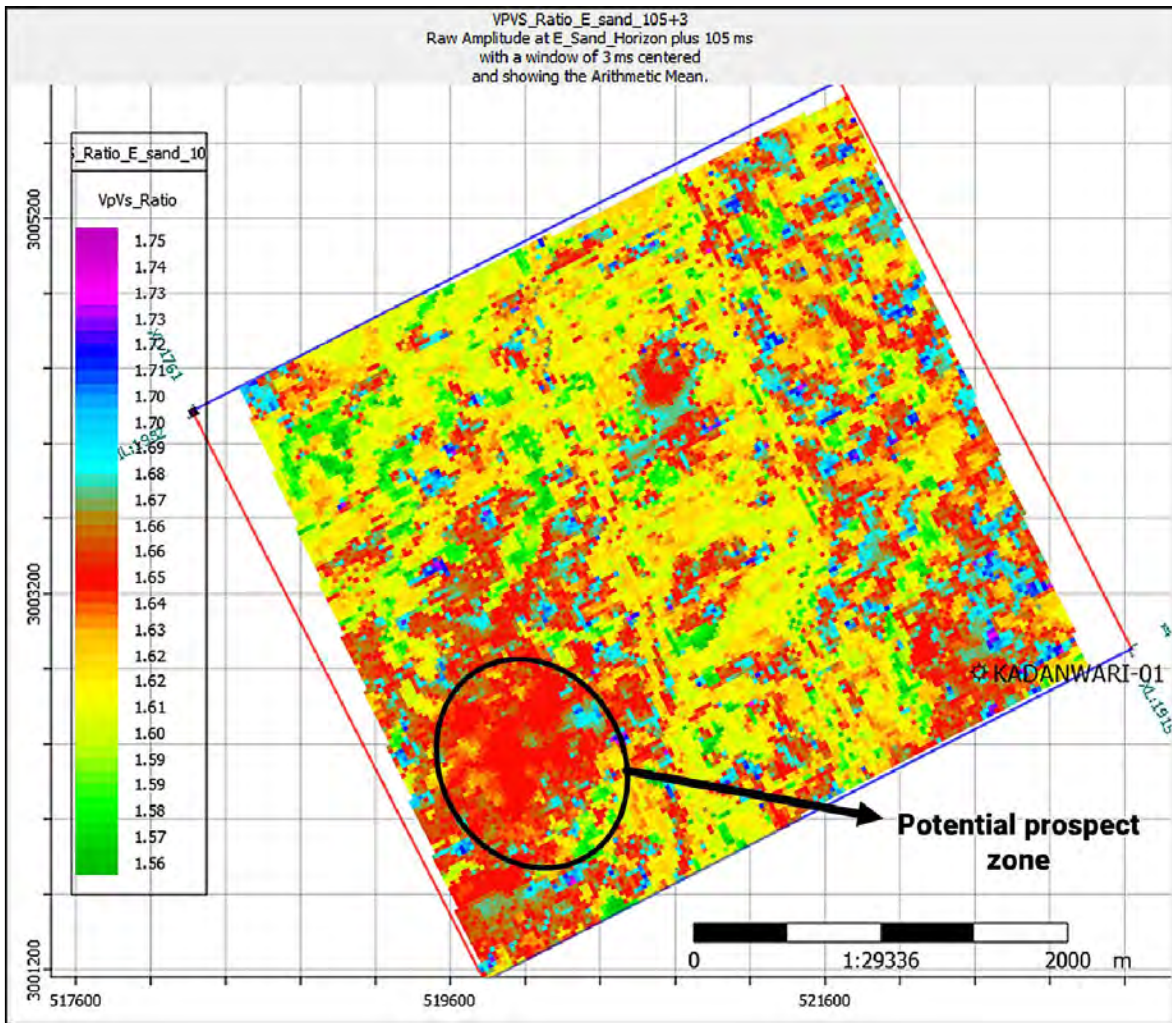


Figure (5.10): Time slice of E-sand and black eclipse represent potential prospect zone.

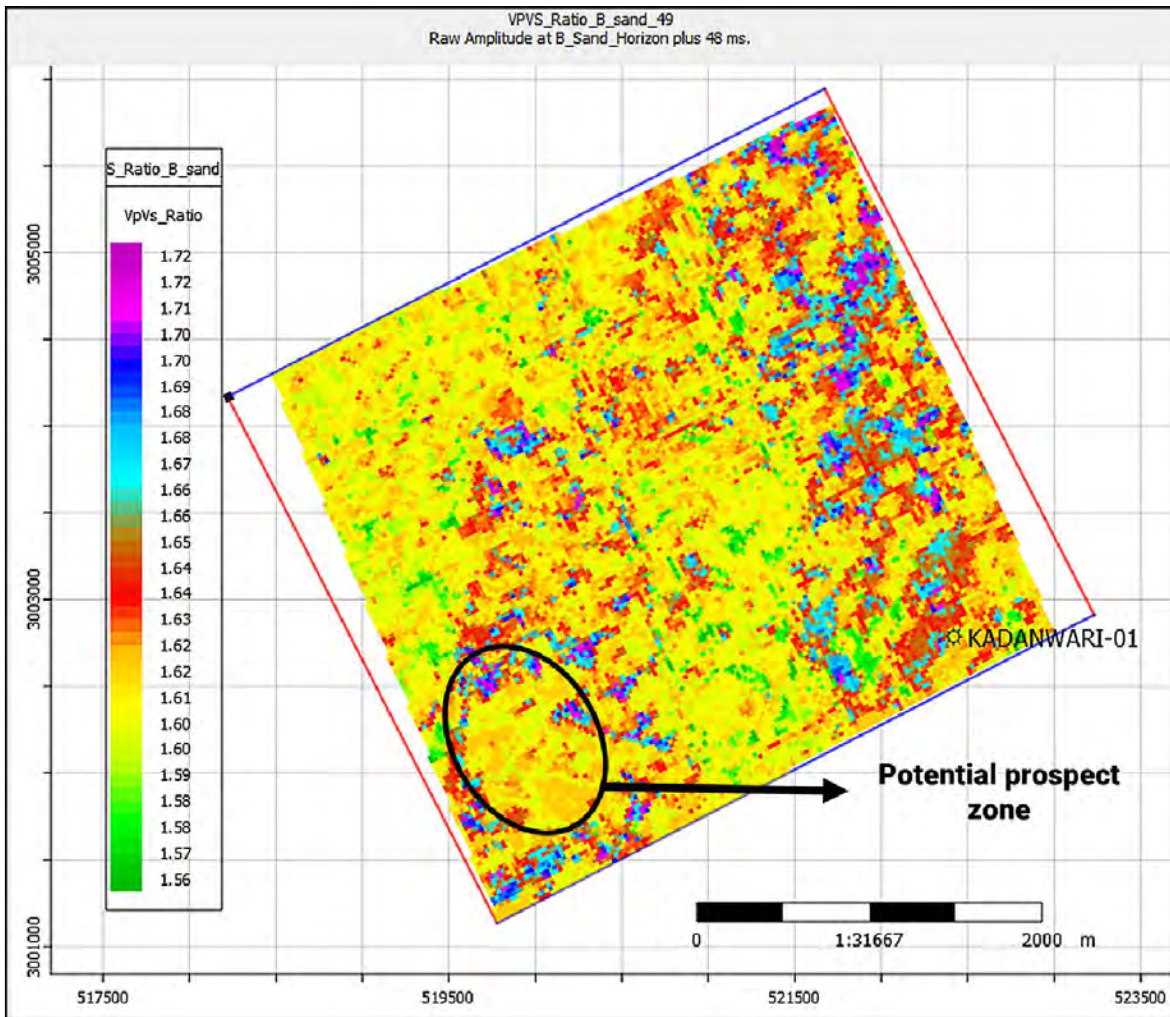


Figure (5.11): Time slice of B-sand and black eclipse represent potential prospect zone.

5.3.3 SPATIAL DISTRIBUTION POSSON'S RATIO:

Passion ratio is used to predict rock behavior and fluid present in pores of formation (Zhang and Bently.,2005).In the presence of hydrocarbon the passion ration must be low approx 0.23 with standard deviation of (SD) 0.3(Abbas et al.,2018).The predicted and observed values of psson's ratio show are very good relation with .983904 correlation show in figure (5.12).While spatial distribution of passion' ratio show in figure(5.13).The Low values of possion's ratio give clear identification of hydrocarbon. Time slice of E-sand & B-sand are shown in figure (5.14 &5.15) depict that kadanwari-well-01 are drilled at low passion's ratio (.22 & .19) values which required for hydrocarbon occurrence. These values are relatively high because we use Vs which is generated by

Han(1986) empirical equation. Black eclipse represent the potential prospect zone which have low values of poisson's ratio and is is good position for drilling new well to increase our production rate.

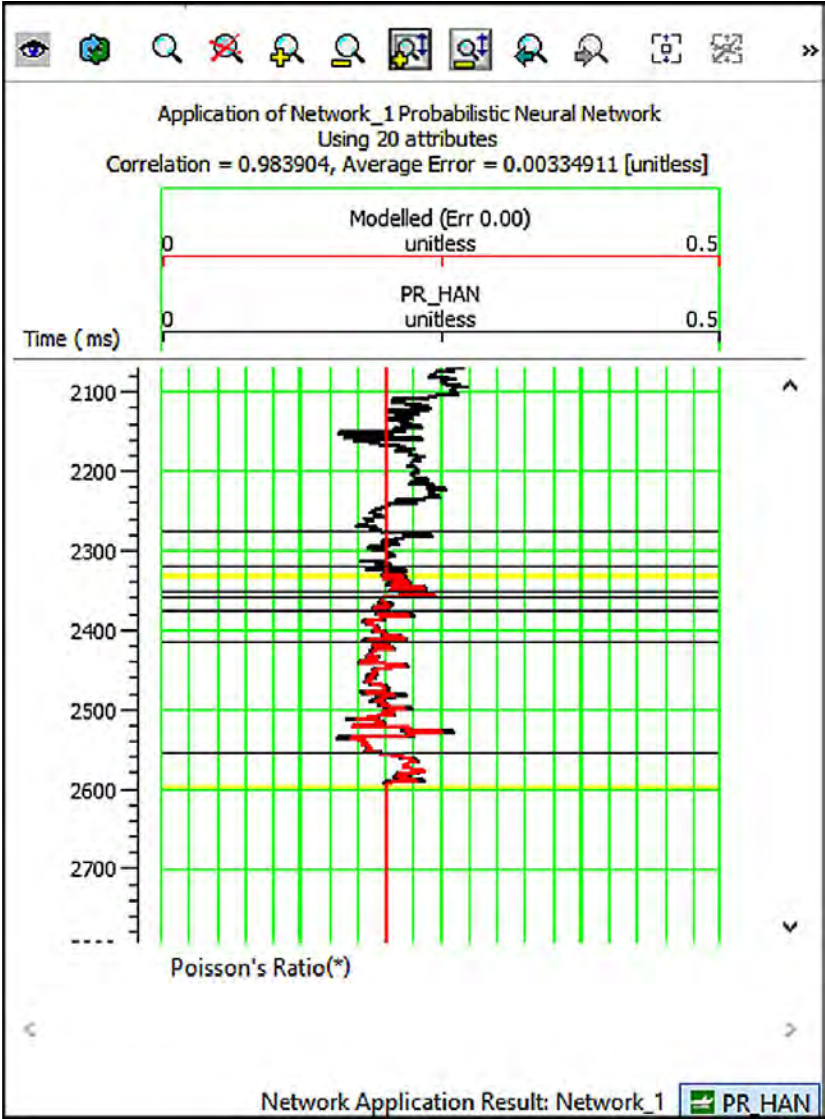


Figure (5.12): Results from PNN of predicted and actual passion's ratio with correlation of 0.983404.

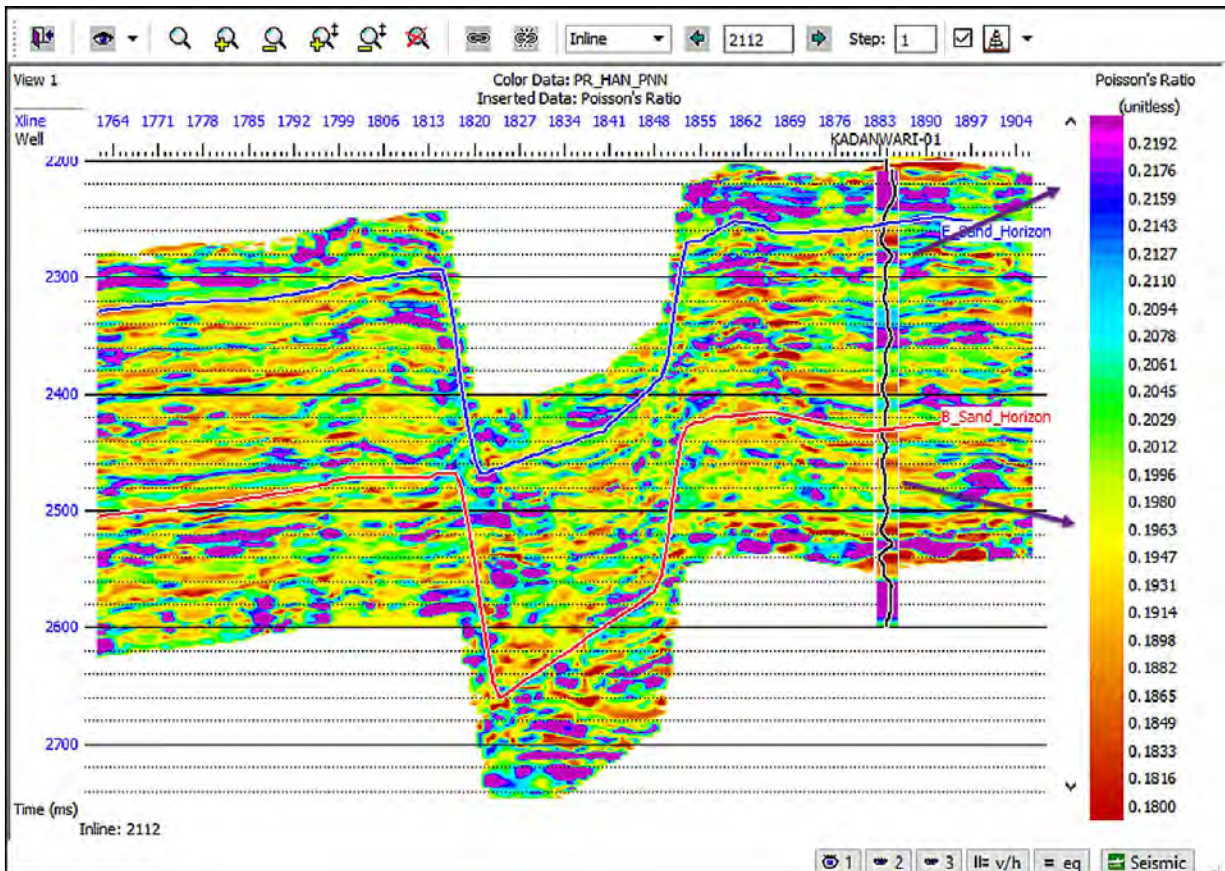


Figure (5.13): Spatial variation of Poisson's ratio for inline 2112 with black arrow represents Low values of E (3318-3339) & B (3507-3797) sand.

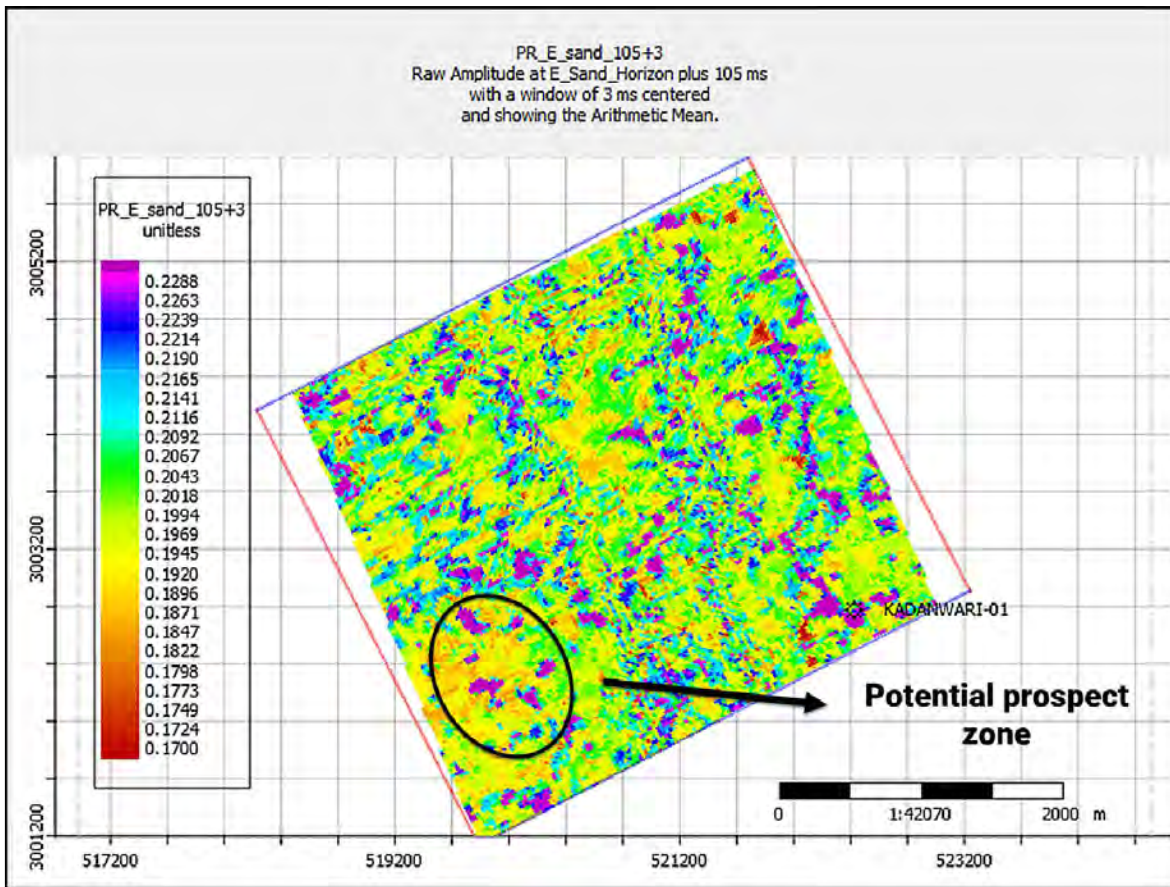


Figure (5.14): Time slice of E-sand with low possion's ratio and black eclipse represent potential prospect zone.

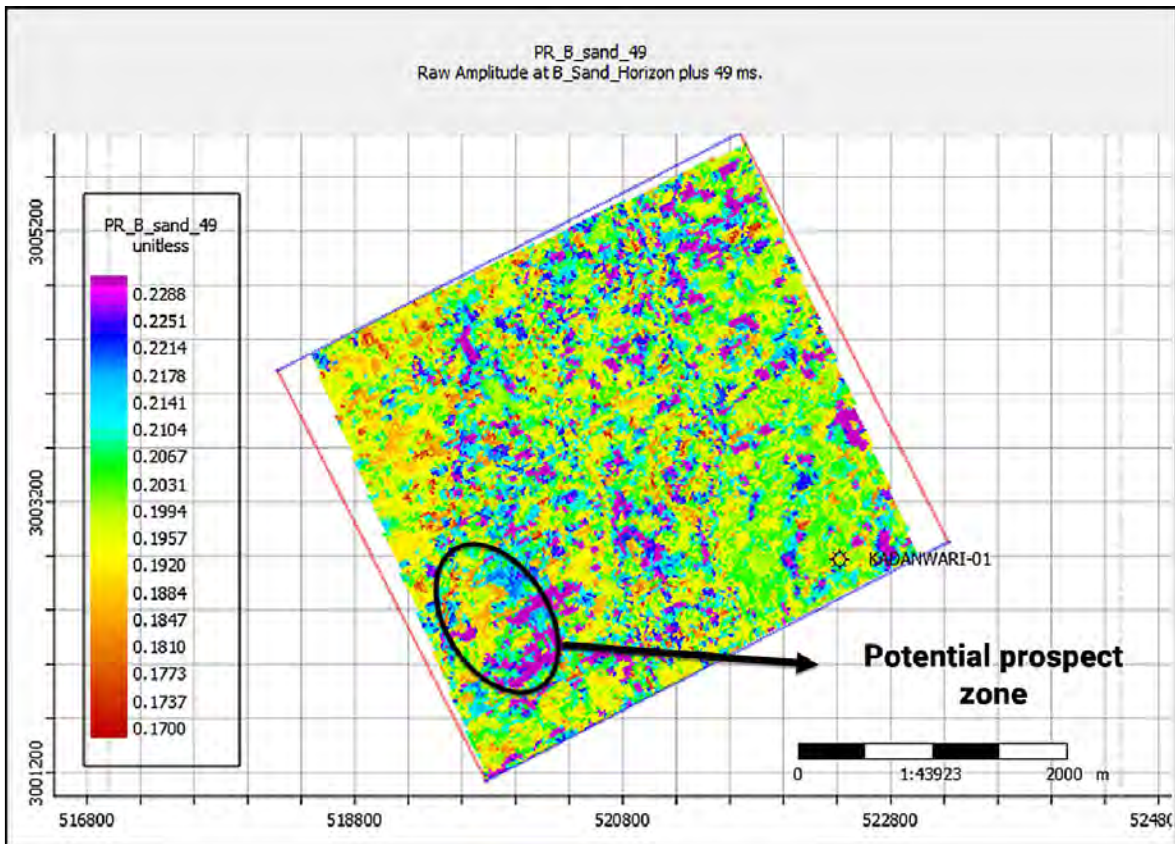


Figure (5.15): Time slice of B-sand with low porosity ratio and black ellipse represent potential prospect zone.

5.3.4 SPATIAL DISTRIBUTION LAMBDA -RHO:

Lambda-rho provides valuable information about lithology and fluid within pore spaces of rock. The combination of lambda and rho help us to separate different fluid bearing zones i.e gas bearing, oil bearing and brine zone. The value of lambda-rho for hydrocarbon saturated rock is less incompressible (Goodway et al.,1997).according to Das and Chatterjee (2018) the range of lambda – rho for hydrocarbon zone should be less or equal to 20gpa and for compacted sand shows some relative close value . To estimate this property spatially the cube of lambda-rho are generated by using PNN and multi attributes networking. Lower value of lambda-rho gives us clear indication of hydrocarbon. The good correlation is observed between predicted and real values shown in figure (5.16) .Spatial distribution of lambda-rho is shown in figure (5.17) which show low values which help full in hydrocarbon identification. Time slice of E-sand & B-sand are shown in figure (5.18 &5.19) depict that kadanwari-well-01 showing low LMR values. LMR values are relatively high because we use S-wave which is generated by Han empirical relation. Black ellipse represents the

potential prospect zone which have low values of LMR and is good position for drilling new well to increase our production rate.

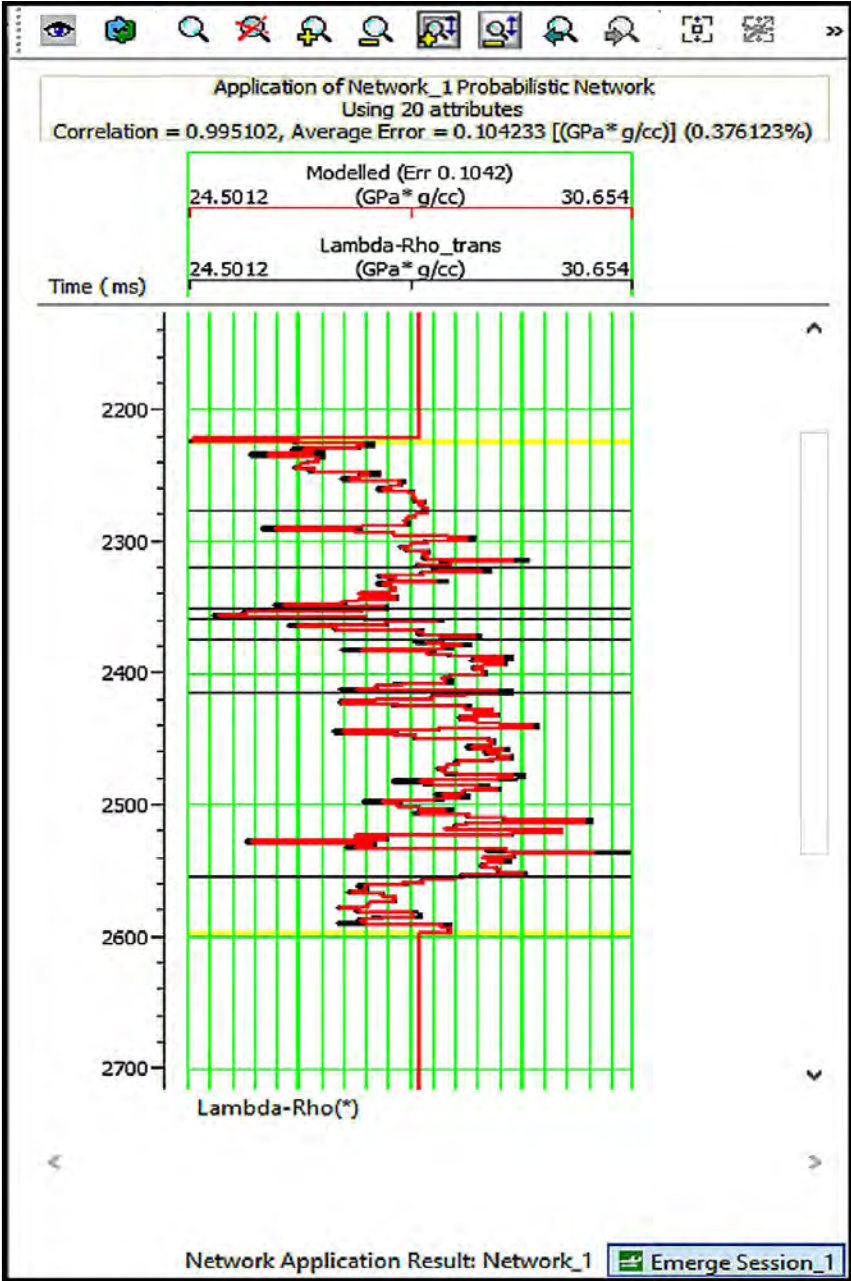


Figure (5.16): Results from PNN of predicted and real LMR with correlation of .995102.

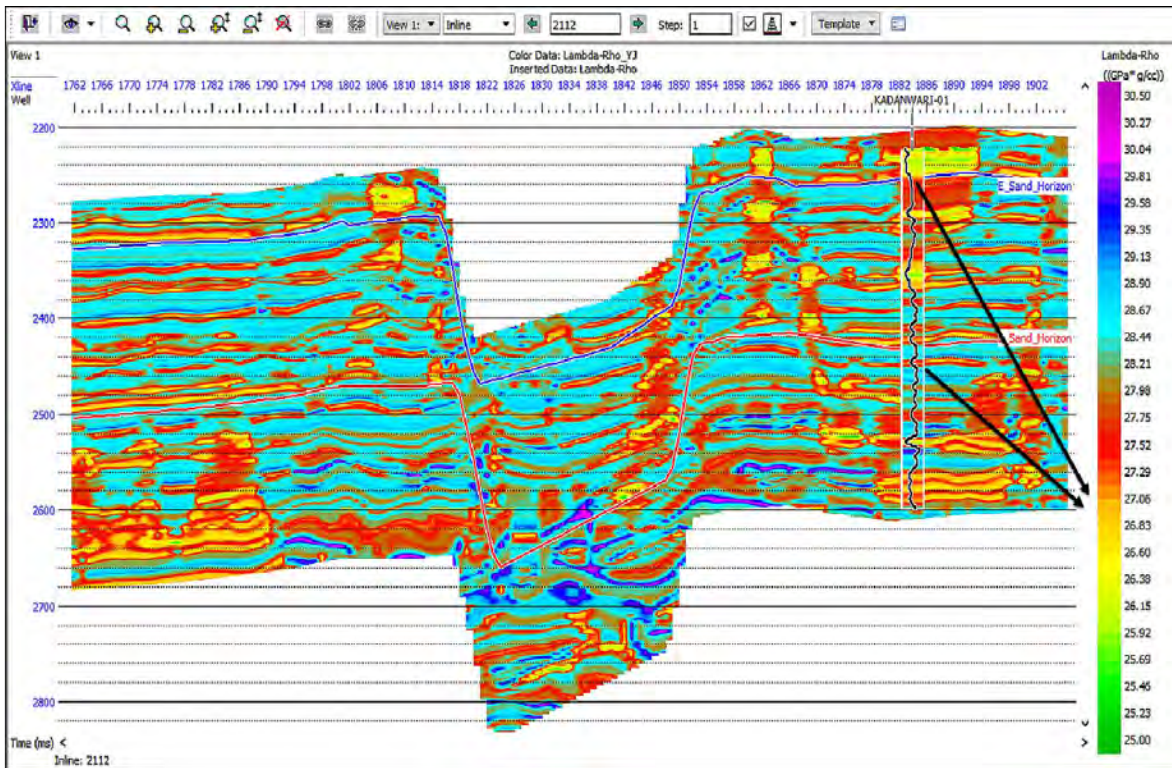


Figure (5.17): Spatial variation LMR for inline 2112 with black arrow represents the value of LMR values of E (3318-3339) & B (3507 -3797) sand.

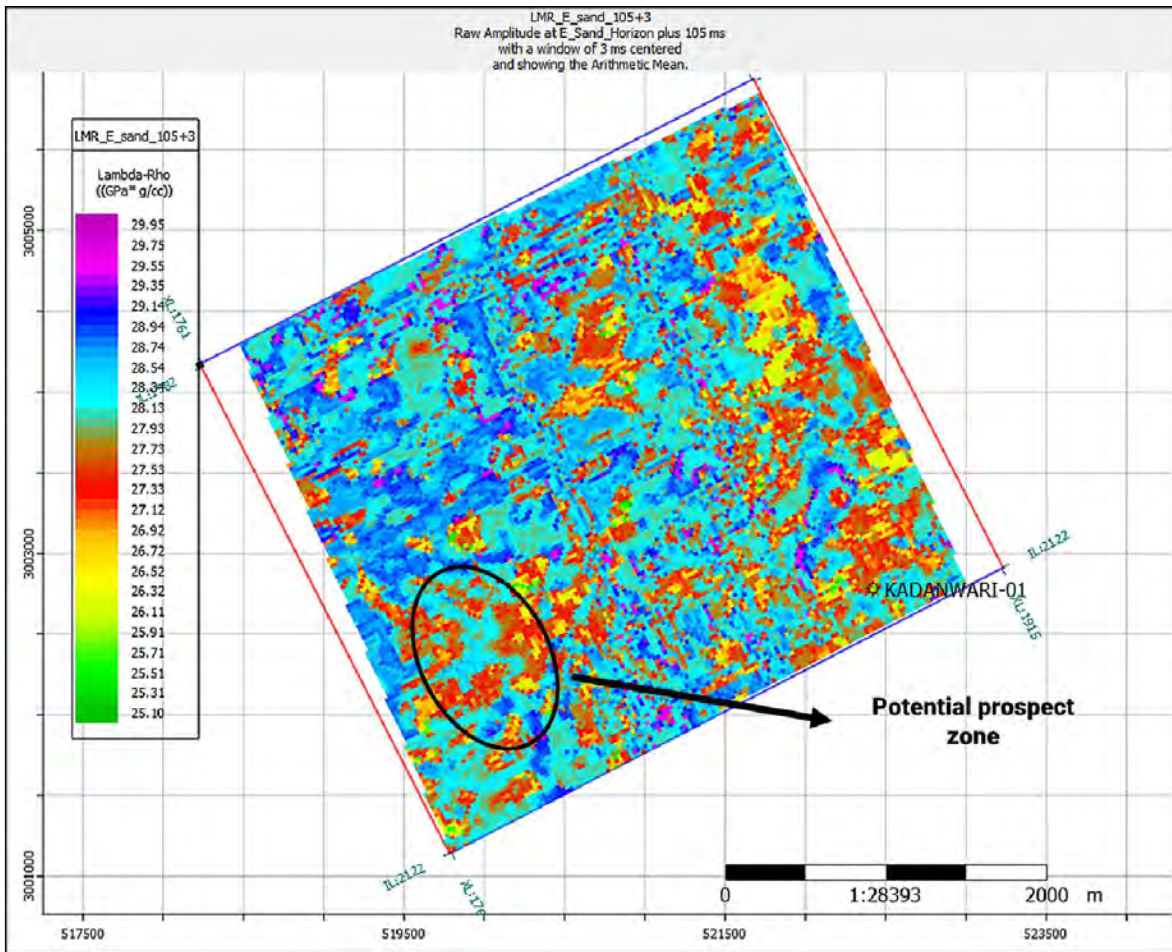


Figure (5.18): Time slice of E-sand with low LMR values and black eclipse represent potential prospect zone.

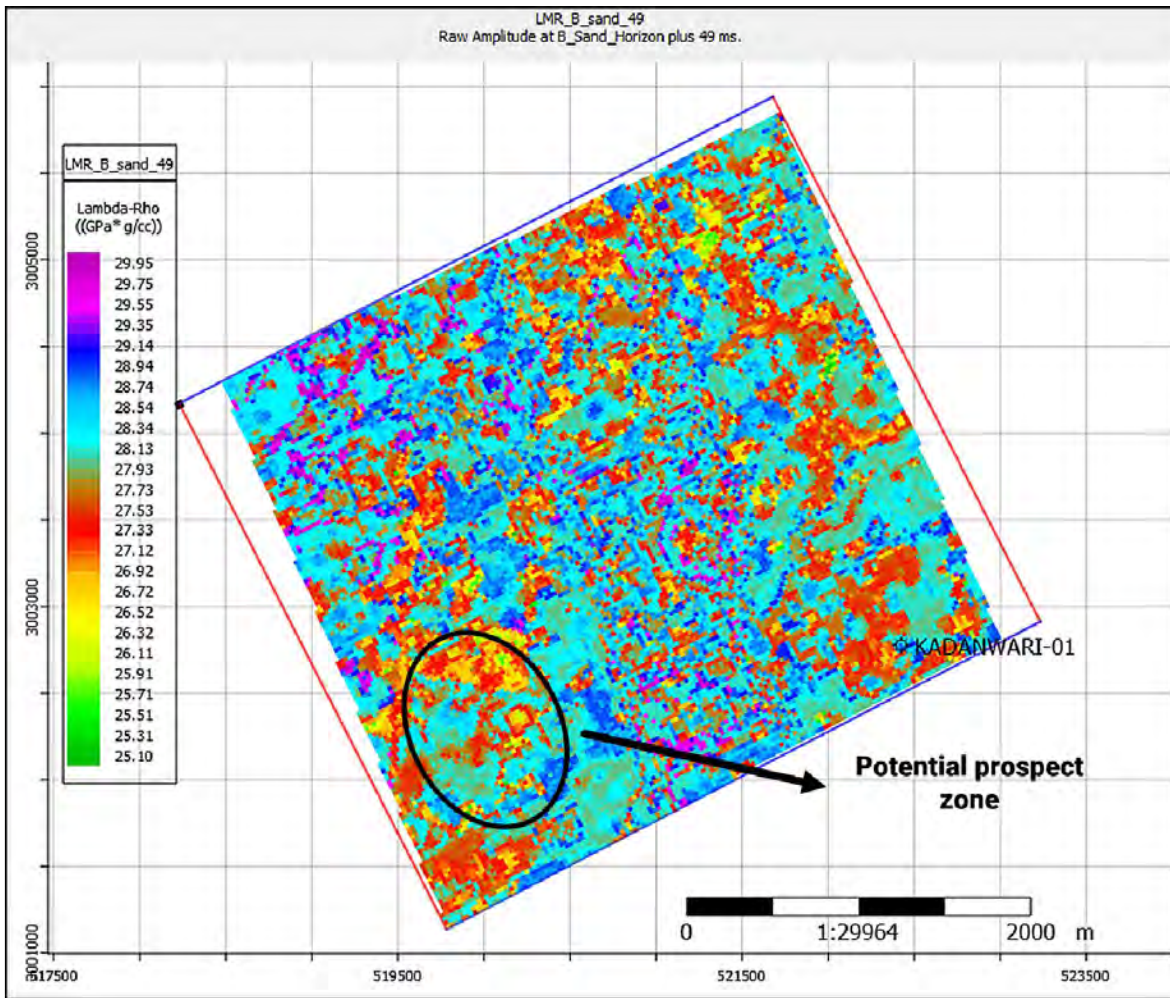


Figure (5.19): Time slice of B-sand with low LMR values and black eclipse represent potential prospect zone.

5.3.5 SPATIAL DISTRIBUTION OF PORE PRESSURE:

The objective of MBI is to calculate properties that are help full in characterizing of the reservoir. The set of attributes and PNN are used to facilitate our interpretation (Pendrel., 2006).Pore pressure gives us a value able information about active compaction trends(abdulaal.,2006).By neural networking linear relationship is attained between predicted and actual pressure values shown in figure (5.20). Spatial variation is predicted in such linearity when moving away from well with the help of PNN. Predicted and actual pressure shows a positive correlation (.984331) shown in figure (5.21).

BY PNN the variation of pore pressure is spatially estimated on seismic 3D cube shown in figure (5.23). But true image is difficult to obtain because of resolution issue. High pressure zone are associated with the reservoir. The study of pore pressure is helpful in identifying cause of failure of well and used to estimate the mud weight(Abdulaa.2016).The high pressure zones are identify in Guru sands which is prediction of hydrocarbon and here we can estimate mud weight in order to reduce risk while drilling. In presence of hydrocarbon pore pressure should be over pressure or under pressure because we know that pore pressure is pressure exerted by fluid on pore spaces of rock at depth.Time slices of E &B sands show high pressure value in figure (5.24 & 5.25).

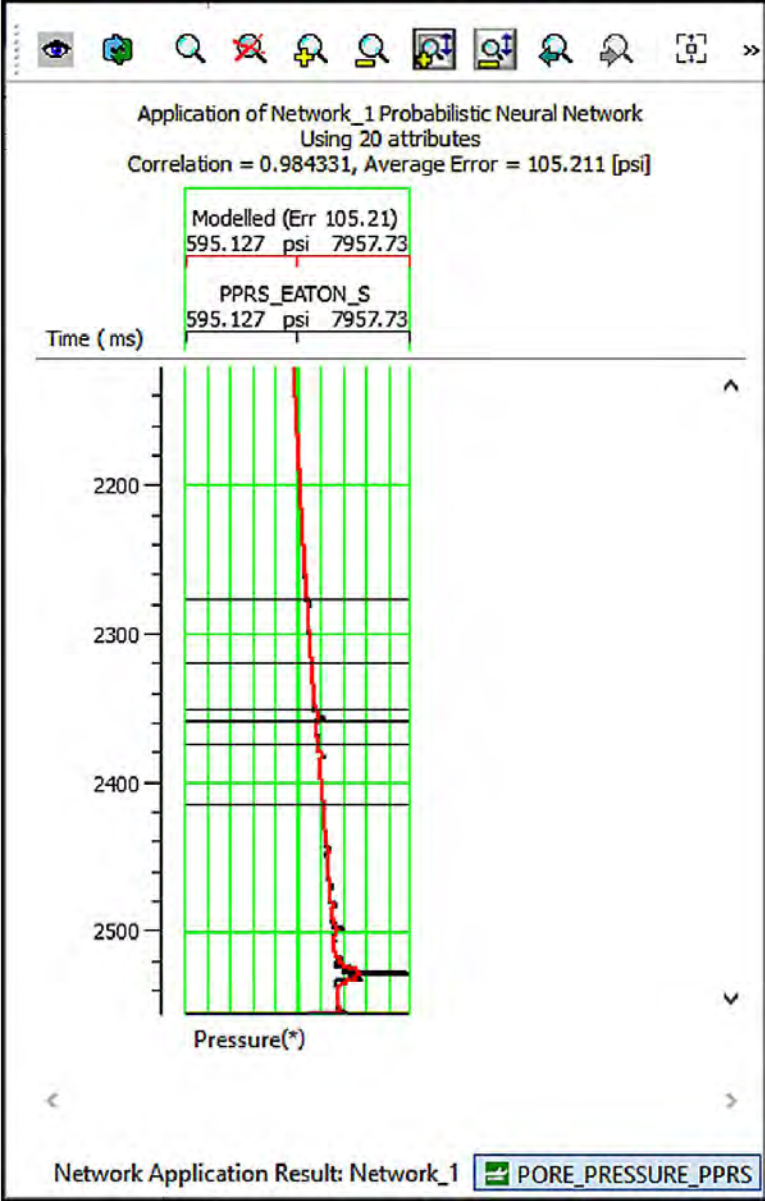


Figure (5.21): Results from PNN of predicted and actual PP with correlation of .984331.

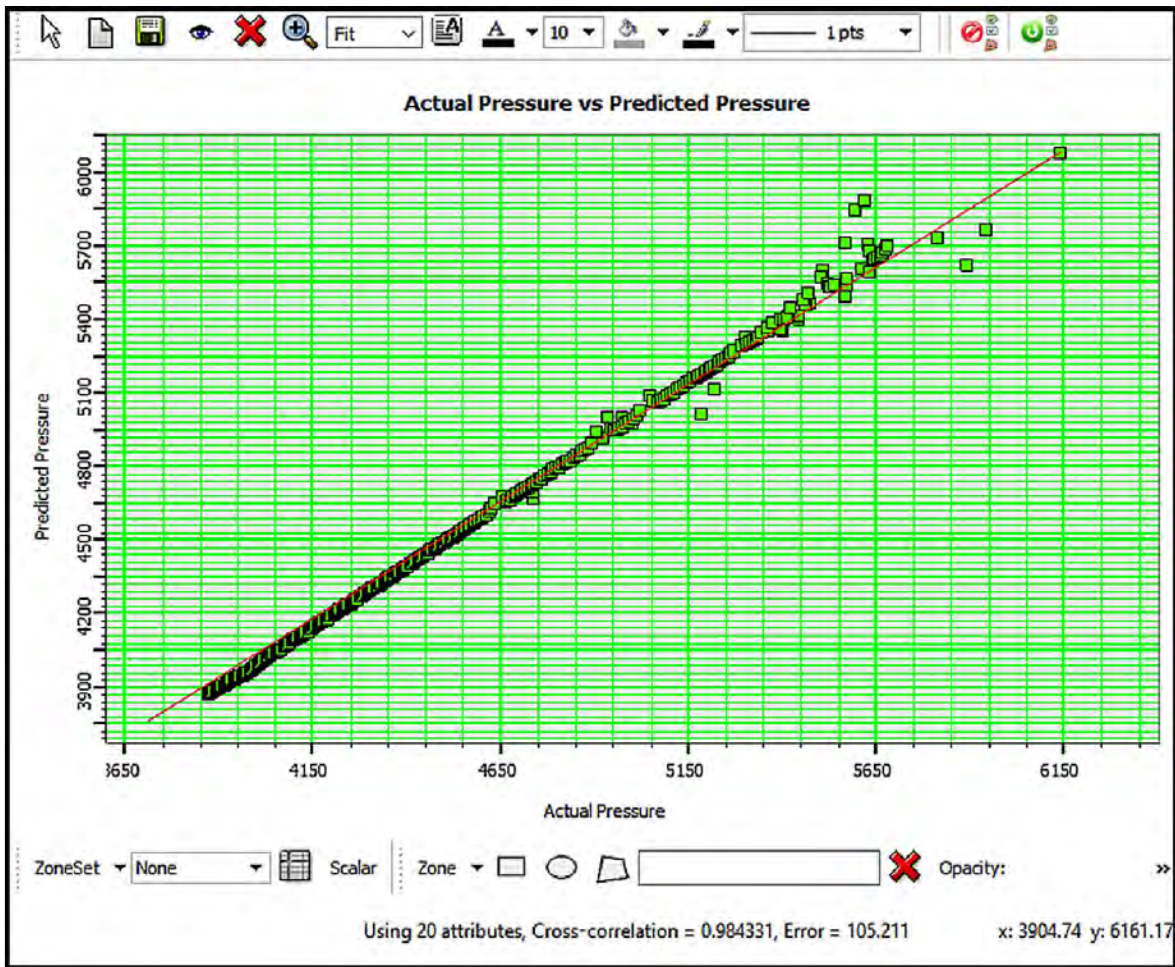


Figure (5.22): Match between predicted and actual pressure.

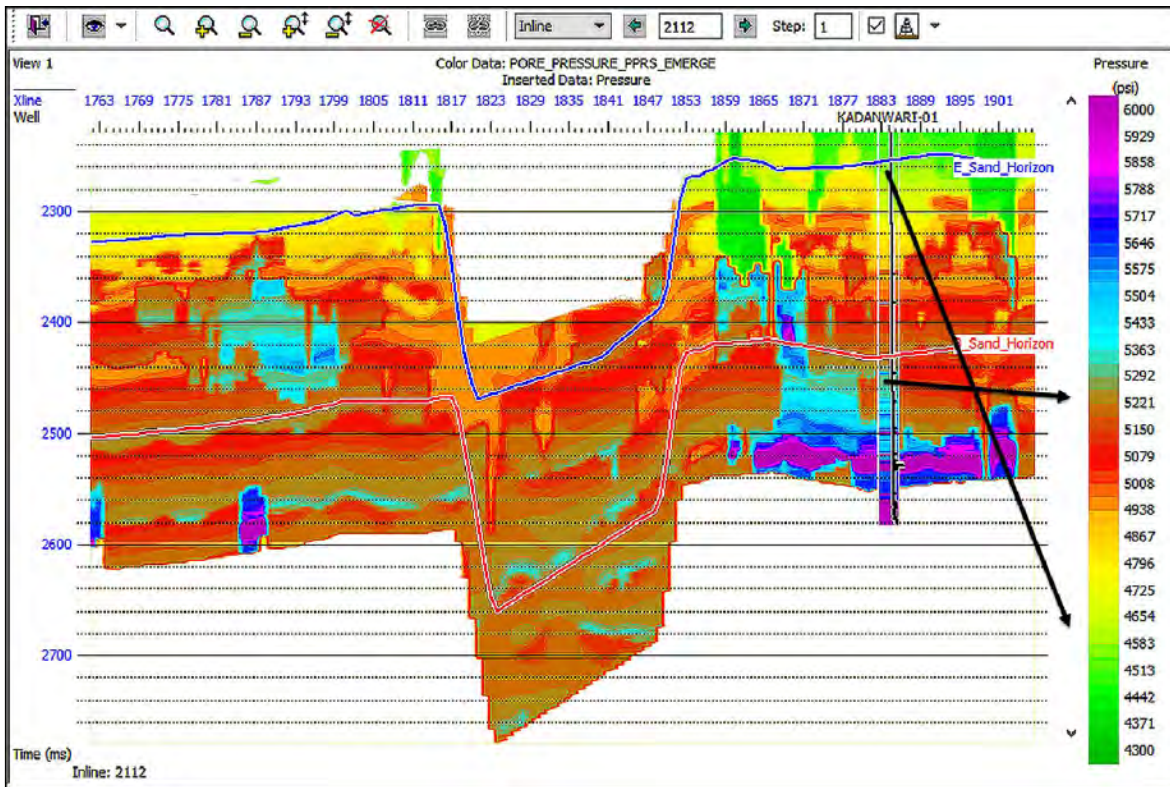


Figure (5.23): Spatial variation of PP for inline 2112 with black arrow represents the high value of Pore pressure for E (3318-3339) & B (3507 -3797) sand.

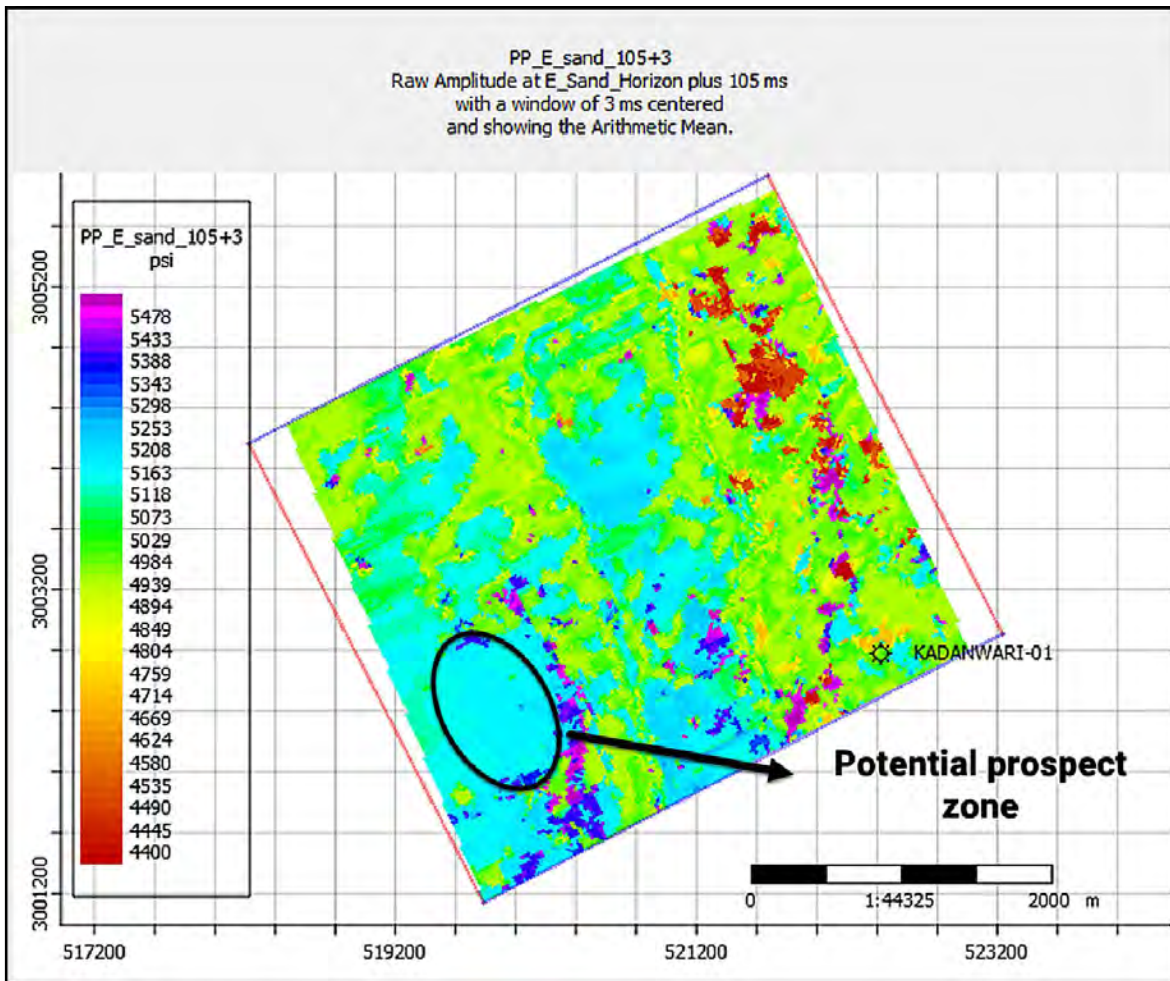


Figure (5.24): Time slice of E-sand with high pore pressure values and black ellipse represent potential prospect zone.

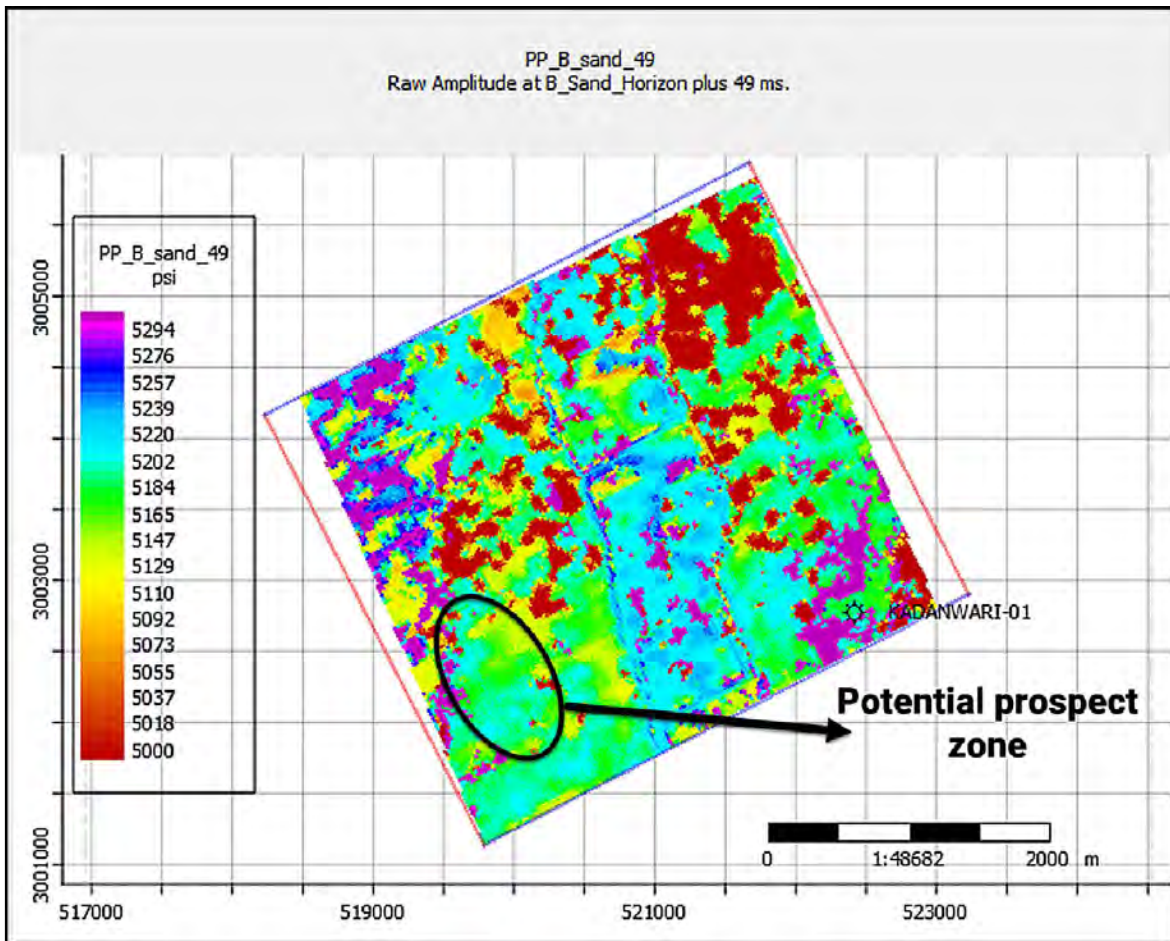


Figure (5.25): Time slice of B-sand with high pore pressure values and black ellipse represent potential prospect zone

5.3.6 SPATIAL DISTRIBUTION OF MINIMUM AND MAXIMUM STRESSES

These stresses are one of the principle stress helpful in prediction of geometry, fracture propagation geometry, barrier zone ,safe window, production behavior of reservoir and borehole stability (Bell.,1996;McLellan 1996;Bell and Babcock 1986;Lancaster & Guidry .,1990;Maleki et al .,2014)).These stress also help us to identify the types of faults. Maximum and minimum, stresses are calculated by poro-elastic model. The stress profile and pore pressure profile show opposite trend in presence of hydrocarbon. Figure (5.21) show .998649 of correlation between predicted and actual pressure. Matching between predictive and actual sigma are shown in Figure (5.22).The spatial distribution of minimum horizontal stress is shown in figure (5.23). Time slices of E &B sands show high Shmin value in figure (5.29 & 5.30).

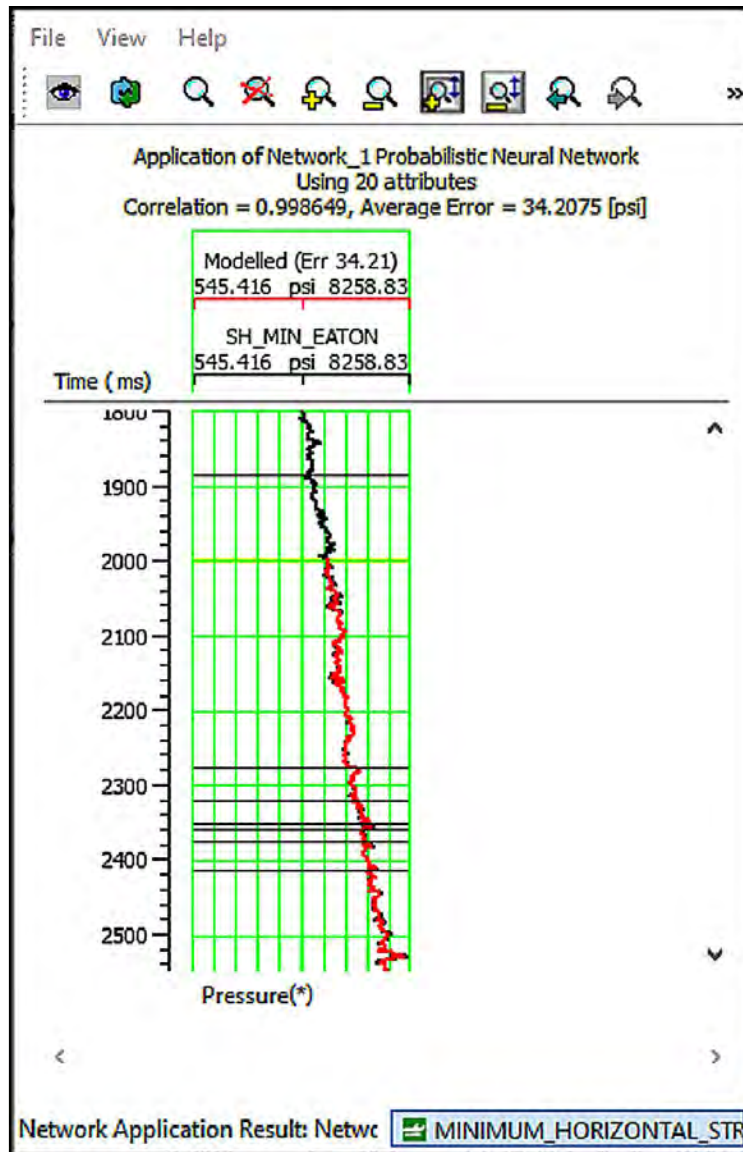


Figure (5.21) : correlation between predicted and actual pressure is.998649.

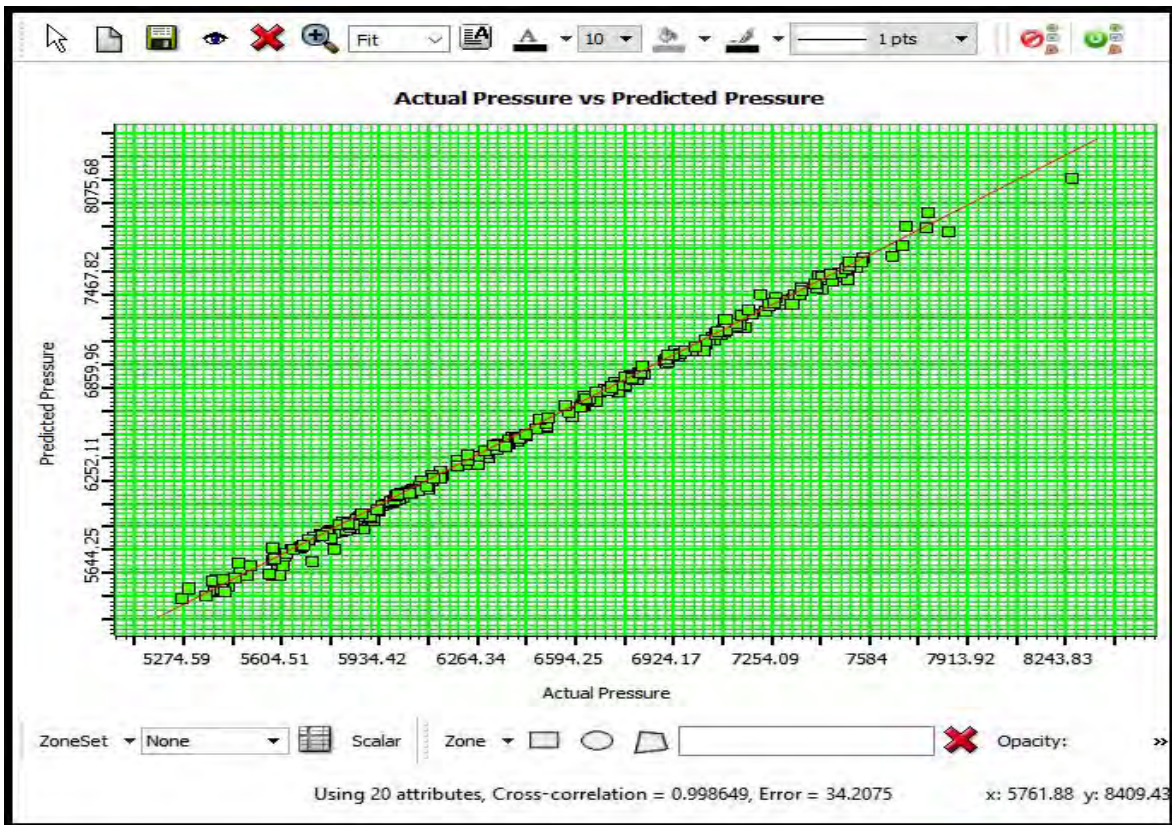


Figure (5.22): Match between predicted and actual pressure.

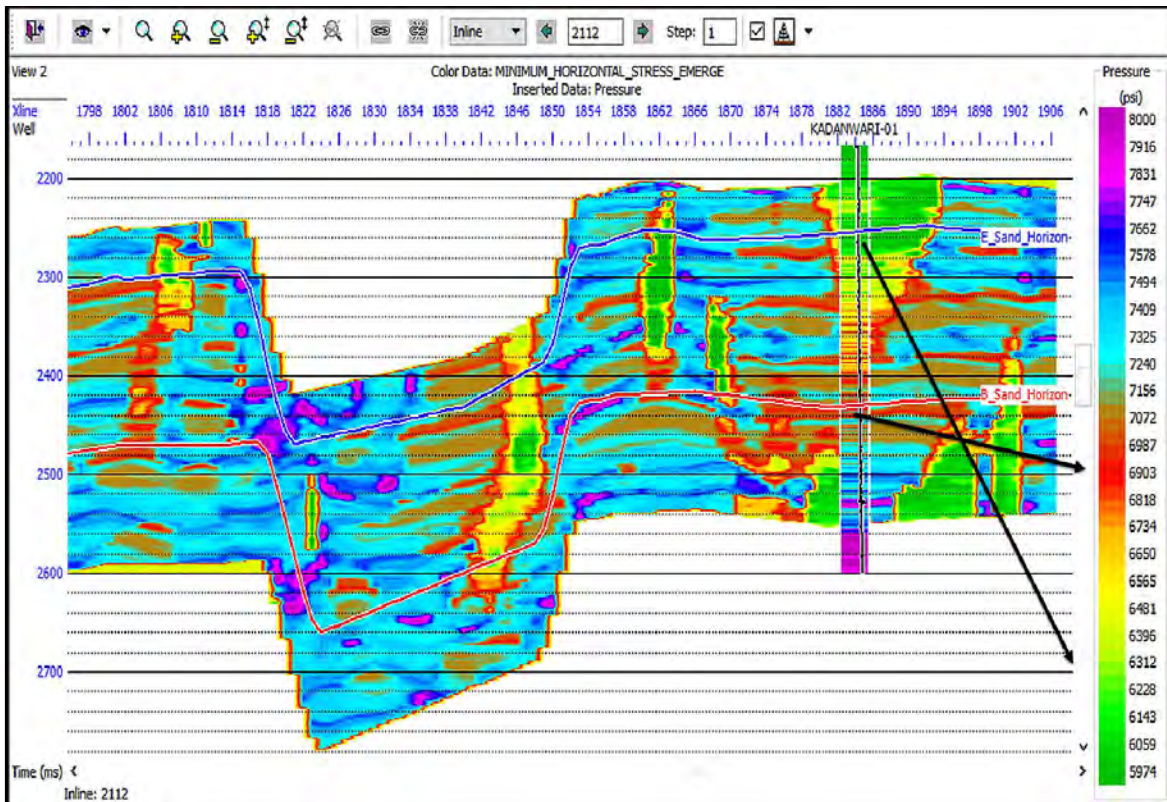


Figure (5.23): Spatial variation of s_{hmin} for inline 2112 with black arrow represents the high value for E (3318-3339) & B (3507 -3797) sand.

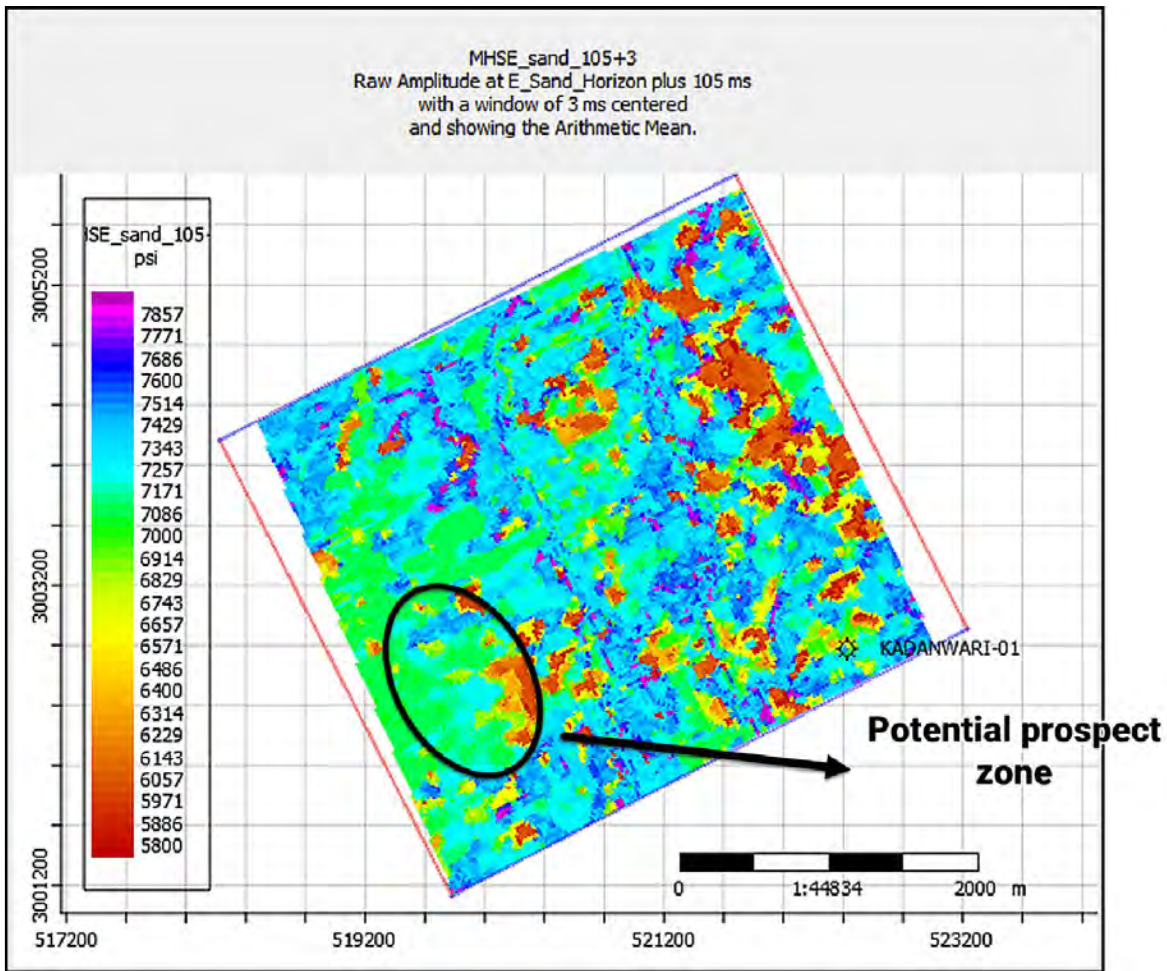


Figure (5.29): Time slice of E-sand with high Shmin values and black eclipse represent potential prospect zone

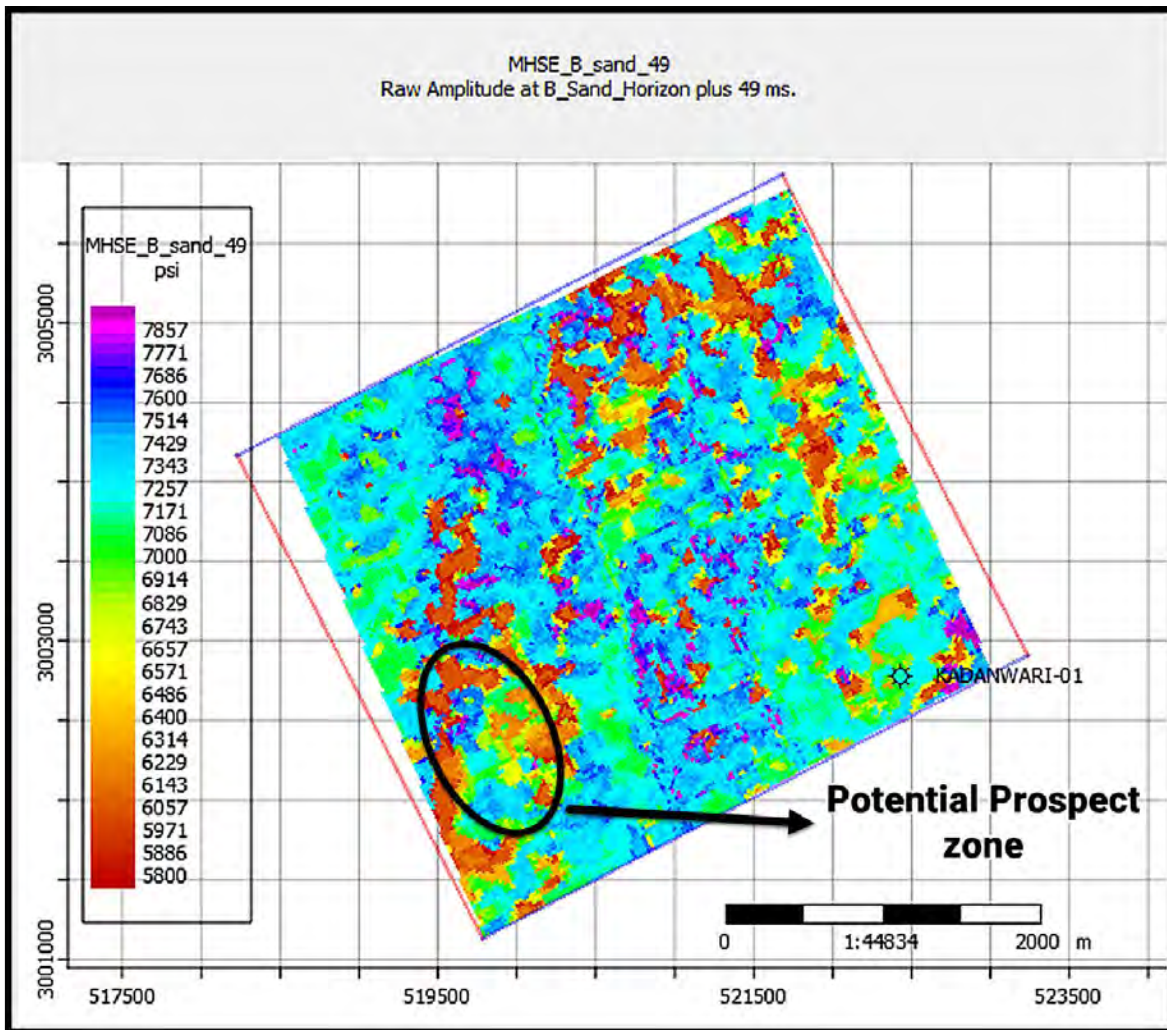


Figure (5.30): Time slice of B-sand with high Shmin values and black eclipse represent potential prospect zone

Spatial distribution of all geo-mechanical properties mimics our petro-physical results. There is strong indication of occurrence of hydrocarbon.

CHAPTER 6

6. DISCUSSIONS AND CONCLUSIONS

6.1 DISCUSSIONS:

We done reservoir evaluation of lower guru sands (E-sand and B-sand) using 3D seismic data and petro-physical data of kadanwari 01 well. Seismic interpretation show negative flower structures which is favourable position for hydrocarbon accumulation (Aziz.,2016). we found positive results from petro-physical analysis of lower Goru sand with good porosity ranges and high hydrocarbon saturation.i.e the effective porosity (8-11%), volume of shale (33-38%) and hydrocarbon saturation (60-80%).

For futher detail reservoir evaluation we done rock physics modeling which is important tool to separate oil and brine zones present in reservoir Dvorkin et al.,2014;Ali et al.,2017).

We calculated low values of lambda-rho , Mu-rho , VpVs ratio and values of P-impedance which give us clear identification of hydrocarbon accumulation. According to Das and chaterjee the low values of lambda -rho, Mu-rho shows low values & VpVs ratio (1.60 to 1.80) proven the hydrocarbon bearing zone. In kadanwari Gas field the sand are compacted and have low porosities as compared to non compacted sands due to these factors our values lie closely to standard values which is clear indication of presence of hydrocarbon. The cross-plotting of these values separate brine and shale zone also (Das & chaterjee)..

The mechanical properties of reservoir is key factor to estimate well stability and reservoir evaluation (Xu et al.,2016;Archer and Rasouli;2012).We estimate the geo-mechanical properties such as young's modulus bulk modulus, shear's modulus, unconfined compressive strength, friction angle, overburden stress, pore pressure, minimum and maximum stress and correlate with the GMP's of same lithological units that are calculate in laboratory (Abbas et al.,2018).We optimized our results to characterized the reservoir and reduce the uncertainty related to hydrocarbon exploration. The results help us to analyze the stability of well during drilling and also minimize the risk while drilling.the calculated rock physics model parameters and geo-mechanical properties of our study area are given in Table (6.1)

Table 6.1 :Rock physics and geo-mechanical values calculated for E & B sand. The standard values are also given .

Rock Physics Parameters	E-Sand	B-Sand	Standard Laboratory Values	Geo-mechanical properties	E-sand	B-sand	Standard GMP's Values
VpVs Ratio	1.63	1.65	1.62-1.80	FANG (deg)	33°	40°	42.35° ± 17°
				E(GPa)	32.68	37.88	27.66±9.98
P-Impedance (m/s)*(g/cc)	~10500	~11200	Low	K(GPa)	5.34	6.906	8.75±3.98
				G(GPa)	5.119	7.00	5.60±2.60
Lambda – Rho	~26	~27	(Gas Sand) Low values	USC(MPa)	52	70	66.38±17
				Mhu-Rho	~34	~38	(Gas Sand) High values

The GMP's and rock physics models are integrated with seismic inversion to estimate the spatial distribution of reservoir properties to seismic scale. this approach enable us to identify the sweet spots over study area. From GMP's analysis we find the potential prospect zone which will results in increasing of reservoir production. This integrated approach enabled us to minimize the risk while drilling for more accuracy the core data and micro seismic data is used.

6.2 CONCLUSIONS

- Seismic interpretation confirm the negative flower structures prevail in study area. Host and graben structure are good position for hydrocarbon accumulation.
- Two Faults are marked in the horst and graben structure showing the extensional regime, tectonics activity making negative flower structures as a whole in area.

- Petro-physical analysis of lower guru E-sand (3318-3339) and B-sand (3505-3797) shows the presence of gas sand
- RMM is true picture of rock mechanical properties and it is key factor to estimate well stability and reservoir evaluation for hydrocarbon reserves.
- Results of geo-mechanical properties also confirm the presence of gas sand , because GMP's values are matched with standard values which are required for potential hydrocarbon zone.
- The spatial distribution of geo-mechanical properties are utilizing seismic inversion for detail information .This integrated approach has enabled us to identify the hydrocarbon prone sand and helps us to minimizing risk related to well stability.
- Time slices of all GMP's give indication of potential prospect zone which increase reservoir production rate.
- It is suggested that rock mechanical properties (RMM) should be utilized in order to find potential prospect zone for drilling and also help us to avoid risks related to drilling.

7. REFERENCES

- Abbas, A. K., Y. M. Al-Asadi, M. Alsaba, R. E. Flori, and S. Alhussainy. 2018. Development of a Geo-mechanical Model for Drilling Deviated Wells through the Zubair Formation in Southern Iraq. SPE/IADC Middle East Drilling Technology Conference and Exhibition. doi:10.2118/189306-ms
- Ali, A., Kashif, M., Hussain, M., Siddique, J., Aslam, I., & Ahmed, Z. (2015). An integrated analysis of petrophysics, cross-plots and Gassmann fluid substitution for characterization of Fimkassar area, Pakistan: A case study. *Arabian Journal for Science and Engineering*, 40(1), 181-193.
- Francis, A. M., & Syed, F. H. (2001, November). Application of relative acoustic impedance inversion to constrain extent of E sand reservoir on Kadanwari Field. In *SPE & PAPG Annual Technical Conference, Islamabad, Pakistan*.
- Gavotti, P., D. C. Lawton, G. Margrave, and J. H. Isaac. (2013). Model-based inversion of low-frequency seismic data. 75th EAGE Conf. and Exhib. European Association of Geoscientists & Engineers. doi:10.3997/2214-4609.20130047
- Hampson, D. P., Russell, B. H., and Bankhead, B. (2005). Simultaneous inversion of pre-stack seismic data. In SEG Technical Program Expanded Abstracts 2005 (pp. 1633-1637). Society of Exploration Geophysicists.
- Ahmad, N., & Chaudhry, S. (2002). Kadanwari Gas Field, Pakistan: a disappointment turns into an attractive development opportunity. *Petroleum Geoscience*, 8(4), 307-316.
- Kadri, I. B. (1995). Petroleum Geology of Pakistan: Pakistan Petroleum Limited. *Karachi, Pakistan*.
- Khan, M. J., & Khan, H. A. (2018). Petrophysical logs contribute in appraising productive sands of Lower Goru Formation, Kadanwari concession, Pakistan. *Journal of Petroleum Exploration and Production Technology*, 8(4), 1089-1098.
- Goodway, W., Chen, T. and Downton, J., 1997, Improved AVO fluid detection and lithology discrimination using Lamé petrophysical parameters: λ/ρ , μ/ρ , & λ/μ fluid stack from P and S inversions, 68th Ann. Int. SEG Mtg, p.183-186.
- Samantaray, S. and Gupta, P., 2008, An interpretative approach for gas zone identification and lithology discrimination using derivatives of λ/ρ and μ/ρ attributes, 7th Biennial International Conference and Exposition on Petroleum Geophysics, Society of Petroleum Geophysicists, Hyderabad, 386–341
- Kazmi, A.H. & Jan, M.Q. 1997. Geology and tectonics of Pakistan. Graphic Publ., Karachi

- Barclay, F., Bruun, A., Rasmussen, K. B., Alfaro, J. C., Cooke, A., Cooke, D and Roberts, R. (2008). Seismic inversion: Reading between the lines. *Oilfield Review*, 20(1), 42-63.
- French, F. R. and McLean, M. R., 1992. Development drilling problems in high-pressure reservoirs. In: Proc SPE Int Meeting Petrol Eng, Beijing, 24-27 March. SPE 22385.
- Goodway, B., Chen T. and Downtown, J 1997, Improved AVO fluid detection and lithology discrimination using Lamé petrophysical parameters, 67th Annual international Meeting, SEG, Expanded Abstracts, 183–186
- Das B, Chatterjee R (2017) Wellbore stability analysis and prediction of minimum mud weight for few wells in Krishna-Godavari Basin, India. *Int J Rock Mech Min Sci* 93:30–37
- Asquith, G. and Gibson, C., 1983, Basic well log analysis for geologists. AAPG methods in exploration series, Tulsa, pp.216
- Cooke, D., and Cant, J. (2010). Model-based seismic inversion: Comparing deterministic and probabilistic approaches. *CSEG Recorder*, 35(4), 29-39.
- Chang, C., Zoback, M. D., & Khaksar, A. (2006). Empirical relations between rock strength and physical properties in sedimentary rocks. *Journal of Petroleum Science Engineering*, 51(3-4), 223–237. doi:10.1016/j.petrol.2006.01.003.
- Fan, X., Zhang, M., Zhang, Q., Zhao, P., Yao, B., & Lv, D. (2020). Wellbore stability and failure regions analysis of shale formation accounting for weak bedding planes in ordos basin. *Journal of Natural Gas Science and Engineering*, 103258
- Fjær, E., Holt, R.M., Horsrud, P., Raaen, A.M., & Risnes, R. (1992). *Petroleum Related Rock Mechanics*, 1st ed., Elsevier, Amsterdam, 346p
- Li, M., and Zhao, Y. (2014). *Prestack Seismic Inversion and Seismic Attribute Analysis*. 10.1016/B978-0-12-410436-5.00007-1.
- Chang, C., Zoback, M.D and Khaksar, A., Empirical relations between rock strength and physical properties in sedimentary rocks. *Journal of Petroleum Science & Engineering*, 51, 223-237, 2006.
- Asquith GB, Krygowski D, Gibson CR (2004) *Basic well log analysis*, American Association of Petroleum Geologists, Tulsa
- Fjær, E., Holt, R. M., Raaen, A. M., Risnes, R., & Horsrud, P. (2008). *Petroleum related rock mechanics* (Vol. 53). Elsevier.
- Kadri IB (1995) *Petroleum geology of Pakistan*, Pakistan Petroleum Limited, Karachi
- Kazmi AH, Jan MQ (1997), *Geology and tectonics of Pakistan*. Graphic publishers, Santa Ana

- Najibi, A.R., Ghafoori, M., Lashkaripour, G.R., 2015. Empirical relations between strength and static and dynamic elastic properties of Asmari and Sarvak limestones, two main oil reservoirs in Iran. *J. Pet. Sci. Eng.* 126, 78e82.
- A log based analysis to estimate mechanical properties and in-situ stresses in a shale gas well in North Perth Basin S. Archer & V. Rasouli (2016). Department of Petroleum Engineering, Curtin University, Australia
- Xu, H., Zhou, W., Xie,R., Da,L., Xiao, C., Shan., Y Zhang,H (2016).Characterization of Rock Mechanical Properties Using Lab Tests and Numerical Interpretation Model of Well Logs
- Factors determining Poisson's ratio John J. Zhang and Laurence R. Bentley (2005).
- Eaton, B.A., 1975. The equation for geopressure prediction from well logs. Society of Petroleum Engineers of AIME, Paper SPE-5544.
- Eyinla, D .S ., & Michael A. Oladunjoye (2014).Estimating Geo-Mechanical Strength of Reservoir Rocks from Well Logs for Safety Limits in Sand-Free Production .
- AI Abdulaal, H.A.(2016). Constraining pore pressure prediction using seismic inversion (Doctoral dissertation).
- Gavotti, P.E. (2014). Model based inversion of broadband seismic data.(Doctoral dissertation).
- Gavotti, P.E. ,Lawton, D.C., Margrave, G.F., Isaac, J.H.(2014).Post stack inversion of Hussar low frequency seismic data.
- Das B , Chatterjee R , Singha DK ,Kumar R (2017). Post-stack seismic inversion and attributes analysis in shallow off shore of Krishna Godanvari basin India.
- Fischetti , A.I.,& Andrade, A (2002).Porosity images from well logs.
- Ali , A., Alves, T.M ., Saad, F. A.,Ullaha, M.,Toqeer,M.,& Hussain,M (2018).resource potential of gas reservoir in south Pakistan and adjacent indain sub continent revealed by post-stack inversion techniques.Jornal of Natural Gaws Science And Engineering.
- Adham, A. (2016).Geo-mechanics model for well bore stability analysis in field" X"North Sumatra Basin.
- Cooke, D.A and Schneider, W.A.,1983.Generized linear inversion of reflection seismic data.
- Danial,K.,A.(2003),Guide to petrophysical interpretation, Austin Texas,USA
- Mahammad , H .Q ., Abbas ,A .,& Dahm ,H.H (2018).Well bore instability analysis for Nahr Umr Formation in Southern Iraq.
- Mavko,G ., Mukerji,T.,&Dvorkin,J (2009).The rock physics hand book.

